ENGINEERING PRINT® PARTICLES FOR PULMONARY DELIVERY OF THERAPEUTICS

Tojan Bassam Rahhal

A dissertation submitted to the faculty at the University of North Carolina at Chapel Hill in partial fulfillment of the requirements for the degree of Doctor of Philosophy in the Division of Molecular Pharmaceutics in the UNC Eshelman School of Pharmacy.

Chapel Hill
2016

Approved by

Joseph M. DeSimone

Elena V. Batrakova

David C. Henke

Shawn D. Hingtgen

James C. Luft

ABSTRACT

Tojan Bassam Rahhal: Engineering PRINT® Particles for Pulmonary Delivery of Therapeutics
(Under the direction of Joseph M. DeSimone)

Pulmonary drug delivery is an attractive new approach to the traditional parenteral route of administration due to its non-invasive nature, convenience, and increased patient compliance. However, there is a need for more efficient delivery of active therapeutics/biologics using dry powders that allow for monodisperse aerosolization and accurate deposition in the lungs, as well as extended residence time and targeting ability. Previous work in our lab demonstrated the aerosolization of monodisperse particles for potential pulmonary use in respiratory diseases. We investigated further by focusing on the effect of particle parameters (size, shape, composition and surface chemistry) on residence time, cellular interactions, and immune responses in the lungs.

We aimed to engineer particles with controlled parameters using Particle Replication in Non-wetting Templates (PRINT®) fabrication technology for ultimate pulmonary delivery of therapeutics. We first assessed the particle compositions and their respective characteristics that would be useful for drug delivery (drug release kinetics, activity, stability, and biocompatibility). We then examined the exclusive effect of surface chemistry for drug delivery and targeting in the lungs by assessing the impact of cationic and anionic surface charges, as well as PEGylation. And lastly we presented the particulate delivery of biologics to the lungs, demonstrating our ability to maintain activity and control deposition and aerosolization.

Future work includes investigating the incorporation of therapeutics for direct targeting in the lungs, such as for tuberculosis using antibiotics that can be delivered directly to the macrophages. We have also provided the groundwork for delivering pulmonary vaccines by establishing cationic particles recruit dendritic cells to the lungs and therefore can be vital in designing pulmonary vaccines. Lastly, there is a future in working with alternative particulate biologics for treatment of cystic fibrosis and other pulmonary diseases. Overall, we have shown how engineering particles by controlling particle parameters can impact and improve pulmonary delivery of therapeutics.

I dedicate this work to my family. My grandfather who showed me what courage is in his fight against brain cancer, my mom and dad who have always supported me as I took on one challenge after the other, my sisters who always made sure I had fun along the way and who have become my role models as they take on life, my grandparents, my cousins, aunts, and uncles, and my entire family in their support and encouragement throughout. My fiancé who has kept me sane in this last year of graduate school and my friends, old and new, whom I could never have survived without- the late movie nights, the numerous study dates, and all the random adventures. And lastly, to Our Three Winners, my friends, Yusor, Deah, and Razan, who despite being taken so young have truly shown me what it means to live a life of service, do good, and to truly be the change you want to see in this world.

ACKNOWLEDGMENTS

I would like to thank my advisor Joseph DeSimone for giving me the opportunity to be a part of his lab, constantly leading by example, and allowing me to pursue activities that I am passionate about in the lab and the community. I do not think I could have been luckier to be in an environment that supports and values service, diversity, and community involvement as much as science. I must also mention that Joe convinced me how awesome twitter is for science! Next, I would like to thank my committee members who have constantly supported my endeavors and guided me throughout, while serving as great role models doing amazing research. Dr. David Henke took me in as his only PhD student to learn the ways of pulmonologists and gave me many opportunities to see the clinical side of my research as well as meet other MDs. Dr. Michael Jay always provided guidance and support throughout and Dr. Shawn Hingtgen continuously inspired me with his breakthrough research and willingness to provide a different perspective to my work. And lastly, Dr. Elena Batrakova, from the time I rotated with you I admired your passion about your research and your approach to science- you definitely taught me a lot, and your unwavering faith in my abilities has meant so much! Dr. Chris Luft, you didn't hesitate to join my committee, and more so have been a wonderful mentor and adviser throughout! You were always there to help guide me with the big decisions, and teaching me how to become a better writer and scientist along the way! Thank you all for being such an inspiration, I am so glad to have you as my mentors.

I would also like to thank Dr. Cathy Fromen; I could not be where I am without her

constant support! She has been a mentor to me from day one of graduate school, teaching me the realities of good science, listening to my rants and showing me what it looks like to be a superwoman in science! Another great mentor that has truly guided me since undergrad, and has continued to be a true friend and advisor is Dr. Erin Banks. Thank You! I cannot say that enough, for without you I would never have been exposed to research and would not have found my passion. Thank you!

Numerous people have supported me in pursuing fellowships, awards, and extracurricular activities. I must start by thanking Crista who has always been there to help me navigate the world of applications, my passions for diversity in science, and has been the source of many wonderful enlightening conversations. Thank you to Vicki who has always put up with all of my logistical questions and my other rambles. Vicki, the DeSimone lab experience would not have been the same without you! I would also like to thank Dr. Mary Napier, who first interviewed me for graduate school and truly confirmed that this was the lab I wanted to be a part of.

I would like to also thank the members of the DeSimone lab. Kevin Chu, thank you for taking me on my first tour of the DeSimone lab and mentoring me on my first PhD research project! Jillian, you made sure I was taken care of as a rotation student and properly trained, and you continued to provide support and answers to any and all my questions- Thank you! Tammy and Marc, thank you for preventing any dull moments in research and joining Cathy and me on our hour long discussions of study designs, and providing me with tips on what movies (from another generation) that I need to see. I think you would be proud to know I finally watched Top Gun and it wasn't awful. Cameron Bloomquist, we started graduate school together and I am so glad that we joined the DeSimone lab the same year. Your work ethic and your approach to science is inspirational, you never hesitate to lend a helping hand and are always available to

hear my rants, or to teach me how to use new equipment! You even volunteered to take part in some of my crazy initiatives on campus, and for your willingness I am very thankful! I am truly so sorry that I have left you to be the only senior student, but I have no doubt you can handle the little ones. I would also like to thank Chintan, James, Charlie, Erin, Cassie, Ashley, Katie, Sarah, Kevin R., Ying, Yi, Shaomin, Lihong and the entire lab family for their constant support, guidance, and wonderful conversations!

I would also like to thank my BBSP family and the entire OGE office! You made my first year at UNC amazing and I am so glad that I joined your program! You have continued to provide me support throughout my graduate career. Thank you! Thank you Ashalla, Jessica, Erin, Sausyty, Anna, Jeff, Josh, Patrick and the entire team! Thank you to the Women in Science team who I have been lucky enough to be a part of and able to help make great things happen on campus! I must also thank my professors that not only taught me, but were also invested in my success. A special thanks to Dr. Hull, Dr. Cho, Dr. Thakker and Dr. Goy!

Throughout my graduate career I have been passionate about providing opportunities for my peers that showed the importance of diversity in our training to be better leaders. I would like to thank Chancellor Folt, who encouraged me to pursue these efforts, and Aaron Todd, Dr. Roy Hawke and Dean White who have all helped support me in pursuing a diversity workshop for ESOP students. I would also like to thank the student committee who helped bring our workshop to fruition. Cameron, Jing, Jim, Nick, and Hao- Thank you for believing in my vision and helping make it a reality. I am really proud of what we put together for the cross-cultural leadership development workshop.

And lastly I would like to thank my family! I have been so fortunate to have them

nearby! My parents who never doubted me and always supported all my decisions, they were the ones to force me to take breaks, and to make sure I was well supplied with home-cooked meals and more importantly desserts. My sisters who have grown so much and are pursuing their own dreams now- I could not be prouder of them and so thankful that they kept me entertained throughout! My cousins (Mariam, Layla, Hamood, Bader, Sara K and Sara R, all of you!) who kept me young and went along on my crazy adventures of laser tag and go-karting! My grandparents, who always prayed for me and encouraged me to pursue my dreams, my aunts and uncles, you have been so supportive, always ready to give me advice, and sometimes just taking me out for a good break, thank you! My friends, really my sisters, Reem, Nada, Lama and Alma, you have kept me sane, reducing my stress levels, encouraging me, and constantly being there for me, Thank you!! Aminah thank you for being the first person I met at UNC and helping me find a place to live while dealing with my VW drives!! My Chapel Hill family, the Moussas! Thank you for being so loving and truly making me feel like I was at home, always ready to have me over for hours of discussions, sweets, and a good time! Hard work and dedication went into this dissertation, but not without the constant support of those who love me and God's will.

TABLE OF CONTENTS

LIST OF FIGURES xiv

LIST OF ABBREVIATIONS xvi

CHAPTER 1. Introduction to Pulmonary Delivery of Therapeutics Using Nanotechnology 1

1.1 Lung Biology 2

1.2 Targeted Delivery to the Lungs 3

1.3 Pulmonary Delivery Devices 4

1.4 Particulate Delivery to the Lungs 5

1.5 Particle Fabrication Methods 8

1.6 Fabrication of Monodisperse Particles: PRINT Technology 9

1.7 Thesis Overview 11

REFERENCES 12

CHAPTER 2. PRINT® Particles of Controlled Composition for the Lung 16

2.1 Introduction 16

2.2 Methods 19

2.2.1 Fabrication of PRINT PLGA Nanoparticles 19

2.2.2 Assessing Stability of PRINT PLGA Nanoparticles 20

2.2.3 Release kinetics for PRINT PLGA: Docetaxel Nanoparticles 20

2.2.4 Fabrication and Characterization of PRINT Hydrogel Particles 21

2.2.5 Fabrication and Characterization of PRINT BuChE Particles 22

2.2.6 Enzyme Activity Assay for PRINT BuChE Particles 23

2.3 Results 23

2.3.1 Particle Fabrication. 23

2.3.2 PLGA Particle Stability. 24

2.3.3 Particle Release Kinetics. 25

2.3.4 BuChE Particle Characterization. 26

2.4 Discussion 28

REFERENCES 32

CHAPTER 3. Nanoparticle Surface Chemistry Impacts Distribution and Uptake by Pulmonary Antigen-Presenting Cells 37

3.1 Introduction 37

3.2 Methods 41

3.2.1 Animals 41

3.2.2 Particle Fabrication, Functionalization and Characterization 41

3.2.3 Pulmonary Administration 42

3.2.4 Biodistribution Study of Cationic and Anionic Nanoparticles 43

3.2.5 Tissue and Cell Preparation 43

3.2.6 Histopathology 44

3.2.7 Flow Cytometry and ELISAs 44

3.2.8 Cytokine Analysis 45

3.2.9 Quantitative Real-Time PCR (qRT-PCR) for Cationic and Anionic Nanoparticle Treated Mice 46

3.2.10 Statistical Analysis 47

3.3 Results 48

3.3.1 Distribution of Cationic and Anionic Nanoparticles in the Lung Following Pulmonary Instillation 48

3.3.2 Cationic and Anionic Nanoparticle Association in Lung Antigen Presenting Cells 49

3.3.3 Effect of Nanoparticle Treatment on Cellular Responses in the Lung 51

3.3.4 mRNA Expression in Lung Homogenate via Quantitative Real-Time PCR (qRT-PCR) for Immune Response Assessment 53

3.3.5 PEGylated and unPEGylated Nanoparticle Cellular Response and Association in the Lung 55

3.4 Discussion 57

REFERENCES 62

CHAPTER 4. Pulmonary Delivery of Butyrylcholinesterase as a Model Biologic to the Lung 68

4.1 Introduction 68

4.2 Methods 71

4.2.1 Animals 71

4.2.2 Protein Source 71

4.2.3 Orotracheal Administration and Residence of BuChE 72

4.2.4 Cytokine Measurements 73

4.2.5 Flow Cytometry 73

4.2.6 Particle Fabrication 74

4.2.7 Enzyme Activity Measurements 75

4.2.8 Cascade Impactor Lung Deposition 75

4.2.9 Dry Powder Insufflation 75

4.2.10 Statistical Analysis 76

4.3 Results 76

4.3.1 Biodistribution of Orotracheal Administrated BuChE in Nude Mouse Model 76

4.3.2 Immunological Assessment of Orotracheal Administration of BuChE in Different Murine Models 78

4.3.3 Fabrication and Utilization of PRINT BuChE Protein Particles to Demonstrate Pulmonary Cascade Impactor Deposition 82

4.3.4 Dry Powder Insufflation of PRINT BuChE Protein Particles in C57BL/6 Mouse Model 83

4.4 Discussion 85

REFERENCES 91

CHAPTER 5. Summary and Outlook 95

5.1 Summary and Future Work 95

5.2 Outlook 99

REFERENCES 102

LIST OF FIGURES

FIGURE 1.1 ANDERSEN CASCADE IMPACTION. 6

FIGURE 1.2. PARTICLE DELIVERY TO THE LUNGS 8

FIGURE 1.3. PRINT® FABRICATION PROCESS. 10

FIGURE 2.1 VARIED COMPOSITIONS OF PRINT PARTICLES OF UNIFORM SIZE AND SHAPE. 24

FIGURE 2.2. STABILITY OF PLGA-PRINT PARTICLES. 25

FIGURE 2.3 . PLGA:DOCETAXEL NANOPARTICLE FABRICATION AND RELEASE KINETICS. 26

FIGURE 2.4. BUCHE ACTIVITY DETECTION. 27

FIGURE 2.5. CHARACTERIZATION OF PRINT BUCHE PARTICLES. 27

FIGURE 3.1. PARTICLE FUNCTIONALIZATION. 41

FIGURE 3.2. REPRESENTATIVE GATING FOR WHOLE LUNG IDENTIFICATION OF APC POPULATIONS AND NP POSITIVE CELLS. 45

FIGURE 3.3. DETERMINING MRNA EXPRESSION. 47

FIGURE 3.4. BIODISTRIBUTION OF INSTILLED PARTICLES 47

FIGURE 3.5. REPRESENTATIVE IMMUNOHISTOCHEMISTRY OF NP-TREATED LUNGS AFTER 72 HRS. 49

FIGURE 3.6 NP ASSOCIATION IN LUNG APCS AT 72 HOURS. 49

FIGURE 3.7. IL-6 CYTOKINE ANALYSIS. 52

FIGURE 3.8 . IL-6 CYTOKINE ANALYSIS. 52

FIGURE 3.9. MRNA EXPRESSION IN LUNG HOMOGENATE. 54

FIGURE 3.10. APC POPULATIONS IN THE LUNG FOLLOWING NP TREATMENT. 55

FIGURE 3.11. CYTOKINE RESPONSE FOR PEG AND UNPEGYLATED PARTICLES. 56

FIGURE 3.12. FLOW CYTOMETRY ANALYSIS OF PEGYLATED AND UNPEGYLATED PARTICLE UPTAKE. 57

FIGURE 4.1 ACTIVITY OF EQBUCHE TAGGED WITH DYLIGHT680. 73

FIGURE 4.2. REPRESENTATIVE FLOW CYTOMETRIC ANALYSIS OF BALF CELLS. 74

FIGURE 4.3. BIODISTRIBUTION OF BUCHE.....77

FIGURE 4.4. ORGAN BIODISTRIBUTION OF BUCHE......78

FIGURE 4.5. BUCHE ACTIVITY CONFIRMATION......79

FIGURE 4.6. CYTOKINE RESPONSES FOLLOWING BUCHE ADMINISTRATION TO THE LUNG......80

FIGURE 4.7. SYSTEMIC CYTOKINE LEVELS......81

FIGURE 4.8. LEUKOCYTE POPULATION IN THE BALF FOLLOWING BUCHE ADMINISTRATION TO THE LUNG..82

FIGURE 4.9. ANDERSEN CASCADE IMPACTION (ACI)......83

FIGURE 4.10. BIODISTRIBUTION OF 1 μM BUCHE DRY POWDER PARTICLES......84

FIGURE 4.11. PRINT® BUCHE IN AQUEOUS ENVIRONMENT......85

LIST OF ABBREVIATIONS

ACI	Andersen Cascade Impactor
ACN	Acetonitrile
AEM	2-Aminoethylmethacrylate
AMs	Alveolar Macrophages
APCs	Antigen-Presenting Cells
BAL	Broncheoalveolar Lavage
BALF	Broncheoalveolar Lavage Fluid
BuChE	Butyrylcholinesterase
CF	Cystic Fibrosis
COPD	Chronic Obstructive Pulmonary Disease
DCs	Dendritic Cells
DPI	Dry Powder Inhaler
EDC	1-Ethyl-3-[3-Dimethylaminopropyl]Carbodiimide Hydrochloride
ELISA	Enzyme-Linked Immunosorbent Assay
FI	Total Fluorescence Intensity
FMO	Fluorescence- Minus One
FPF	Fine Particle Fraction
GSD	Geometric Standard Deviation
H&E	Hematoxylin And Eosin
HBSS	Hank's Buffered Saline Solution
HGF	Human Growth Factor
HPLC	High Performance Liquid Chromatography
HP4A	Tetra(ethylene glycol) monoacrylate
i.m.	Intramuscular
i.p.	Intraperitoneal
i.v.	Intravenous

IACUC	Institutional Animal Care and Use Committee
IVIS	*In Vivo* Imaging System
LN	Lymph Node
LPS	Lipopolysaccharide
MFO	Median Fluorescence Intensity
MHC	Major Histocompatibility Complex
MMAD	Mass Median Aerodynamic Diameter
NHS	N-hydroxysulfosuccinimide
NP	Nanoparticle
Nude	$Foxn1^{Nu/Nu}$
OP	Organophosphate
PEG	Poly(Ethylene Glycol)
PEG5k-SCM	PEG5k-Succinimidyl Carboxymethyl Ester
PET	Poly(ethylene Terephthalate
PLGA	Poly(lactic-co-glycolic-acid)
pMDIs	Pressured Metered Dose Inhalers
PRINT	Particle Replication in Non-Wetting Templates
PVOH	Polyvinyl Alcohol
qRT-PCR	Quantitative Real-Time Polymerase Chain Reaction
SEM	Scanning Electron Microscopy
TEM	Transmission Electron Microscopy
TGA	Thermal Gravimetric Analysis
TPO	Diphenyl(2,4,6-Trimethylbenzyol)Phosphine
UT	Untreated
ζ -	Anionic
ζ+	Cationic

CHAPTER 1. Introduction to Pulmonary Delivery of Therapeutics Using Nanotechnology

According to the Center for Disease Control and Prevention, pulmonary diseases are the third leading cause of death second to cancer and heart disease.[1] We must understand the implications of patient, clinician, and scientist interaction in order to advance current standard of care. In the realm of lung diseases patients struggle to sustain normal lives, while clinicians utilize every accessible therapeutic to help improve quality of life. Scientists have the power to create new approaches for existing therapeutic delivery that can provide more effective treatments and aid clinicians in improving patient care. Therefore, as scientists we must pursue collaboration with pulmonologists to fill in the gaps to provide cost-effective, patient-friendly, and efficacious therapies for treating lung diseases. Here we present the use of precision-engineered particles for delivery of therapeutics with hopes to improve the current pulmonary treatment options.

Pulmonary delivery of therapeutics faces many challenges in formulation and delivery. For example, one must avoid potential degradation of the therapeutic en route to the lungs as well as overcome the rapid clearance and absorption in the lung. Furthermore, the therapeutic must be formulated to maintain stability in the device being used, as well as demonstrate aerosol characteristics for the desired deposition. In this work, we provide an introduction to the many factors influencing design of an ideal nanotechnology and pulmonary treatment combination that results in therapeutic particles with increased efficacy, optimal aerosol characteristics, and convenient administration.

1.1 Lung Biology

The lung is a target organ for alternative delivery of therapeutics as it provides a large surface area for drug absorption, reduced drug-metabolizing enzyme content, and avoidance of the first pass metabolism, which all aid in delivering therapeutics for both local and systemic treatments.[2–4] The architecture of the lung starts at the trachea, progresses to the bronchi, branches out to the bronchioles and lastly ends at the alveoli, where it meets the epithelial lining and pulmonary capillaries. Between the trachea and the bronchioles there are 17 divisions, which allow for increased surface area, reduced airway size and decreased air velocity as they branch further to the alveoli.[5] The alveoli have a thin layer of fluid and mucus surrounding them that allows for proper gas exchange, but can also be useful for drug absorption.[6] The alveolar region of the deep lung is the ideal target for systemic drug exposure due to increased surface area, while the secondary bronchi make ideal targets for extended drug release in the lung.[5]

The main functions of the lungs are to transfer oxygen from the air to the blood and to release carbon dioxide from the blood to the air. Also, the lungs play a role in the body's defenses against harmful substances in the air, such as smoke, pollution, bacteria, or viruses. The multiple clearance mechanisms (mucociliary clearance, phagocytosis, and metabolic degradation) can prevent therapeutic delivery. Understanding lung deposition characteristics can guide aerosol design for avoidance of mucocilliary clearance in the upper airways and direct targeting of the deep lung. Design of particle parameters can impact interactions with the mucus layers, as some surface chemistries can lead to particle aggregation and rapid elimination from the lung, while other modifications can enhance residence time at the sites of absorption.[6] In addition, there is also intricate cellular involvement that is central in engineering targeted therapeutics. The lung contains antigen-presenting cells (APCs), which include dendritic cells

(DCs) and alveolar macrophages (AMs).[4,7–12] AMs tend to phagocyte foreign material including particles, especially those of 1-2 μm in size.[2] They are able to detect foreign material, engulf it, and secrete cytokine/chemokine signals to recruit immune cells like DCs.[13] DCs have been accepted as one of the most important antigen presenting cells due to their ability to take up the foreign material, recruit more DCs to the site, and then travel to the nearest lymph node to activate T cells and initiate an immune response. [7,11,12] Chapter 3 provides further detail on lung cells and the immune system.

1.2 Targeted Delivery to the Lungs

Due to the sophistication of the lung, the target will vary; a therapeutic particle may be needed in the lung space, in the AMs, or to recruit DCs. If the intricate lung structure and cellular mechanisms are understood, they can be utilized to aid in targeted delivery. In the case of COPD or asthma, the main goal is effective bronchodialation or anti inflammation in the lung without systemic exposure, which therefore requires a treatment targeting the bronchiole region.[9,1414,15] In these diseases, patients have reduced airflow due to the thickening of the bronchial walls and the increased mucus production, making it more important for use of precisely engineered particles that can bypass the upper lung region and maintain extended release in the deep lung. [5]

Being able to control targeting or de-targeting of AMs would harness using the lung's built-in mechanisms for enhanced treatments.[6] For example, targeting AMs in diseases like tuberculosis, a bacterial lung infection that affects about one-third of the world's population, would provide useful.[10] The AMs engulf this bacterium and send the proper signals to recruit DCs, but the bacteria continue to survive within the immune cells (primarily AMs). [10,16] Treatments for tuberculosis would benefit from a targeted use of anti-bacterial(s) in particles that would reside in AMs harboring the bacteria. On the other hand, de-targeting AMs is useful for

increasing drug bioavailability in the lungs, having slow therapeutic release, and for systemic delivery.[17] For example, in lung cancer it is important for the therapeutic particle to have long residence time in the lung and extended therapeutic release in order to deliver the chemotherapeutic to the tumor.[18] Therefore, in treating diseases like lung cancer, particles must be engineered to have the ideal parameters (composition, surface chemistry, size and shape) to avoid AM uptake and maintain residence time for long-term treatment.

In the development of pulmonary vaccines, the focus is on recruiting DCs that sample antigens and relay that information to the T cells via the lymph nodes as described earlier.[8] Typical parenteral vaccines require an adjuvant, which can amplify the immune reaction.[19] However, the ability of polymers to induce a sufficient immune response has been established.[19] Therefore, particles can be specifically engineered to have preferential association with DCs by readily incorporating antigens, maintaining antigen stability, and triggering desired immune responses without the need for an adjuvant. .[20] Currently, multiple nanoparticle based vaccines of different compositions have been approved for human use.[20] Delivery of therapeutics using nanoparticles has the potential to improve current approaches to treatments while improving drug accumulation at target sites and decreasing systemic toxicity where applicable.[21–23] Furthermore, particles with controlled aerosol properties will allow for direct deposition in the lungs to protect against respiratory diseases. Overall, understanding the anatomical and cellular complexity involved with the treatment of different lung diseases will aid in engineering better therapeutics.

1.3 Pulmonary Delivery Devices

In order to successfully utilize engineered particles for treating pulmonary diseases, we must first understand the delivery devices. Pulmonary drug delivery first dates back to the ancient Egyptians (1554 BC) with a steam based mist delivery, which has since evolved to be

nebulizers.[24] Nebulizers are mainly used on hospitalized intubated patients, or for delivery of large drug doses in liquid form.[25] They are bulky and typically take a long duration (10-20 minutes) for delivery of therapeutics, lending to potential drug degradation. In the early 1900s, pressured metered dose inhalers (pMDIs) were developed for propellant based liquid formulation delivery containing drug, propellant, and excipients in order to prevent drug aggregation and allow for dispersion of the heterogeneous droplets.[6] pMDIs quickly became popular due to their small size, reliability, and long shelf life.[3,14] However, optimal dosing is very dependent on coordination of patient breathing which may result in highly variable and limited deposition of the entire dose (i.e. only 20% reaches the alveoli).[3,5]

Lastly dry powder inhalers (DPIs) were developed for delivery of dry powders or solids with no propellants allowing for enhance therapeutic stability and increased patient compliance.[15] For example, cystic fibrosis (CF) patients, who typically receive lengthy anti-pseudomonal treatments via nebulizer multiple times a day, could benefit from a single, convenient DPI dose.[14] DPI use is dependent on formulating aerosols with optimal dispersion and deposition characteristics.[15] Despite the device employed to deliver a pulmonary therapeutic, the size, composition, and stability of the aerosol formulation are vital for efficient delivery to the lungs.

1.4 Particulate Delivery to the Lungs

Use of nanotechnology for parenteral drug delivery has been in the spotlight for decades, while recent advances have been made for its use in pulmonary delivery.[8] Pulmonary delivery of nano-based therapeutics allows for more active lung targeting by using new formulations of therapeutics commonly administered as soluble drug intravenously for direct lung delivery.

Furthermore, therapeutic particles can also allow for reducing multiple dose treatments to a single pulmonary dose and engineered to utilize or bypass the pulmonary defense mechanisms.

Characterizing a particle's aerodynamic size is an essential in determining the probability of effectively depositing in the lung and appropriately delivering therapeutics. The aerodynamic particle size is used to compare any particle to a standard sphere, which allows for a baseline characterization and serves as a predictor of aerosol deposition.[9] Particles greater than 10 µm will deposit in the mouth and trachea, 5 to 10 µm particles will deposit in the upper airways, and 1 to 5 µm particles deposit in the respiratory zone (bronchi and alveolar region).[2,8,15] Therefore, particles in the 1-5 µm size range are ideal for avoiding exhalation or upper airway deposition.[2,15] It is important to note that even though lung anatomy is different between humans and rodents, no significant impact on aerosol deposition characterization has been found.[26]

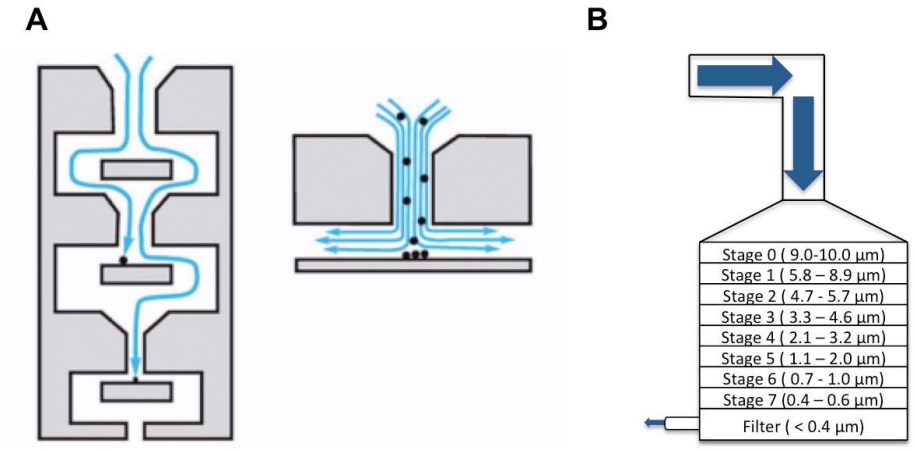

Figure 1.1 Andersen Cascade Impaction. Particles smaller than the cutoff diameter on each stage will deposit on lower stages. (A) Visualization of particles at a stage (adapted from Lewis *et al.* 2011. Pharm. Tech.)[27] (B) Associated cutoff diameters for particles at each stage.

Aerosol properties of particles are determined using an Andersen Cascade Impactor (ACI) with eight stages that correlate to human lung depostion.[28] ACI can provide insight on the mass median aerodynamic diameter (MMAD) of particles, predicting where it will deposit in a

human model and how it compares to other particles. Particle deposition within the ACI depends on the inertial momentum of the particles as they are pulled through the stages of collection plates containing openings with decreasing diameter via a vacuum. If the particle is smaller than the diameter of the holes within the collection plate, it will flow past the stage and impact on a lower stage.[29,30] The ACI setup allows for controlling flow rates and pressure drops to mimic the human model. Figure 1.1 shows the stages and relevant cut off diameters.

Several studies have been conducted to investigate the effect of particle size and deposition. Patton *et al.* summarized how monodisperse particles in different size ranges could deposit in different regions of the lung (Figure 1.2).[2] Weers *et al.* assessed particle deposition for single bolus administrations and confirmed that particle aerodynamic diameter impacts deposition, with 1 μm diameters primarily depositing in the alveoli and diameters of 5 μm in the conducting airways and alveoli.[14] Being able to control particle size, shape, and surface chemistry can lead to much needed targeted deposition and potentially controlled therapeutic release in the lungs.

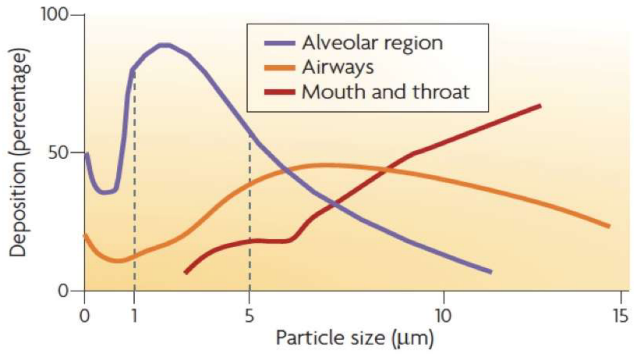

Figure 1.2. Particle Delivery to the Lungs. Larger monodisperse particles deposit in the airways, mouth or throat while smaller particles deposit in the alveolar region. (Figure taken from Patton *et al.* 2007. Nature Reviews.)[2]

1.5 Particle Fabrication Methods

There are numerous particle fabrication techniques that have been explored for pulmonary delivery. Particles must be able to encapsulate sufficient drug, maintain activity of cargo, and have aerosol characteristics optimal for deposition. One commonly used method is solvent evaporation with oil-in-water emulsifications for encapsulating soluble drugs, resulting in mostly polydisperse particles with limited drug loading and mass production capabilities.[31] Another technique, spray drying, is a scalable process and consists of drug-loaded microspheres that are exposed to a heated air jet, with various solvents, temperatures, and evaporation steps, resulting in a dry powder.[31] Spray-dried particles are suitable dry powder formulations, however, the fabrication process limits control of particle shape and size, resulting in polydisperse particles, which can therefore lack the aerosol dispersion properties needed for targeted pulmonary delivery.[31] A recent breakthrough in pulmonary delivery of particles was the 2015 FDA approval of Afrezza, one of the earliest inhaled macromolecules for systemic delivery. Afreeza is made up of insulin microspheres that were freeze dried for dry powder delivery with an average diameter of 2-3 μm.[15] It provided a faster onset of action and higher bioavailability compared to other pulmonary insulin formulations.[15] Ultimately, the fabrication method chosen is dependent on the desired application of the particles.

Considering existing particle fabrication techniques, there is still a need for fabricating monodisperse particles with controllable parameters. Many different compositions (natural and synthetic polymers, liposomes, gold, etc.) can be used with the varying fabrication techniques to address this concern.[8] However, the majority of current fabrication techniques are specific to

certain compositions and therefore, the properties of the particles are limited. Monodisperse particles enable more controlled deposition and uniformity in cargo loading, controlled release and delivery efficiencies.[32] Furthermore, monodisperse particles allow for a systematic investigation of particle parameters that can contribute to optimal aerosol characteristics in pulmonary delivery. The best approach would be to utilize a fabrication method that is amenable to different compositions and can form monodisperse particles with the benefits of high loading and optimal deposition characteristics in order to increase the therapeutic efficacy.

1.6 Fabrication of Monodisperse Particles: PRINT Technology

Particle Replication in Non-wetting Templates (PRINT®) technology allows for precise control of an unlimited array of size, shape, and surface chemistry options.[33–36] PRINT® is a top-down particle fabrication technology that allows the engineering of precisely defined particles. Utilizing phtotolithography techniques, micro- and nano- patterns are etched into a master template, which is used to make perfluoropolyether molds.[33] The mold is filled with the chosen pre-particle composition via capillary forces, followed by a heated lamination to a high surface energy material. Solidification of the materials in the mold is done by vitrification, crystallization, or gelation dependent on the pre-particle composition used. An immediate peeling away of the laminated layer allows for the removal of any excess filing, resulting in monodisperse micro- or nano- particles.[35] An adhesive layer is used to remove the particles from the mold. Then the adhesive is dissolved away resulting in a suspension of monodisperse particles.[37] Particles can then be purified, lyophilized or modified as needed. Figure 1.3 illustrates the general fabrication process used for all particles presented in this dissertation.

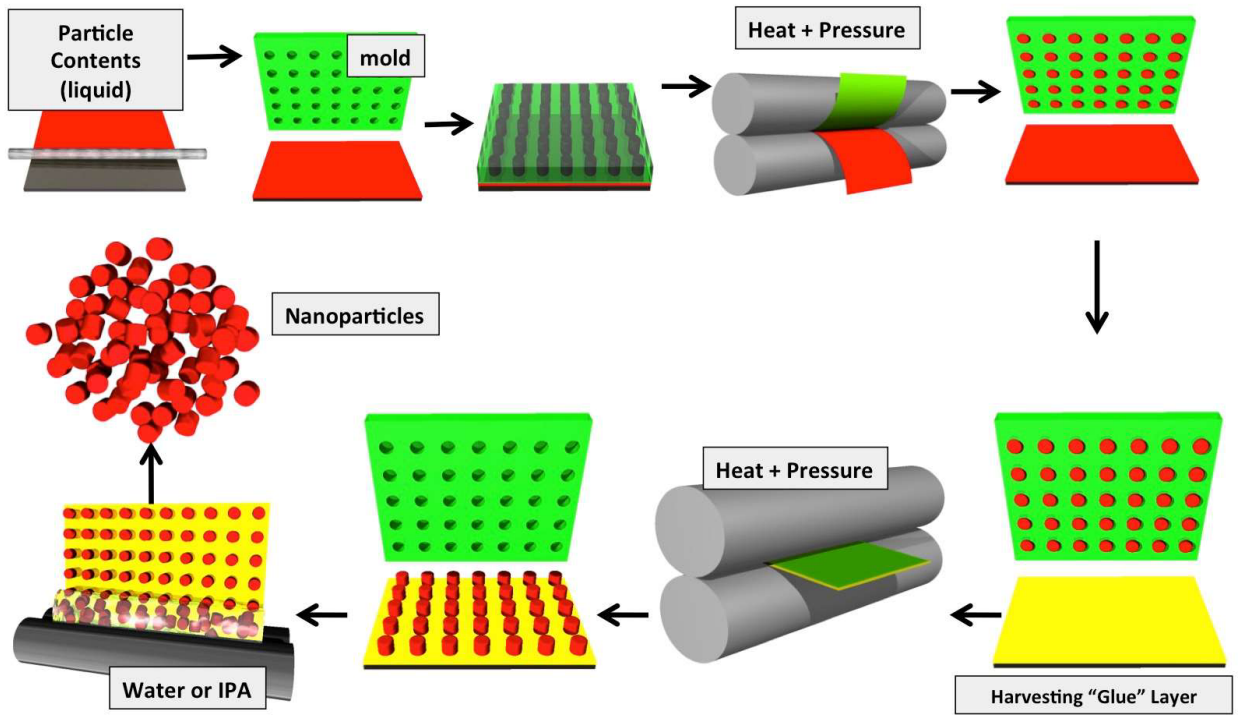

Figure 1.3. PRINT® Fabrication Process. A thin film of the therapeutic/polymer or respective composition is drawn across a poly(ethylene terephthalate)(PET) delivery sheet (red), applied to the face of the mold (green), and then passed through a heated nip. The particles are removed from the mold by attaching a polyvinyl alcohol (PVOH) adhesive harvesting layer (yellow) and passing the pair through the nip. The harvesting layer is split from the mold and then dissolved in water or isopropanol alcohol creating an aqueous suspension of monodisperse particles.

The PRINT process was also scaled up for a more continuous fabrication in the 'roll to roll' set up, which is accessible at the DeSimone lab and at Liquidia Technologies. The 'roll to roll' allows for mass production of particles for potential use in larger pre-clinical and clinical trials. PRINT particles of varying sizes and shapes have been fabricated using biocompatible compositions, such as poly(D-lactic acid), poly(lactic-co-glycolic-acid) (PLGA), and poly(ethylene glycol) (PEG), with the ability to encapsulate various cargo such as imaging contrast agents, dyes, therapeutics like doxorubicin and paclitaxel, and biologics.[32–34,36–41]

1.7 Thesis Overview

In this thesis we focus on engineering particles of different parameters (composition, size, shape and surface chemistry) for use with pulmonary delivery. We hypothesize that utilizing PRINT to precisely and independently control particle parameters will provide an understanding of each parameter's effect on the route of administration and therapeutic application. We predict engineering particles for use with DPI can provide high delivery efficiencies with high drug loading. We specifically investigate the role of particle composition, surface chemistry, and delivery of biologics to the lung. In Chapter 2, we discuss fabrication of particles using different compositions (PLGA, Hydrogel PEG, and Butyrylcholinesterase) and the impact on route of administration. Previous work, using PRINT, has shown cationic particles result in an adjuvant-like effect after pulmonary delivery[39], however, the cellular mechanism involved with this observation has not yet been investigated. Therefore, in Chapter 3, we systematically examine the effect surface chemistry and functionalization of hydrogel particles has on interactions with the lung, specifically at the cellular level. In Chapter 4, we introduce our unique ability to fabricate an entirely active biologic particle with optimal aerosol characteristics for pulmonary delivery. Nanomolding of protein (insulin and albumin) particles has been previously explored with PRINT [34], but in Chapter 4 we aim to address the lacking *in vivo* studies, particle activity analysis, and therapeutic pulmonary application. And lastly, in Chapter 5 we discuss the future outlook for PRINT particles in pulmonary delivery.

REFERENCES

(1) Xu, J.; Murphy, S. L.; Kochanek, K. D.; Bastian, B. A. National Vital Statistics Reports Deaths : Final Data for 2009. *Natl. Cent. Heal. Stat.* **2012**, *60* (3), 1–117.

(2) Patton, J. S.; Byron, P. R. Inhaling Medicines: Delivering Drugs to the Body through the Lungs. *Nat. Rev. Drug Discov.* **2007**, *6* (January), 67–74.

(3) Keller, M. Innovations and Perspectives of Metered Dose Inhalers in Pulmonary Drug Delivery. *Int. J. Pharm.* **1999**, *186* (1), 81–90.

(4) Azarmi, S.; Roa, W. H.; Löbenberg, R. Targeted Delivery of Nanoparticles for the Treatment of Lung Diseases. *Adv. Drug Deliv. Rev.* **2008**, *60* (8), 863–875.

(5) O'Donnell, K. P.; Smyth, H. D. C. Macro- and Microstructure of the Airways for Drug Delivery. In *Controlled Pulmonary Drug Delivery*; Smyth, H. D. C., Hickey, A. J., Eds.; Springer: New York, 2011; pp 1–20.

(6) El-sherbiny, I. M.; El-baz, N. M.; Yacoub, M. H. Review Article Inhaled Nano- and Microparticles for Drug Delivery. **2015**, 1–14.

(7) Moon, J. J.; Irvine, D. J.; Huang, B. Engineering Nano- and Micro- Particles to Tune Immunity. *Adv Mater.* **2012**, *24* (28), 3724–3746.

(8) Kunda, N. K.; Somavarapu, S.; Gordon, S. B.; Hutcheon, G. A.; Saleem, I. Y. Nanocarriers Targeting Dendritic Cells for Pulmonary Vaccine Delivery. *Pharm. Res.* **2013**, *30* (2), 325–341.

(9) Sakagami, M. In Vivo, in Vitro and Ex Vivo Models to Assess Pulmonary Absorption and Disposition of Inhaled Therapeutics for Systemic Delivery. *Adv. Drug Deliv. Rev.* **2006**, *58* (9-10), 1030–1060.

(10) Guilliams, M.; Lambrecht, B. N.; Hammad, H. Division of Labor between Lung Dendritic Cells and Macrophages in the Defense against Pulmonary Infections. *Mucosal Immunol.* **2013**, *6* (3), 464–473.

(11) Hassan, M.; Lau, R. Effect of Particle Shape on Dry Particle Inhalation: Study of Flowability, Aerosolization, and Deposition Properties. *AAPS PharmSciTech* **2009**, *10*, 1252–1262.

(12) Kleinstreuer, C.; Zhang, Z.; Li, Z.; Roberts, W.; Rojas, C. A New Methodology for Targeting Drug-Aerosols in the Human Respiratory System. *Int. J. Heat Mass Transf.* **2008**, *51*, 5578–5589.

(13) Roberts, R. a.; Shen, T.; Allen, I. C.; Hasan, W.; DeSimone, J. M.; Ting, J. P. Y. Analysis of the Murine Immune Response to Pulmonary Delivery of Precisely Fabricated Nano- and Microscale Particles. *PLoS One* **2013**, *8* (4).

(14) Weers, J. G.; Bell, J.; Chan, H.-K.; Cipolla, D.; Dunbar, C.; Hickey, A. J.; Smith, I. J. Pulmonary Formulations: What Remains to Be Done? *J. Aerosol Med. Pulm. Drug Deliv.* **2010**, *23 Suppl 2*, S5–S23.

(15) Yang, M. Y.; Chan, J. G. Y.; Chan, H. K. Pulmonary Drug Delivery by Powder Aerosols. *J. Control. Release* **2014**, *193*, 228–240.

(16) Sharma, R.; Saxena, D.; Dwivedi, A. K.; Misra, A. Inhalable Microparticles Containing Drug Combinations to Target Alveolar Macrophages for Treatment of Pulmonary Tuberculosis. *Pharm. Res.* **2001**, *18* (10), 1405–1410.

(17) Edwards, D. A. Large Porous Particles for Pulmonary Drug Delivery. *Science (80-.).* **1997**, *276* (5320), 1868–1872.

(18) Kim, I.; Byeon, H. J.; Kim, T. H.; Lee, E. S.; Oh, K. T.; Shin, B. S.; Lee, K. C.; Youn, Y. S. Doxorubicin-Loaded Highly Porous Large PLGA Microparticles as a Sustained-Release Inhalation System for the Treatment of Metastatic Lung Cancer. *Biomaterials* **2012**, *33* (22), 5574–5583.

(19) Pulliam, B.; Sung, J. C.; Edwards, D. a. Design of Nanoparticle-Based Dry Powder Pulmonary Vaccines. *Expert Opin. Drug Deliv.* **2007**, *4* (6), 651–663.

(20) Zhao, L.; Seth, A.; Wibowo, N.; Zhao, C. X.; Mitter, N.; Yu, C.; Middelberg, A. P. J. Nanoparticle Vaccines. *Vaccine* **2014**, *32* (3), 327–337.

(21) Maeda, H.; Bharate, G. Y.; Daruwalla, J. Polymeric Drugs for Efficient Tumor-Targeted Drug Delivery Based on EPR-Effect. *Eur. J. Pharm. Biopharm.* **2009**, *71* (3), 409–419.

(22) Maeda, H.; Sawa, T.; Konno, T. Mechanism of Tumor-Targeted Delivery of Macromolecular Drugs, Including the EPR Effect in Solid Tumor and Clinical Overview of the Prototype Polymeric Drug SMANCS. *J. Control. Release* **2001**, *74* (1-3), 47–61.

(23) Maeda, H.; Wu, J.; Sawa, T.; Matsumura, Y.; Hori, K. Tumor Vascular Permeability and the EPR Effect in Macromolecular Therapeutics: A Review. *J. Control. Release* **2000**, *65* (1-2), 271–284.

(24) Sanders, M. Pulmonary Drug Delivery: An Historical Overview. In *Controlled Pulmonary Drug Delivery*; Smyth, H. D. C., Hickey, A. J., Eds.; Springer: New York, 2011; pp 51–73.

(25) Hertel, S. P.; Winter, G.; Friess, W. Protein Stability in Pulmonary Drug Delivery via Nebulization. *Adv. Drug Deliv. Rev.* **2014**, *93*, 79–94.

(26) Fernandes, C. A.; Vanbever, R. Preclinical models for pulmonary drug delivery http://www.uclouvain.be/cps/ucl/doc/farg/documents/FernandesVanbeverEODD2009.pdf (accessed Mar 16, 2015).

(27) Lewis, D.; Copley, M. Inhaled Product Characterization Calculating Particle-Size

Distribution Metrics. *Pharm. Technol.* **2011**, 33–37.

(28) van Oort M, D. B. Cascade Impaction of Mdis and Dpis: Induction Port, Inlect Cone, and Preseparator Lid Designs Recommended for Inclusion in the General Test Chapter Aerosols. *Pharmacopeial Forum* **1996**, *22*, 2204–2210.

(29) Perry, J.; Reuter, K.; Kai, M. P.; Herlihy, K.; Jones, S.; Luft, J. C.; Napier, M. E.; Bear, J. E.; Desimone, J. M. Pegylated Print Nanoparticles: The Impact of Peg Density on Protein Binding, Macrophage Association, Biodistribution, and Pharmacokinetics. *Nano Lett.* **2012**, *12*, 5304–5310.

(30) Mitchell, J. P.; Nagel, M. W. Cascade Impactors for the Size Characterization of Aerosols from Medical Inhalers: Their Uses and Limitations. *J. Aerosol Med.* **2003**, *16* (4), 341–377.

(31) Makadia, H.; Siegel, S. Poly Lactic-Co-Glycolic Acid (PLGA) as Biodegradable Controlled Drug Delivery Carrier. *Polymers (Basel).* **2011**, *3* (3), 1377–1397.

(32) Fromen, C. A.; Shen, T. W.; Larus, A. E.; Mack, P.; Maynor, B. W.; Luft, J. C.; DeSimone, J. M. Synthesis and Characterization of Monodisperse Uniformly Shaped Respirable Aerosols. *Am. Inst. Chem. Eng.* **2013**, *0* (00), 405–410.

(33) Rolland, J. P.; Maynor, B. W.; Euliss, L. E.; Exner, A. E.; Denison, G. M.; DeSimone, J. M. Direct Fabrication and Harvesting of Monodisperse, Shape-Specific Nanobiomaterials. *J. Am. Chem. Soc.* **2005**, *127* (28), 10096–10100.

(34) Kelly, J. Y.; DeSimone, J. M. Shape-Specific, Monodisperse Nano-Molding of Protein Particles. *J. Am. Chem. Soc.* **2008**, *130* (16), 5438–5439.

(35) Merkel, T. J.; Herlihy, K. P.; Nunes, J.; Orgel, R. M.; Rolland, J. P.; DeSimone, J. M. Scalable,Shape-specific,Top-down Fabrication Methods for the Synthesis of Engineered Colloidal Particles. *Langmuir* **2010**, *26* (16), 13086–13096.

(36) Euliss, L. E.; DuPont, J. A.; Gratton, S.; DeSimone, J. Imparting Size, Shape, and Composition Control of Materials for Nanomedicine. *Chem. Soc. Rev.* **2006**, *35* (11), 1095–1104.

(37) Garcia, A.; Mack, P.; Williams, S.; Fromen, C.; Shen, T.; Tully, J.; Pillai, J.; Kuehl, P.; Napier, M.; DeSimone, J. M.; Maynor, B. W. Microfabricated Engineered Particle Systems for Respiratory Drug Delivery and Other Pharmaceutical Applications. *J. Drug Deliv.* **2012**, *2012*, 1–10.

(38) Shen, T. W.; Fromen, C. A.; Kai, M. P.; Luft, J. C.; Rahhal, T. B.; Robbins, G. R.; DeSimone, J. M. Distribution and Cellular Uptake of PEGylated Polymeric Particles in the Lung Towards Cell-Specific Targeted Delivery. *Pharm. Res.* **2015**.

(39) Fromen, C. A.; Robbins, G. R.; Shen, T. W.; Kai, M. P.; Ting, J. P. Y. Controlled Analysis of Nanoparticle Charge on Mucosal and Systemic Antibody Responses

Following Pulmonary Immunization. *Proc. Natl. Acad. Sci. U. S. A.* **2015**, *112* (2), 488–493.

(40) Kai, M. P.; Keeler, A. W.; Perry, J. L.; Reuter, K. G.; Luft, J. C.; O'Neal, S. K.; Zamboni, W. C.; Desimone, J. M. Evaluation of Drug Loading, Pharmacokinetic Behavior, and Toxicity of a Cisplatin-Containing Hydrogel Nanoparticle. *J. Control. Release* **2015**, *204*, 70–77.

(41) Reuter, K. G.; Perry, J. L.; Kim, D.; Luft, J. C.; Liu, R.; DeSimone, J. M. Targeted PRINT Hydrogels: The Role of Nanoparticle Size and Ligand Density on Cell Association, Biodistribution, and Tumor Accumulation. *Nano Lett.* **2015**, *15* (10), 6371–6378.

CHAPTER 2. PRINT® Particles of Controlled Composition for the Lung [1]

2.1 Introduction

Therapeutics are commonly administered in soluble form via parenteral routes for direct systemic exposure. Recently, advances in nanotechnology have set the stage for delivery of drugs, proteins, vaccines, and many more therapeutics using particle carriers to treat numerous diseases.[1] Particles provide the potential for extended drug half-life, reduced toxicity, improved efficacy and increased selectivity.[2–4] Furthermore, the amenability of particle compositions provides an open door for innovating new effective treatments for multiple applications and routes of administration. We are specifically interested in how this applies to lung diseases.

Current treatment of pulmonary diseases relies on systemic administration of particles for passive lung targeting. Numerous studies have been conducted to show increased drug

---

[1] This chapter includes work previously published in the following:

Gharpure KM, Chu KS, Bowerman CJ, Miyake T, Pradeep S, Mangala SL, Han HD, Rupaimoole R, Armaiz-Pena GN, Rahhal TB, Wu SY, Luft JC, Napier ME, Lopez-Berestein G, DeSimone JM, Sood AK. Metronomic Docetaxel in PRINT Nanoparticles and EZH2 Silencing Have Synergistic Antitumor Effect in Ovarian Cancer. Mol Cancer Ther. 2014 Jul;13(7):1750-7. doi: 10.1158/1535-7163.MCT-13-0930. Epub 2014 Apr 22. PubMed PMID: 24755199. Cover Feature

Fromen CA, Rahhal TB, Shen TW, Robbins GR, Kai MP, Luft JC, Ting JP, DeSimone JM. Nanoparticle Surface Charge Impacts Distribution, Uptake [1] and Lymph Node Trafficking by Pulmonary Antigen-Presenting Cells. Nanomedicine: Nanotechnology, Biology, and Medicine. Dec. 2015. Cover Feature. http://dx.doi.org/10.1016/j.nano.2015.11.002

Shen TW, Fromen CA, Kai MP, Luft JC, Rahhal TB, Robbins GR, DeSimone JM. Distribution and Cellular Uptake of PEGylated Polymeric Particles in the Lung Towards Cell-Specific Targeted Delivery. Pharmacetucial Research. April 2015. doi: 10.1007/s11095-015-1701-7

Rahhal TB, Fromen CA, Wilson E, Kai MP, Shen TW, Luft JC, DeSimone JM. Pulmonary Delivery of Butyrylcholinesterase as a Model Protein to the Lung. Molecular Pharmaceutics. March 2016.

concentrations in the lung post-intravenous administration, however more recent work, has shown no significant difference between nanoparticle and free drugs in the lung with parenteral administration.[5–7] This is not to say that there have not been a few nanoparticles (NPs) developed that have been more successful then the free drug counterpart in lung accumulation post-intravenous administration.[5,8–10] For example, the well-known Abraxane, an albumin based placitaxel NP formulation, was successfully administered intravenously for treating non-small cell lung cancer. Despite Abraxane showing promising results for tumor reduction, it is hypothesized that due to the rapid particle dissolving the NP design may be aiding in initial administration and circulation versus actual lung targeting ability.[5,11] Overall, systemic delivery of therapeutics for lung targeting is limited by enzymatic degradation in the liver, shorter half-life, exposure to healthy tissue and low efficacy.[12]

An alternative approach to IV administration is the direct administration of NPs to the target organ. In the lung, this involves inhaled drug development. However, the limiting factor is that current particle design lacks a fine control on shape and size to obtain ideal aerosol and deposition characteristics while maintaining high loading and drug efficacy post formulation. [5,12,13] Current lung diseases like asthma, chronic obstructive pulmonary disease (COPD), cystic fibrosis (CF), lung edema, lung transplant rejection, infections and many more can benefit from targeted treatments delivered to the lungs directly.[14–17] Developing particles for this purpose using different compositions, shapes, and sizes would be advantageous.

The existing array of compositions for particle fabrication provides unique advantages and customization for the therapeutic need or target. NP formulations range from liposomal to polymer-based with the ability to incorporate drugs, ligands, coatings, and more for therapeutic use. Polymeric particles are used due to their biocompatibility and ability to tune release of

drugs. Poly(lactic-co-glycolic-acid) (PLGA) compositions have been a "stalwart" due to the ability to control degradation based on the polymeric ratio of the two main components, as well as the efficient clearance from the body upon degradation.[7,18] Another commonly used composition is hydrogels, which provide high biocompatibility and biodegradability.[13] Various cargos have been incorporated into hydrogels including chemotherapy, antibodies, and antibiotics.[19–21] Importantly, surface properties provided by different compositions can be further varied through use of targeting ligands or PEG stealthing chemistries. Determining the ideal particle composition is dependent on fabrication method, target site, and desired physiological outcome.

A third composition of interest is biologics. Pulmonary delivery of biologics via particle carriers has been explored and still has many challenges. As mentioned, delivery of biologics for pulmonary diseases is mainly limited to parenteral routes of administration that have high systemic exposure and potential toxicity, lack active targeting, and are burdensome to patients.[14,22] Biologics are susceptible to protein degradation and loss of activity during fabrication. It is hypothesized that using particle carriers for pulmonary administration of biologics would allow for higher dosing efficiency, targeted delivery, stable formulations, and increased patient compliance.[22] This is dependent on having a platform for developing particles suitable for pulmonary delivery that can maintain the protein activity as well as be delivered in a more convenient manner. For example, CF patients have long needed an effective delivery of DNase to aid in breaking down the sputum build up in the lungs. Recently Pulmozyme® was approved as a nebulized protein for CF, but it presents problems including the lack of convenience, the bulky nature of the device, long delivery times, susceptibility to protein degradation and lack of enzyme stability.[23–25] Given the complicated interplay between the NP

composition and the biological outcome, employing a platform that allows for exquisite control over engineering particle parameters is required to address unmet needs.

We propose to combine the ability to engineer optimal particles with the interchangeability of compositions (dependent on the desired goal) for treatment via any route of administration. In this chapter we highlight, characterize, and discuss how particle parameters dictate biodistribution, particle/cargo activity, stability, and release kinetics. Additionally, these data provide direction, identify opportunities, and incorporate analytics to expand particle compositions for novel therapeutic applications in pulmonary delivery. We focused on three particle compositions: PLGA, hydrogel and Butyrylcholinesterase (BuChE) using Particle Replication in Non-wetting Templates (PRINT) technology for the production of particles of uniform size and shape within the desired respirable range (1-5 μm).

2.2 Methods

2.2.1 Fabrication of PRINT PLGA Nanoparticles

Cylindrical PLGA NPs of [d] = 80 nm; [h] = 320 nm were fabricated using PRINT, as discussed in Chapter 1. Briefly, Poly (D,L- lactide- co-glycolide) (Sigma Aldrich lactide:glycolide (85:15)) at 20 mg/ml was dissolved in chloroform (Fisher Scientific) and 150 μl was used to create a thin film using a #5 Myer Rod (R.D. Specialties) on a polyethylene terephthalate (PET) sheet. The solvent was evaporated with heat and a 80x320 mold (Liquidia Technologies) was used to fabricate the particles as discussed earlier (Figure 1.3). Particle size and polydispersity index was determined using dynamic light scattering (Malvern Instruments Nano-ZS) and imaged via scanning electron microscopy (SEM) (Hitachi S- 4700 Cold Cathode Field Emission Scanning Electron Microscope). NPs were pipetted (50 μl) onto a glass slide, allowed to dry, and then coated with a 3nm thick gold palladium alloy using a Cressington 108

auto-sputter coater before imaging. NPs were also imaged via transmission electron microscopy (TEM) (JEOL 100 CX II).

2.2.2 Assessing Stability of PRINT PLGA Nanoparticles

80 x 320 nm PLGA NPs were mixed with plasma at a 1:1 ratio with phosphate buffered saline and shaken at 37°C. At set time points, NPs were removed and washed with water 20 times by tangential flow filtration to remove plasma proteins (mPES hollow fiber filter with 0.05 μm pore size, Spectrum Labs). To determine any changes at each time point the particles were then collected on a filter and qualitatively analyzed using SEM and TEM.

2.2.3 Release kinetics for PRINT PLGA: Docetaxel Nanoparticles

To assess release kinetics for determination of future efficacy, cylinders of [d] = 55 nm; [h] = 70 nm were fabricated. Cylinders were fabricated via PRINT continuous production using a 'roll to roll' instrument, as described earlier, with a modified particle composition of 50:50 PLGA(85:15) and Docetaxel. Particles were washed two times in sterile water and aliquoted onto glass slides for SEM imaging.

Particle composition was determined using standard high performance liquid chromatography (HPLC) methods.[26] A C18 reverse phase column (Agilent Technology series 1200) was used with a linear gradient of 100% water to 100% acetonitrile for 10 minutes followed by a 100% acetonitrile 5 minute run at 1 ml/min and 205 nm detection wavelength. Samples and standards for both PLGA and docetaxel were prepared in acetonitrile (ACN).

To determine release of docetaxel *in vitro*, a 1 L phosphate buffered saline (1x) bath was prepared at 37C, with 100 μl of NP solution loaded into a dialysis cassette (20k MW cutoff) placed in the bath. At each timepoint, NP solution was collected and centrifuged. 300 μl of ACN was added to each pellet, vortexed, and placed on shaker for 30 minutes. Samples were then

centrifuged and supernatant was placed in HPLC vials for analysis. This allowed for determining the amount of docetaxel released compared to the initial amount of docetaxel present in the system.[26]

2.2.4 Fabrication and Characterization of PRINT Hydrogel Particles

Hydrogel particles are fabricated via PRINT as described in Chapter 1 following established protocols.[27,28] Briefly, a solution of dissolved monomers is prepared in methanol. Solvents and buffers of reagent grade were obtained by Fisher Scientific. PRINT molds were provided by Liquidia Technologies. Pre-particle reagents of 2-aminoethylmethacrylate (AEM), poly(ethylene glycol)$_{700}$ diacrylate (Mn-700 DA, PEG$_{700}$DA) and diphenyl(2,4,6-trimethylbenzoyl)phosphine oxide (TPO) were obtained from Sigma; tetra(ethylene glycol) monoacrylate (HP$_4$A) was synthesized in house via previously described methods.[29] Fluorescent dye maleimide-Dylight 650 was obtained from Fisher. Coupling reagents for the carboiimide conjugation of 1-ethyl-3-[3-dimethylaminopropyl]carbodiimide hydrochloride (EDC) and N-hydroxysulfosuccinimide (s-NHS) were obtained from Thermo Fisher.

The monomers combined in the pre-particles solution include: HP$_4$A, a hydrophilic monomer, AEM, an amine containing monomer to provide functionality for further modifications, and TPO, a photoinitiator. Fluorescent dye was included as needed. After a film is drawn, the filled mold, in this case 80 x 320 nm, undergoes an additional step to the traditional PRINT method; it is placed in a UV curing chamber (λ= 365 nm) to allow for crosslinking of the monomers. Then the particles were harvested and sputter-coated with 1-5 nm of Au/Pd (Cressington Scientific Instruments) and imaged with Scanning Electron Microscopy (Hitachi model S-4700) to monitor NP morphology. NP size and zeta potential were measured by

dynamic light scattering (Zetasizer Nano ZS, Malvern Instruments, Ltd.) and thermogravimetric analysis (TGA) (Q5000, TA Instruments) was used to determine NP concentrations.

2.2.5 Fabrication and Characterization of PRINT BuChE Particles

Tetrameric Equine Butyrylcholinesterase (referred to as BuChE in this thesis) (ID#C7512) was purchased from Sigma Aldrich and used directly with no further purification. 1 μm BuChE protein particles were fabricated via a PRINT method adapted from Xu *et al.*[30] α-D-Lactose and glycerol were purchased from Acros. Briefly, a 15% (w/v) solution of 37.5% BuChE, 37.5% α-D-Lactose and 25% glycerol by weight was used to cast a film on a PET sheet. Following heat gun application, the transparent film was laminated onto PRINT mold with 1 μm disc features (provided by Liquidia Technologies). The top-heated laminator was set to 73 °C with a laminating pressure of 100 psi. Particles were then removed from the filled mold by a second lamination step at the same settings onto a Plasdone™ covered PET sheet. The Plasdone film containing particles was then dissolved in isopropanol to obtain 1 μm BuChE particles. The BuChE particles were washed with isopropanol multiple times to remove α-D-Lactose, glycerol, and residual Plasdone resulting in a primarily protein particle. The particles were further characterized via TGA (TA Q5000) for concentration and SEM (using a 2 nm thick gold palladium alloy coating) (Hitachi model S-4700) for size and shape confirmation.

Particle enzymatic cholinesterase activity was measured using a colorimetric butyrylthiocholine-based assay described below to confirm protein content and accurate dosing. The particle composition was determined via HPLC , based on previously published protocols.[30] Briefly, a known concentration of particles was dispersed in water, then, BuChE was filtered out (Amicon Ultra, 0.5 ml , MWCO 30k). The filtrate (containing glycerol and lactose) was analyzed using HPLC and the concentrate was measured to confirm BuChE concentration. A Hi-plex Ca

column (Agilent, 300 x 7.7 mm, 8 μm) was used with a mobile phase of pure water over 35 minutes with a flow rate of 0.6 mL/min with an evaporative light scattering detector at 30C. Area under the curve was measured for a Lactose peak at 9.3 minutes and a glycerol peak at 16.3 minutes to determine particle composition using a lactose and glycerol standard curve.

2.2.6 Enzyme Activity Assay for PRINT BuChE Particles

Total cholinesterase levels were measured, with an increase in levels attributed to dosed BuChE, therefore, BuChE activity was considered anything above the established baseline. VITROS CHE DT Slides for cholinesterase detection were used for all sample analysis with the VITROS Chemistry Products DT Specialty Calibrator kit per the standard operating protocol. The assay involves cholinesterase hydrolyzing butyrylthiocholine to thiocholine, which reduces the potassium ferricyanide to potassium ferrocyanide. Reference spectrophotometry was then used to monitor the rate of color loss. The UNC-Chapel Hill Animal Clinical Chemistry Core performed the assay.

2.3 Results

2.3.1 Particle Fabrication.

PLGA particles of [d] = 80 nm; [h] = 320 nm were fabricated and imaged via SEM (Figure 2.1A). Hydrogel particles of [d] = 80 nm; [h] = 320 nm were fabricated and imaged via SEM (Figure 2.1B). Hydrogel (ζ+) NP characterization showed a Z-Average diameter = 273 $\pm$ 10 nm and polydispersity index of 0.06 $\pm$ 0.02, with a charge of 45 $\pm$ 3 mV. Particles made of our model biologic, BuChE, were fabricated using [d] = 1 μm; [h] = 1 μm mold and imaged via SEM in Figure 2.1C.

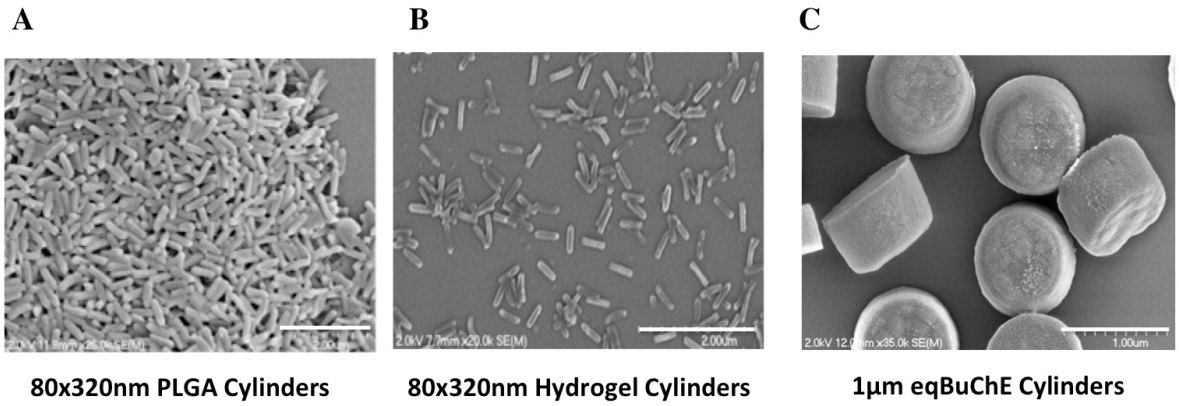

Figure 2.1 Varied compositions of PRINT particles of uniform size and shape. Representative Scanning Electron Microscopy Images of (A) PLGA Cylinders (d=80 nm ; h=320 nm) (Scale bar: 2 µm) (B) Hydrogel Cylinders (d=80 nm ; h=320 nm) (Scale bar: 2 µm) (C) eqBuChE Cylinders (d=1 µm; h= 1 µm) (Scale bar: 1 µm)

2.3.2 PLGA Particle Stability.

Understanding particle stability prior to loading therapeutics is important for accurate drug delivery. NP characterization showed a Z-Average diameter = 235.9 $\pm$ 3.20 nm and polydispersity index of 0.061 $\pm$ 0.002 in plasma at day 0 for the 80x320 nm PLGA particles. Figure 2.2 shows SEM and TEM images initially at day 0. PLGA NPs can be seen to maintain size and shape over three days (Figure 2.2A). However, by the end of the week, the particles swell in size, suggesting uptake of water and ultimately degradation (Figure 2.2B).

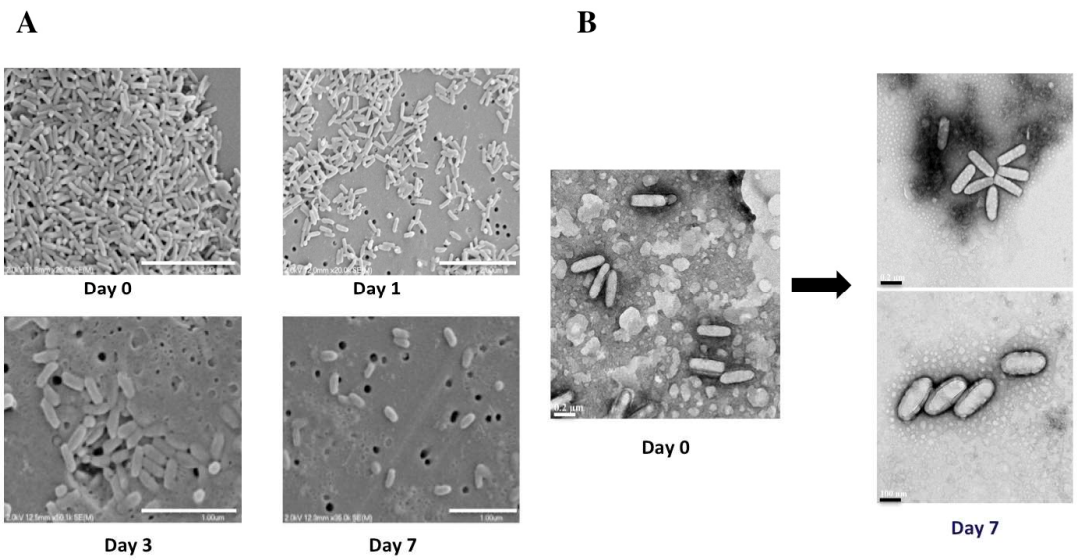

Figure 2.2. Stability of PLGA-PRINT Particles. (A) SEM images of particles over time in plasma (Scale Bars: Day 0 and 1= 2.00 µm, Day 3 and 7= 1.00 µm) (B) TEM images of particles over time in plasma (Scale Bars: Day 0 = 0.2 µm, Day 7 Top = 0.2 µm, Day 7 Bottom =100nm).

2.3.3 Particle Release Kinetics.

For release kinetics, particles characterization resulted in a Z-Average diameter of 115 $\pm$ 0.6 nm and polydispersity index of 0.128 $\pm$ 0.02 as imaged in Figure 2.3A. HPLC analysis confirmed particles were loaded with our model therapeutic, docetaxel, at 56%, with 38% release of docetaxel by 24 hours (Figure 2.3B).

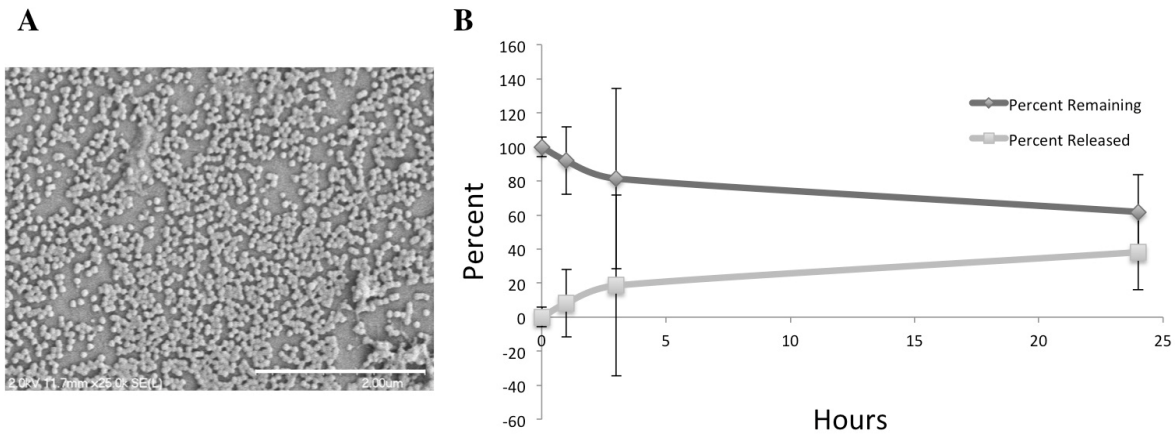

Figure 2.3 . PLGA:Docetaxel Nanoparticle Fabrication and Release Kinetics. (A) SEM image of [d] = 55 nm; [h] = 70 nm PLGA:Docetaxel particles(scale bar 2.0 μm) (B) Docetaxel Release from PLGA:Docetaxel nanoparticles over 24 hours (n=3/timepoint).

2.3.4 BuChE Particle Characterization.

We fabricated cylindrical PRINT particles with a diameter of 1 μm and a height 1 μm (Figure 2.1C). It was important to confirm protein activity of the particles throughout processing. Therefore, we evaluated two assays, the VITROS assay discussed in the methods, and a BuChE specific assay, DetectX (Arbor Assays, K1016-F1) to identify the most robust method to quantify BuChE activity. We found comparable findings to our VITROS assay; yet, the VITROS system provided results in a more accurate, consistent and time/cost effective manner. Assay consistency and BuChE stability was confirmed as shown in Figure 2.4. Importantly, protein activity, crucial for therapeutic use, was maintained throughout processing (Figure 2.5A). Following fabrication, the particle composition was determined via HPLC, establishing the majority of the particles were composed of BuChE, with lactose and glycerol removed during the post-fabrication processing (Figure 2.5B). Particles made of higher activity BuChE exhibited similar compositions shown in Figure 2.5C.

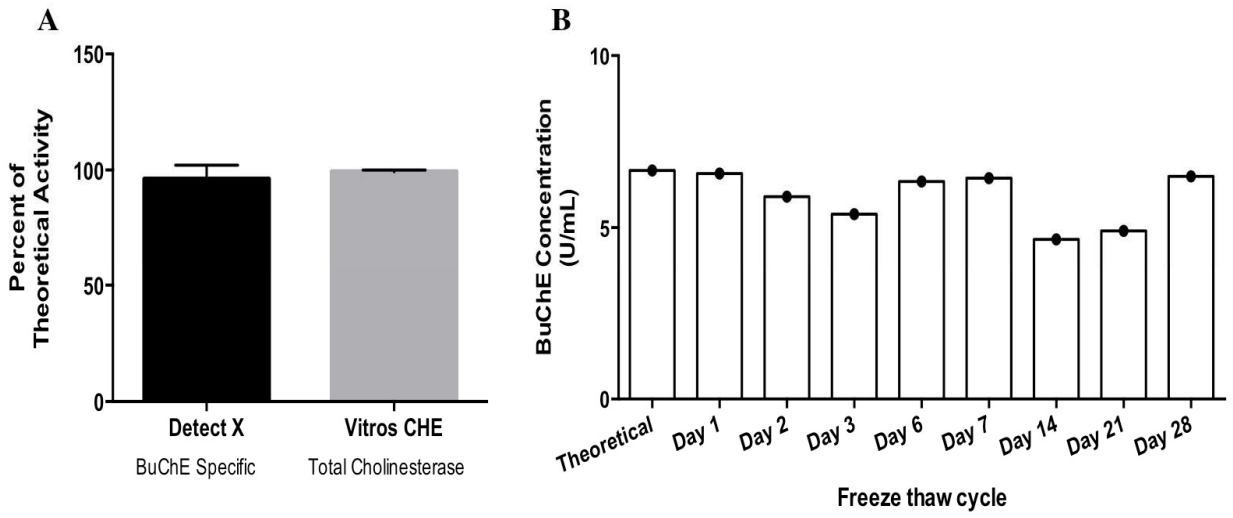

Figure 2.4. BuChE Activity Detection. Known BuChE concentrations were tested in each assay and BuChE detection ability of two assays with a representative sample of n=5, DetectX, a BuChE specific assay versus Vitros ChE , a total cholinesterase detection assay was plotted (A). Validation of BuChE activity with repeated freeze-thaw cycles utilizing VITROS ChE assay was also graphed (B). BuChE used in all studies had a maximum of 7 freeze thaw cycles. Vitros ChE assay was used in this paper after thorough assessment of both assay options.

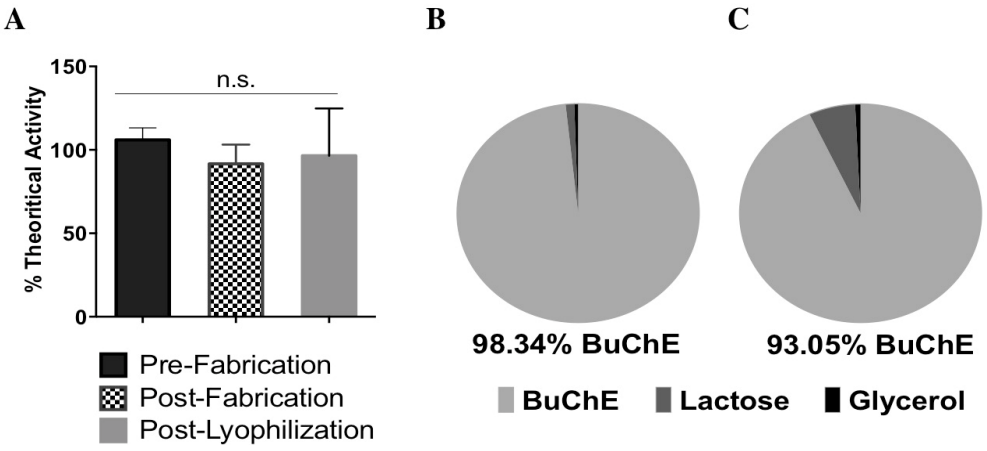

Figure 2.5. Characterization of PRINT BuChE Particles. (A) Representative BuChE activity maintained throughout fabrication process (n.s., not significant; two-way ANOVA with Tukey's multiple comparisons test). Composition of particles as determined by high performance liquid chromatography for (B) eqBuChE (50 U/mg) (6 independent batches) and (C) eqBuChE (331 U/mg) with lactose and glycerol plasticizers.

2.4 Discussion

Employing PRINT particle technology, we investigated the use of three particle compositions with potential clinical application for particle-based therapeutic delivery. In this work, we used and characterized a biocompatible polymer (PLGA), a modifiable monomer composition (hydrogel), and a model biologic (BuChE) for particle fabrication. Current particle production platforms lack the ability to have precise control over particle shape, size, surface chemistry, and drug release rates.[20,31] We utilized PRINT technology to address concerns of translating therapeutics to multiple parenteral and non-parenteral routes of administration. We demonstrated the ability to improve drug-loading efficiency, provide targeted delivery, reduce systemic toxicity, and use different compositions in mono-disperse particles with promising aerosol characteristics for direct pulmonary delivery.

PLGA is a common biodegradable and FDA approved polymer used in particle fabrication.[17] PRINT PLGA particles have been used for parenteral treatments and we predict they would be idea for non-parenteral routes as well. Key considerations for effective treatments are NP stability, therapeutic loading, and release kinetics. Determining the long-term fate of the carrier is important to toxicity because most therapy, like chemotherapy, requires repeat dosing. Additionally, this is important because many drug delivery systems use high molecular weight polymers to provide sustained drug release. We sought to determine the *ex vivo* degradation time and stability of PRINT PLGA particles by assessing change in cylindrical NPs of [d] = 80 nm; [h] = 320 nm in a blood plasma environment, over the time span of one week. Results demonstrated that our PRINT PLGA particles are stable for 3 days and begin to swell at one week, indicating potential for controlled release therapy, therefore supporting rationale to continue advancing these particles.[32]

Drug loading has been a challenge in many nanotechnology platforms. We utilized a common chemotherapeutic, docetaxel, for incorporation into our particles. Docetxael has toxic systemic side effects due to the high dosing and limited reach to the target site.[7] We used PLGA:Docetaxel particles for investigating effects on ovarian cancer showing an approximate 80% reduction in tumor weight after three intraperitoneal injections a week.[32] Furthermore, our lab has shown intravenous administration of these particles had higher plasma exposure and tumor accumulation, as well as reduced clearance as compared to only Taxotere, a soluble docetaxel, treatment.[26] Our PRINT particle loading is higher than typical docetaxel loaded particles, which average at 10%.[26,33–35] Previous work in our lab established that the 80x320 nm particles, loaded with 33.5% docetaxel, release nearly 100% by 24 hours, while 200x200 nm particles, loaded with 45.2% docetaxel, release 70% by 24 hours. In comparison, the 55x70 nm particles presented here were loaded with 56% docetaxel and had 38% release by 24 hours. This shows promising ability for controlled drug release and enhanced residence times. Investigating this ability for high therapeutic loading and differentiated efficacy based on particle size provides promising groundwork for pulmonary delivery of our NPs.

Hydrogel particles are routinely used as parenteral oral therapeutics for pulmonary diseases due to the lack of controlling particle parameters that dictate targeting ability.[19] Common inhaled hydrogel formulations are rapidly cleared by alveolar macrophages, lack specific targeting, and have limited aerosolization.[31] Current work with swellable hydrogels for pulmonary delivery has become popular to evade macrophage uptake and maintain good aerosol characteristics. These particles vary in size from 1-5 μm prior to administration and then swell once in the airways.[15,19–21,36,37] However, swellable hydrogel particles face the same challenges of limited drug loading and non-uniform shape and size, all of which are important for optimal

pulmonary delivery.[20,21] Using hydrogels with the PRINT platform can revolutionize pulmonary administration because these factors are easily controlled allowing hydrogel particles to be further customized with an array of surface chemistry modifications and drug loading potential for pulmonary delivery. [15,27,38] We are able to load therapeutics, add targeting ligands, and surface coatings, as well as fabricate various shapes.[27,28,38,39] We have confirmed (unpublished) that PRINT particle shape can impact alveolar macrophage affinity for uptake. Being able to modify our hydrogel particles is promising for vaccine development, which relies on cellular initiation of immune responses. This can be triggered or avoided with varying surface chemistries ranging from particle charge to surface coatings, as will be discussed in Chapter 3.

Currently, administration of biologics faces many challenges including maintaining activity of the proteins so that they can be therapeutic upon delivery, having a high loading in the particles to be effective, and demonstrating good aerosol characteristics for targeted deposition.[40,41] Employing PRINT, we were able to fabricate protein particles using BuChE, a nonspecific cholinesterase enzyme that has demonstrated to function as a prophylactic countermeasure against organophosphate nerve agents [42–44], while maintaining activity in these uniform size and shape particles. BuChE particles would be ideal for protection of the lungs against organophosphate poisoning since inhalation is the primary route of exposure, as well as for patients with pseudocholinesterase deficiency.[45–48] We demonstrated that PRINT BuChE particles have maintained activity, as well as the ability to have uniform size that is crucial for targeted deposition into the lungs, which will be further discussed in Chapter 4. PRINT particles can also be lyophilized to form dry powder particles for use in a convenient dry powder inhaler (DPI). DPI provides the advantages of particle and protein stability that is lacking in nebulizer

treatments.[49] Demonstrating our ability to work with biologics for effective pulmonary delivery opens doors for numerous clinical applications with other biologics.

Therapeutically loaded NPs of different compositions are needed for treatment of lung cancer, COPD, CF and many more pulmonary diseases.[14–17] However, pulmonary delivery faces many challenges including the need for controlled release therapeutic formulations to address for diseases like COPD and asthma that require multiple doses per day and would benefit from a single convenient dose allowing for extended drug release.[22] If pulmonary treatment options can be developed to include particles with high drug loading, higher drug delivery efficiency, and extended drug release patients could potentially experience less severe side effects and improved therapy compliance. We have demonstrated that PRINT can be used for fabrication of multiple compositions with ideal particle features (size, shape, loading, stability etc.). Our PLGA formulation has shown good stability, drug loading and release kinetics, while the hydrogel particles can be effectively customized depending on the desired therapeutic need.[27] And lastly our biologic-based NPs allow for an array of clinical use. Overall, our work shows the feasibility of loading different therapeutics to target the various pulmonary diseases.

REFERENCES

(1) Casettari, L.; Castagnino, E.; Stolnik, S.; Lewis, A.; Howdle, S. M.; Illum, L. Surface Characterisation of Bioadhesive PLGA/chitosan Microparticles Produced by Supercritical Fluid Technology. *Pharm. Res.* **2011**, *28* (7), 1668–1682.

(2) Maeda, H.; Bharate, G. Y.; Daruwalla, J. Polymeric Drugs for Efficient Tumor-Targeted Drug Delivery Based on EPR-Effect. *Eur. J. Pharm. Biopharm.* **2009**, *71* (3), 409–419.

(3) Maeda, H.; Sawa, T.; Konno, T. Mechanism of Tumor-Targeted Delivery of Macromolecular Drugs, Including the EPR Effect in Solid Tumor and Clinical Overview of the Prototype Polymeric Drug SMANCS. *J. Control. Release* **2001**, *74* (1-3), 47–61.

(4) Maeda, H.; Wu, J.; Sawa, T.; Matsumura, Y.; Hori, K. Tumor Vascular Permeability and the EPR Effect in Macromolecular Therapeutics: A Review. *J. Control. Release* **2000**, *65* (1-2), 271–284.

(5) Azarmi, S.; Roa, W. H.; Löbenberg, R. Targeted Delivery of Nanoparticles for the Treatment of Lung Diseases. *Adv. Drug Deliv. Rev.* **2008**, *60* (8), 863–875.

(6) Rolland, A.; Collet, B.; Le Verge, R.; Toujas, L. Blood Clearance and Organ Distribution of Intravenously Administered Polymethacrylic Nanoparticles in Mice. *J. Pharm. Sci.* **1989**, *78* (6), 481–484.

(7) Wang, H.; Xu, Y.; Zhou, X. Docetaxel-Loaded Chitosan Microspheres as a Lung Targeted Drug Delivery System: In Vitro and in Vivo Evaluation. *Int. J. Mol. Sci.* **2014**, *15* (3), 3519–3532.

(8) Zara, G. P.; Cavalli, R.; Fundarò, A.; Bargoni, A.; Caputo, O.; M.R. Gasco. Pharmacokinetics of Doxorubicin Incorporated in Solid Lipid Nanospheres (SLN),. *Pharmacol. Res.* **1999**, *40* (3), 281–286.

(9) Santhi, K.; Dhanaraj, S. A.; Koshy, M.; Ponnusankar, S.; Suresh, B. Study of Biodistribution of Methotrexate-Loaded Bovine Serum Albumin Nanospheres in Mice,. *Drug Dev. Ind. Pharm.* **2000**, *26* (12), 1293–1296.

(10) Löbenberg, R.; Araujo, L.; Briesen, H. Von; Rodgers, E.; J. Kreuter. Body Distribution of Azidothymidine Bound to Hexyl-Cyanoacrylate Nanoparticles after I.v. Injection to Rats,. *J. Control. Release* **1998**, *50* (1-3), 21–30.

(11) Green, M. R.; Manikhas, G. M.; Orlov, S.; Afanasyev, B.; Makhson, A. M.; Bhar, P.; M.J. Hawkins. Abraxane®, a Novel Cremophor®-Free, Albumin- Bound Particle Form of Paclitaxel for the Treatment of Advanced Non-Small- Cell Lung Cancer. *Ann. Oncol.* **2006**, *17* (8), 1263–1268.

(12) Kuzmov, A.; Minko, T. Nanotechnology Approaches for Inhalation Treatment of Lung Diseases. *J. Control. Release* **2015**, *219*, 500–518.

(13) Mahmud, A.; Discher, D. E. Lung Vascular Targeting through Inhalation Delivery: Insight from Filamentous Viruses and Other Shapes. *IUBMB Life* **2011**, *63* (8), 607–612.

(14) Kim, I.; Byeon, H. J.; Kim, T. H.; Lee, E. S.; Oh, K. T.; Shin, B. S.; Lee, K. C.; Youn, Y. S. Doxorubicin-Loaded Highly Porous Large PLGA Microparticles as a Sustained-Release Inhalation System for the Treatment of Metastatic Lung Cancer. *Biomaterials* **2012**, *33* (22), 5574–5583.

(15) El-Sherbiny, I. M.; Smyth, H. D. C. Controlled Release Pulmonary Administration of Curcumin Using Swellable Biocompatible Microparticles. *Mol. Pharm.* **2012**, *9*, 269–280.

(16) Roy, I.; Vij, N. Nano-Delivery in Airway Diseases: Challenges and Therapeutic Applications. *Nanomedicine* **2010**, *6* (2), 237–244.

(17) Makadia, H.; Siegel, S. Poly Lactic-Co-Glycolic Acid (PLGA) as Biodegradable Controlled Drug Delivery Carrier. *Polymers (Basel).* **2011**, *3* (3), 1377–1397.

(18) Pulliam, B.; Sung, J. C.; Edwards, D. a. Design of Nanoparticle-Based Dry Powder Pulmonary Vaccines. *Expert Opin. Drug Deliv.* **2007**, *4* (6), 651–663.

(19) Du, J.; Du, P.; Smyth, H. Hydrogels for Controlled Pulmonary Delivery. *Ther. Deliv.* **2013**, 1293–1305.

(20) Selvam, P.; El-Sherbiny, I. M.; Smyth, H. D. C. Swellable Hydrogel Particles for Controlled Release Pulmonary Administration Using Propellant-Driven Metered Dose Inhalers. *J. Aerosol Med. Pulm. Drug Deliv.* **2011**, *24* (1), 25–34.

(21) Du, J.; El-Sherbiny, I. M.; Smyth, H. D. Swellable Ciprofloxacin-Loaded Nano-in-Micro Hydrogel Particles for Local Lung Drug Delivery. *AAPS PharmSciTech* **2014**, *15* (6), 1535–1544.

(22) Weers, J. G.; Bell, J.; Chan, H.-K.; Cipolla, D.; Dunbar, C.; Hickey, A. J.; Smith, I. J. Pulmonary Formulations: What Remains to Be Done? *J. Aerosol Med. Pulm. Drug Deliv.* **2010**, *23 Suppl 2*, S5–S23.

(23) Hertel, S. P.; Winter, G.; Friess, W. Protein Stability in Pulmonary Drug Delivery via Nebulization. *Adv. Drug Deliv. Rev.* **2014**, *93*, 79–94.

(24) Pressler, T. Review of Recombinant Human Deoxyribonuclease (rhDNase) in the Management of Patients with Cystic Fibrosis. *Biologics* **2008**, *2* (4), 611–617.

(25) Sung, J. C.; Padilla, D. J.; Garcia-Contreras, L.; Verberkmoes, J. L.; Durbin, D.; Peloquin, C. A.; Elbert, K. J.; Hickey, A. J.; Edwards, D. A. Formulation and Pharmacokinetics of Self-Assembled Rifampicin Nanoparticle Systems for Pulmonary Delivery. *Pharm. Res.* **2009**, *26* (8), 1847–1855.

(26) Chu, K. S.; Hasasn, W.; Rawal, S.; Walsh, M. D.; Enlow, E. M.; Luft, J. C.; Bridges, A. S.; Kuijer, J. L.; Napier, M. E.; Zamboni, W. C.; DeSimone, J. M. Plasma, Tumor and

Tissue Pharmacokinetics of Docetaxel Delivered via Nanoparticles of Different Sizes and Shapes in Mice Bearing SKOV-3 Human Ovarian Carcinoma Xenograft. *Nanomedicine* **2013**, *9* (5).

(27) Shen, T. W.; Fromen, C. A.; Kai, M. P.; Luft, J. C.; Rahhal, T. B.; Robbins, G. R.; DeSimone, J. M. Distribution and Cellular Uptake of PEGylated Polymeric Particles in the Lung Towards Cell-Specific Targeted Delivery. *Pharm. Res.* **2015**.

(28) Perry, J.; Reuter, K.; Kai, M. P.; Herlihy, K.; Jones, S.; Luft, J. C.; Napier, M. E.; Bear, J. E.; Desimone, J. M. Pegylated Print Nanoparticles: The Impact of Peg Density on Protein Binding, Macrophage Association, Biodistribution, and Pharmacokinetics. *Nano Lett.* **2012**, *12*, 5304–5310.

(29) Guzman, J.; Iglesias, M.; Riande, E. Synthesis and Polymerization of Acrylic Monomers with Hydrophilic Long Side Groups. *Polymers (Basel).* **1997**, *38*, 5227–5232.

(30) Xu, J.; Wang, J.; Luft, J. C.; Tian, S.; Owens, G.; Pandya, A. a.; Berglund, P.; Pohlhaus, P.; Maynor, B. W.; Smith, J.; Hubby, B.; Napier, M. E.; Desimone, J. M. Rendering Protein-Based Particles Transiently Insoluble for Therapeutic Applications. *J. Am. Chem. Soc.* **2012**, *134*, 8774–8777.

(31) Wanakule, P.; Liu, G. W.; Fleury, A. T.; Roy, K. Nano-inside-Micro: Disease-Responsive Microgels with Encapsulated Nanoparticles for Intracellular Drug Delivery to the Deep Lung. *J. Control. Release* **2012**, *162* (2), 429–437.

(32) Gharpure, K. M.; Chu, K. S.; Bowerman, C. J.; Miyake, T.; Pradeep, S.; Mangala, S. L.; Han, H.-D.; Rupaimoole, R.; Armaiz-Pena, G. N.; Rahhal, T. B.; Wu, S. Y.; Luft, J. C.; Napier, M. E.; Lopez-Berestein, G.; DeSimone, J. M.; Sood, A. K. Metronomic Docetaxel in PRINT Nanoparticles and EZH2 Silencing Have Synergistic Antitumor Effect in Ovarian Cancer. *Mol. Cancer Ther.* **2014**, *13* (7), 1750–1757.

(33) Dong, X.; Mattingly, C. A.; Tseng, M. T.; Cho, M. J.; Liu, Y.; Val, R.; Mumper, R. J. Doxorubicin and Paclitaxel-Loaded Lipid-Based Nanoparticles Overcome Multi-Drug Resistance by Inhibiting P-Gp and Depleting ATP. *Cancer Res.* **2009**, *69* (9), 3918–3926.

(34) Chenga, J.; Teplya, B. A.; Sherifia, I.; Sunga, J.; Luthera, G.; Gua, F. X.; Levy-Nissenbauma, E.; Radovic-Morenob, A. F.; Robert Langera, b, c, and O. C. F. Formulation of Functionalized PLGA-PEG Nanoparticles for In Vivo Targeted Drug Delivery. *Biomaterials* **2007**, *28* (5), 869–876.

(35) Hrkach, J.; Von Hoff, D.; Ali, M. M.; Andrianova, E.; Auer, J.; Campbell, T.; De Witt, D.; Figa, M.; Figueiredo, M.; Horhota, A.; Low, S.; McDonnell, K.; Peeke, E.; Retnarajan, B.; Sabnis, A.; Schnipper, E.; Song, J. J.; Song, Y. H.; Summa, J.; Tompsett, D.; Troiano, G.; Van Geen Hoven, T.; Wright, J.; LoRusso, P.; Kantoff, P. W.; Bander, N. H.; Sweeney, C.; Farokhzad, O. C.; Langer, R.; Zale, S. Preclinical Development and Clinical Translation of a PSMA-Targeted Docetaxel Nanoparticle with a Differentiated Pharmacological Profile. *Sci. Transl. Med.* **2012**, *4* (128), 128ra39–ra128ra39.

(36) EL-SHERBINY, I. M.; MCGILL, S.; SMYTH, H. D. C. Swellable Microparticles as Carriers for Sustained Pulmonary Drug Delivery. *J. Pharm. Sci.* **2009**, *99* (5), 2343–2356.

(37) El-sherbiny, I. M.; El-baz, N. M.; Yacoub, M. H. Review Article Inhaled Nano- and Microparticles for Drug Delivery. **2015**, 1–14.

(38) Reuter, K. G.; Perry, J. L.; Kim, D.; Luft, J. C.; Liu, R.; DeSimone, J. M. Targeted PRINT Hydrogels: The Role of Nanoparticle Size and Ligand Density on Cell Association, Biodistribution, and Tumor Accumulation. *Nano Lett.* **2015**, *15* (10), 6371–6378.

(39) Kai, M. P.; Keeler, A. W.; Perry, J. L.; Reuter, K. G.; Luft, J. C.; O'Neal, S. K.; Zamboni, W. C.; Desimone, J. M. Evaluation of Drug Loading, Pharmacokinetic Behavior, and Toxicity of a Cisplatin-Containing Hydrogel Nanoparticle. *J. Control. Release* **2015**, *204*, 70–77.

(40) Mansour, H. M.; Rhee, Y. S.; Wu, X. Nanomedicine in Pulmonary Delivery. *Int. J. Nanomedicine* **2009**, *4*, 299–319.

(41) Garcia, A.; Mack, P.; Williams, S.; Fromen, C.; Shen, T.; Tully, J.; Pillai, J.; Kuehl, P.; Napier, M.; DeSimone, J. M.; Maynor, B. W. Microfabricated Engineered Particle Systems for Respiratory Drug Delivery and Other Pharmaceutical Applications. *J. Drug Deliv.* **2012**, *2012*, 1–10.

(42) Bajgar, J.; Bartošova, L.; Fusek, J.; Jun, D.; Kuča, K. Equine Butyrylcholinesterase Protects Rats against Inhalation Exposure to Sublethal Sarin Concentrations. *Arh. Hig. Rada Toksikol.* **2006**, *57* (4), 391–395.

(43) Mumford, H.; E Price, M.; Lenz, D. E.; Cerasoli, D. M. Post-Exposure Therapy with Human Butyrylcholinesterase Following Percutaneous VX Challenge in Guinea Pigs. *Clin. Toxicol. (Phila).* **2011**, *49* (4), 287–297.

(44) Graham, J. R.; Wright, B. S.; Rezk, P. E.; Gordon, R. K.; Sciuto, A. M.; Nambiar, M. P. Butyrylcholinesterase in Guinea Pig Lung Lavage: A Novel Biomarker to Assess Lung Injury Following Inhalation Exposure to Nerve Agent VX. *Inhal. Toxicol.* **2006**, *18* (7), 493–500.

(45) Darvesh, S.; Hopkins, D. a; Geula, C. Neurobiology of Butyrylcholinesterase. *Nat. Rev. Neurosci.* **2003**, *4* (February), 131–138.

(46) Soliday, F. K.; Conley, Y. P.; Henker, R. Pseudocholinesterase Deficiency : A Comprehensive Review of Genetic, Acquired, and Drug Influences. *AANA* **2010**, *78* (4), 313–320.

(47) Doctor, B. P.; Saxena, A. Bioscavengers for the Protection of Humans against Organophosphate Toxicity. *Chem. Biol. Interact.* **2005**, *157-158*, 167–171.

(48) Alexander, D. R. Pseudocholinesterase Deficiency. *Medscape*; WebMD, 2015.

(49) Shoyele, S. A.; Slowey, A. Prospects of Formulating Proteins/peptides as Aerosols for Pulmonary Drug Delivery. *Int. J. Pharm.* **2006**, *314* (1), 1–8.

CHAPTER 3. Nanoparticle Surface Chemistry Impacts Distribution and Uptake by Pulmonary Antigen-Presenting Cells[2]

3.1 Introduction

Respiratory drug delivery can target local lung diseases such as asthma, COPD, or lung cancer and can also deliver therapeutics systemically, including delivery of insulin for diabetes management, or antigens for vaccination.[1–4] Controlling particle parameters would be advantageous for achieving optimal aerosol characteristics and targeted deposition. [4–8] Engineered particles can be designed such that aerosol properties, lung deposition, and cellular interactions are independently taken into consideration.[4,9–11] While there is extensive literature describing how physical particle properties can influence aerodynamic diameter and thus pulmonary deposition, there is minimal understanding of how these same particle properties influence interactions with lung cells and their subsequent immune responses.[4,11] This chapter will discuss the effect of PRINT particle parameters on residence time, cellular interactions, and immune responses in the lungs.

---

[2] This work was previously published in :

Fromen CA, Rahhal TB, Shen TW, Robbins GR, Kai MP, Luft JC, Ting JP, DeSimone JM. Nanoparticle Surface Charge Impacts Distribution, Uptake and Lymph Node Trafficking by Pulmonary Antigen-Presenting Cells. Nanomedicine: Nanotechnology,Biology, and Medicine. Dec. 2015. Cover Feature. http://dx.doi.org/10.1016/j.nano.2015.11.002

Shen TW, Fromen CA, Kai MP, Luft JC, Rahhal TB, Robbins GR, DeSimone JM. Distribution and Cellular Uptake of PEGylated Polymeric Particles in the Lung Towards Cell-Specific Targeted Delivery. Pharmacetucial Research. April 2015. doi: 10.1007/s11095-015-1701-7

We hypothesize that modifying particle surface chemistry will impact pulmonary cell uptake and can be useful for optimizing inhaled therapeutics (particulate vaccines, cell-specific targeted delivery and extended release of therapeutics). Nanoparticles (NPs) have been explored as pulmonary vaccine carriers, due to their ability to diffuse through mucosa, target or de-target alveolar macrophages (AM), and co-deliver both adjuvants and antigens.[3,12–17] Amongst the numerous cell types present in the lung, of particular interest are antigen presenting cells (APCs), which comprise B cells, dendritic cells (DC) and macrophages.[1,12,15,18–21] AMs, the main phagocytic cell in the lung, roam the airway epithelium, where they are responsible for internalizing, sequestering, and digesting any foreign material.[16,19,22,23] While they are generally considered APCs, their main function in the lung is more maintenance and clearance, rather than initiating adaptive responses.[19,22,23] Due to the nature of AMs they end up harboring disease targets, such as infectious bacteria like tuberculosis.[24] Targeting AMs with therapeutic NPs would be beneficial for various disease treatments.

In contrast, lung DCs are considered "professional" APCs and act as a sentinel in the lung; monitoring and sampling foreign material to elicit adaptive immune responses.[12,20,21] Lung DCs are responsible for internalizing foreign particulates, digesting and presenting antigen by major histocompatibility complex (MHC) II, migrating to lymph nodes (LNs), and educating T cells.[1,19–21,25–28] In the lung, there are two conventional myeloid-derived DC subsets, CD11b and CD103 DCs, which have distinct functions.[19,20,29] CD103 DCs protrude through the lung epithelium, are considered the main migratory population, and have been implicated in skewing the lung towards Th1, Th2 and Th17 responses given different stimuli.[16,19,20,27–31] While CD11b DCs can also migrate to the LNs, they have been shown to prime IgA production in the lung and are the major producers of soluble protein mediators, chemokines, and cytokines.[16,18,20,26,30,31]

These cells are found predominately under the basement membrane in the conducting airways.[19] Understanding which particle parameters DC prefer to take up may be advantageous for vaccine applications or immunomodulation therapies.[12,13,19,27,32,33] NP strategies capable of preferentially targeting either AMs or these DCs subtype are expected to result in superior responses for disease treatments or vaccination, respectively.

To date, the role of NP charge on lung APC association remains poorly understood, as the majority of vaccination studies have focused on anionic NP carriers.[13,34] These formulations follow design principles of pathogen mimicry, as the majority of both bacteria and viruses have surfaces with acidic isoelectric points.[35,36] However, recent work from our group has demonstrated that pulmonary vaccination with cationic NPs can enhance local and systemic antibody production to a model antigen, as compared to otherwise equivalent anionic NPs.[10] While these results indicate that NP charge is a key variable to immune responses in the lung, the underlying cellular mechanisms responsible for this deviation in immune response remain unclear. Understanding these lung processes is critical in the ultimate identification of NP design features capable of producing an optimized, controlled immune response.

Furthermore, there is a growing interest in studying precisely engineered drug carriers for local and systemic delivery to the lung.[10,37,38] Drug carriers can take advantage of the ease of access, large absorptive surface area, and reduced enzymatic activity, but must circumvent the lung's highly efficient particle clearance mechanisms in order to successfully deliver their payload.[39–41] Surface coating NPs with poly(ethylene glycol) [PEG] has been studied extensively for intravenous administration of drug carriers. This surface modification increases the particle's surface hydrophillicity and subsequently minimizes protein opsonization thereby limiting cellular uptake and extending circulation times.[28–31] Given the overwhelming evidence that

PEGylation inhibits macrophage uptake in IV applications, PEGylation has also been investigated in the context of pulmonary drug delivery.[17] PEGylation has been successfully used to extend the half-life of antibodies, small molecule drugs, and other proteins in the lung.[42–45] Various particles (liposomes, polymeric micelles, and dendrimers) containing PEG in their formulation have been evaluated for pulmonary delivery.[10,17,42,46–49] Finally, PEG coatings have also been studied in the lung in the context of mucocilliary transport, as a high density PEG coating can promote mucus penetration of nano- and micro- particles in the lung[50,51] Despite this extensive history of utilizing PEG to enhance pulmonary drug/particle delivery, there has been surprisingly limited work done to explore the *in vivo* cellular fate and inflammatory response to PEG-modified micro- and nano-particles.

As such, the goal of this work is to understand the cellular lung mechanisms involved in the processing of cationic and anionic NPs, as well as PEGylated NPs. As seen in previous work, we hypothesize that increased antibody production is the result of increased association of cationic NPs with lung DC subtypes, as well as a slight adjuvant effect of the charge associated with the NP itself.[10] We also hypothesize that an additional PEG surface coating with anionic NPs could extend residence time. To further elucidate the role of NP surface parameters on cellular activity in the lung, we utilized the Particle Replication In Non-wetting Templates (PRINT) technique to fabricate hydrogel-based NPs of identical size and shape that varied only in surface charge or in surface chemistry. We investigated the role of NP charge and PEGylation, respectively, on uptake by APCs, cytokine and chemokine recruitment, and subsequent residence times in order to identify key cellular mechanisms involved in lung NP immune responses for pulmonary delivery of therapeutics.

3.2 Methods

3.2.1 Animals

All studies were conducted in accordance with National Institutes of Health guidelines for the care and use of laboratory animals and approved by the Institutional Animal Care and Use Committee (IACUC) at UNC. C57BL/6 (Jackson Laboratories) were maintained in pathogen-free facilities at UNC and used between 8-15 wks.

3.2.2 Particle Fabrication, Functionalization and Characterization

Hydrogel particles were fabricated as described in Chapter 2. Briefly, amine-containing 80 nm x 320 nm hydrogel rod-shaped (ζ+)NP were fabricated with a continuous roll-to-roll PRINT method. Pre-particle solutions contained 1% TPO (photoinitiator), 20% AEM (functional groups), 10% $PEG_{700}DA$ (crosslinker), 0-2% functional fluorescent dye (maleimide-Dylight 650, Fisher), 68-9% HP_4A (monomer) by weight. For (ζ-)NPs , (ζ+)NPs in DMF were incubated with 100 M excess succinic anhydride for 30 minutes, washed first with borate buffer pH 9.5 and then three additional washes in water.

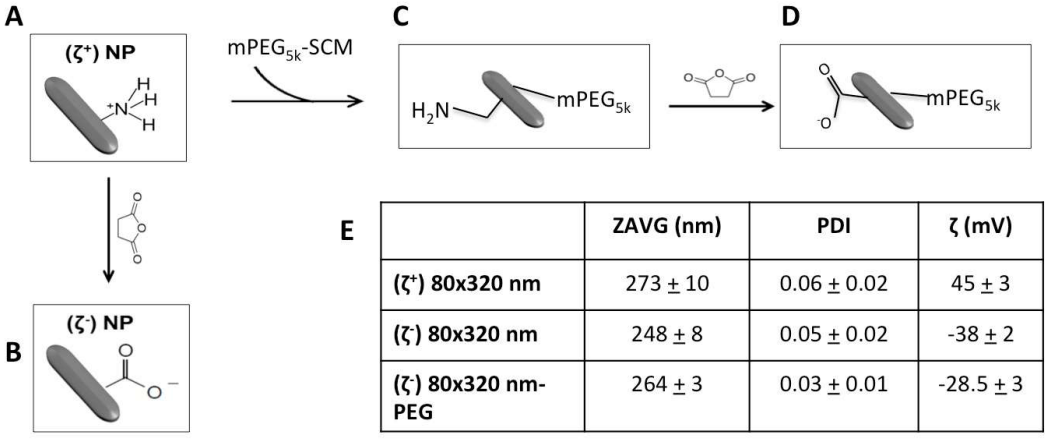

E

	ZAVG (nm)	PDI	ζ (mV)
(ζ+) 80x320 nm	273 ± 10	0.06 ± 0.02	45 ± 3
(ζ-) 80x320 nm	248 ± 8	0.05 ± 0.02	-38 ± 2
(ζ-) 80x320 nm-PEG	264 ± 3	0.03 ± 0.01	-28.5 ± 3

Figure 3.1. Particle Functionalization. Fabrication of (A) Cationic particles via PRINT® followed by incubation with succinic anhydride for (B) Anionic particles. Cationic particles were reacted with PEG_{5k}-succinimidyl carboxymethyl ester for (C)$mPEG_{5k}$ functionalization followed

by quenching of the amines with succinic anhydride resulting in (D) anionic PEGylated particles. Representative particle characterization for all three particle types (E).

For PEGylated NPs, the amine functional handles on (ζ+) NPs were reacted with PEG5k-succinimidyl carboxymethyl ester (PEG5k-SCM, Creative PEGworks) for a PEG layer on the particle surface, as has been established in previous lab protocols.[52] PEG (ζ+) NPs were then succinylated to quench remaining free amine groups and to form PEG (ζ-)NPs. UnPEGylated particles are the (ζ-)NPs. The functionalization of the particles is illustrated in Figure 3.1.

Samples were sputter-coated with 1-5 nm of Au/Pd (Cressington Scientific Instruments) and imaged with Scanning Electron Microscopy (Hitachi model S-4700. NP size and zeta potential were measured by dynamic light scattering (Zetasizer Nano ZS, Malvern Instruments, Ltd.) and thermogravimetric analysis (TGA) (Q5000, TA Instruments) was used to determine NP concentrations.

3.2.3 Pulmonary Administration

Orotracheal administrations followed established protocols.[10,53] Mice were anesthetized with isofluorane, followed by orotracheal instillation of 50 µl of particles. For PEGylation studies, 50 µg of particles was administered. Mice were suspended via the incisors vertically, and the tongue was shifted to allow for direct administration into the trachea via a pipette. The mouse was kept in the vertical position for several breaths to insure instillation, while the nose was gently occluded. In studies with a positive control of lipopolysaccharide (LPS) a dose of 20 µg/50 µl was used. In studies with CpG as a positive control, 2.5 µg/50 µl was used. And lastly, 50 µl of PBS was used as the negative control. CpG-B 1826 oligonucleotide (5′-TCCATGACGTTCCTGACGTT-3′) and LPS were obtained from Sigma Aldrich.

3.2.4 Biodistribution Study of Cationic and Anionic Nanoparticles

Female, C57BL/6 mice (n=4) were dosed 88 μg of the respective NP (positive or negative 80 nm x 320 nm Dylight 650 hydrogels) in 50 μl PBS orotracheally. Blood and broncheoalveolar lavage fluid (BALF) were collected at 24 and 72 hours with a single 1 mL PBS flush. Organs were then harvested for IVIS® Lumina optical imaging (Caliper Life Sciences, emission filter Cy5.5 and excitation filter 640 nm) and radiant efficiency per gram was determined. Following harvest, lungs were dissociated into a single cell suspension, placed in TRIzol® (Invitrogen) and stored before extracting RNA for RT-qPCR.

3.2.5 Tissue and Cell Preparation

Whole blood was obtained through cardiac puncture and collected in heparin-coated eppendorfs; from these, serum was obtained by centrifugation. Following perfusion of 10 mL PBS, broncheoalveolar lavage (BAL) was performed. BAL was performed by inserting a cannula in an incision in the trachea and flushing the lungs with 1 mL Hank's buffered saline solution (HBSS) (three sequential washes for BALF cell collection). BALF was obtained by centrifugation, separating BALF cells from supernatant. For single cell lung suspensions, lungs were resected, physically agitated and digested in 5 mg/mL Collagenase D, 20 units/mL DNase in HBSS with 2% FBS for 1 hour at 37 °C. These cells were then passed through a 70 μm sieve and overlaid on a Lymphoprep gradient to isolate lung lymphocytes. For histology sectioning, lungs were inflated through the cannula with a mixture of 1:1 PBS:OCT using gravity inflation; inflated lungs were embedded in OCT (Fisher) and flash frozen using an isopentane, dry ice slurry. For cationic and anionic particle studies, mice were harvested at 24 and 72 hours. For PEGylation studies, mice were harvested at 1,7, and 28 days.

3.2.6 Histopathology

Lung histology was performed by K. McNaughton in the UNC Histology Facility of the Department of Cell and Molecular Physiology. Frozen serial sections (thickness 7 μm) were obtained using a Leica 1950 cryostat, mounted to a glass slide and underwent staining. Hematoxylin and eosin (H&E) staining was performed by the core facility. Additional staining of $CD11c^+$ sections was performed by fixing the slides in chilled acetone for 2 minutes, then blocking and staining with Alexa Fluor 555 Phalloidin, anti-CD11c (Invitrogen), Alexa Fluor 488 Rabbit Anti-Rat IgG (H+L) (Invitrogen), and 14 mM DAPI (Invitrogen).

3.2.7 Flow Cytometry and ELISAs

Single cell suspensions from tissues were kept on ice and blocked with anti-CD16/32 (Fc block, eBioscience) and stained with the following antibodies to mouse cell surface molecules; I-A/I-E-PE-Cy7, CD11b-APC-Cy7, CD11c-PB, F4/80-PE-Cy5, CD45-BV510, CD103-PE, CD3-BV510, CD19-PE-Cy7, were from BioLegend. For PEGylation studies, the antibodies used were CD45-PacBlue, CD11c-PE, MHCII-PE-Cy7, and Ly6-G-AF700. Cells were fixed using 2-4% PFA in PBS. All data were collected using LSRII (BD Biosciences) flow cytometer and analyzed using FlowJo software (Tree Star).

Briefly, in the lung, macrophages and DCs were identified as $CD45^+CD11c^+$ populations and were separated by MHC II expression. Macrophages were defined as $CD45^+CD11c^+MHC11^{lo}$, and DCs were identified as $CD45^+CD11c^+MHC11^{hi}$ (Figure 3.2).

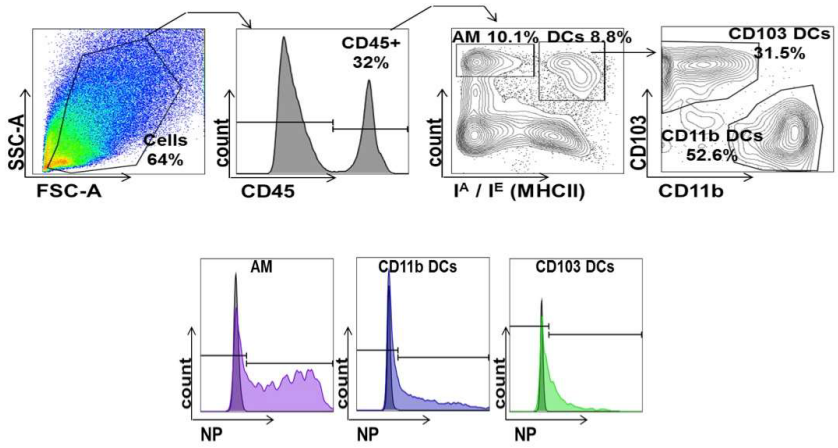

Figure 3.2. Representative gating for whole lung identification of APC populations and NP positive cells.

For further characterization, the MHC II^{lo} macrophages were confirmed to be F4/80^{+} and CD11b^{-} MHC II^{hi} DCs were further separated into a CD103^{+}, CD11b^{-} population, identifying the CD103 DCs, and a CD103^{-}CD11b^{+} population of CD11b DCs. Following population identification, each cell population was analyzed for NP fluorescence, gated by the PBS-treated, NP fluorescence-minus one (FMO) control. NP association was quantified as the percentage of each cell type, which had a detectable signal in the NP channel. From the NP positive gate, the median fluorescence intensity (MFI) per cell was also determined.

3.2.8 Cytokine Analysis

Enzyme-linked immunosorbent assay (ELISA) kits for IL-6, TNF-α, and IL-1β were purchased from BD Biosciences and used following manufacturer's suggestions on BALF and Serum samples. MIP-2 ELISA was purchased from R&D Systems. For BALF and serum obtained from mice treated with (ζ+)NPs and (ζ-)NPs, IL-6 levels were measured with CpG as a positive control and PBS as a negative control as described above. For assessment of (ζ+)NPs effect on the immune system, mice were treated with particles and then, 1 hour later, dosed with

LPS via instillation; IL-6 levels were measured in BALF and Serum. For PEGylation studies, PEGylated and unPEGylated particles were administered as described above, with LPS as a positive control. IL-6 and MIP-2 levels were then measured.

3.2.9 Quantitative Real-Time PCR (qRT-PCR) for Cationic and Anionic Nanoparticle Treated Mice

Mouse lungs from biodistribution study were used for qRT-PCR analysis. RNA isolation was performed from single cell suspensions of whole lung cells using TRIzol® (Invitrogen) followed by reverse transcription per standard protocol.[54] Briefly, Fast Real Time 7500 (Applied Biosystems) was used. Each primer was at a final concentration of 200 nM, Power Sybr Green 1X, 2 µl of template (cDNA dilution 1:10 for housekeeping genes, dilution of 1:4 for target genes). All samples were run in triplicate. qRT-PCR was performed for murine *Il-6, Il-4, Tnf-α, Il-12α, I1-12β, Cxcl10, lfn-γ, Tgfβ-1, Ccl2, and Il-10*, normalized to *Gapdh* using SYBR®-Green (Applied Biosystems), with the primer sets in (Figure 3.3).

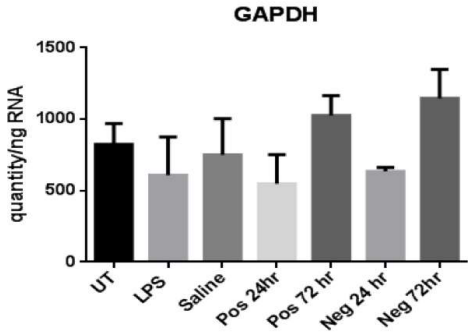

Gene	Forward	Reverse
IL-6	5′-CAACCACGGCCTTCCCTACTT-3′	5′-CACGATTTCCCAGAGAACATGTG-3′
IL-4	5′-GGCATTTTGAACGAGGTCACA-3′	5′-GACGTTTGGCACATCCATCTC-3′
TNF−α	5′-CCCTCACACTCAGATCATCTTCT-3	5′-GCTACGACGTGGGCTACAG-3′;
IL-12α	GCTTCTCCCACAGGAGGTTT	CTAGACAAGGGCATGCTGGT
IL-12β	GGAGACACCAGCAAAACGAT	GATTCAGACTCCAGGGGACA
CXCL10	TGCTGGGTCTGAGTGGGACT	rev: GGATAGGCTCGCAGGGATGA
INF-γ	5′-TCAAGTGGCATAGATGTGGAAGAA-3′	5′-TGGCTCTGCAGGATTTTCATG-3′
GAPDH	5′-CCTCGTCCCGTAGACAAAATG-3′	5′-TCTCCACTTTGCCACTGCAA-3′
TGF-β1	sense- 5' -ACCATGCCAACTTCTGTCTG-3'	antisense=5'- CGGGTTGTGTTGGTTGT AGA -3'
CCL2	ATTGGGATCATCTTGCTGGT	CCTGCTGTTCACAGTTGCC
IL10	sense: 5'- CCCTTTGCTATGGTGTCCTT-3'	antisense- 5' -TGGTTTCTCTTCCCAAGACC- 3'

Figure 3.3. Determining mRNA expression. (A) qRT-PCR for mRNA expression of *GAPDH* by single cell suspensions of lung cells treated with either (ζ^+)NP or (ζ^-)NP and homogenized at 24 hours and 72 hours. Data are presented as quantity of amplified molecules in a 20uL qRT-PCR reaction per ng of RNA. UT and LPS treatments shown for 24 hours. n=4 with bar representing SD. (B) Primer sets for qRT-PCR

3.2.10 Statistical Analysis

Statistical analyses were performed with GraphPad Prism version 6. Analysis of groups was performed as indicated in figures, where asterisks (or hashtags) indicate p values of *≤0.05, **≤0.01, ***≤0.001 and n.s indicating not significant. NP batches, cell assays, and immunization studies were repeated in at least two independent experiments, with the number of replicates (NPs, cells, mice) indicated in figures.

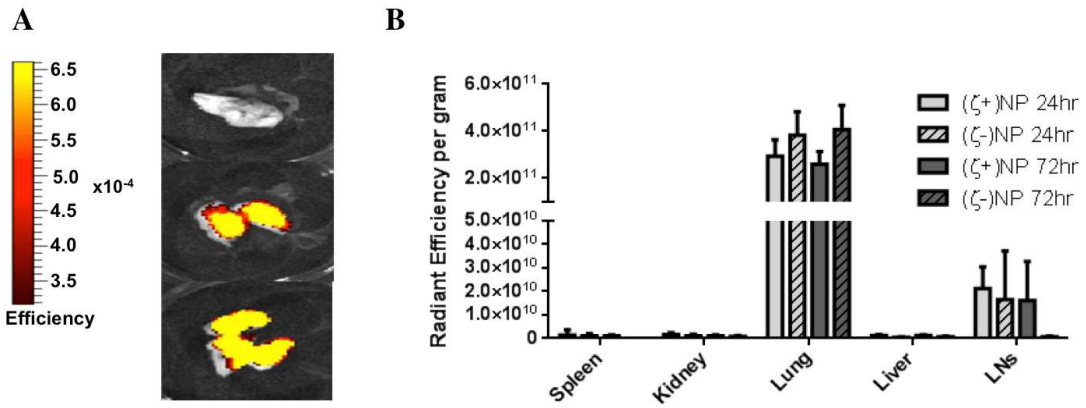

Figure 3.4. Biodistribution of Instilled Particles. (A) Representative IVIS imaging. From top to bottom: Saline, (ζ^+)NP, and (ζ^-)NP negative at 24 hours. Scale bar ranges from 3.14e-4 to 6.61e-4. (B) Organ distribution of instilled particles at 24 and 72 hours. n=4 with bar representing SD. Statistics performed by 1-way ANOVA within groups with Tukey multiple comparisons test, n.s.

3.3 Results

3.3.1 Distribution of Cationic and Anionic Nanoparticles in the Lung Following Pulmonary Instillation

In order to compare anionic and cationic NPs, we first quantified bulk organ distribution following pulmonary instillation in mice. NPs of (ζ+)NP and (ζ-)NP were fabricated as described previously[10] with the addition of a fluorescent dye to enable visualization throughout the organ tissue using an IVIS imaging system. Examples of lung fluorescence images are shown in Figure 3.4. Organs were resected at 24 and 72 hours to determine NP localization within this timeframe (Figure 3.4B). At both time points, NP fluorescence was detected above baseline in the lung and mediastinal lymph nodes, with no statistical difference between these groups. This indicated that NPs were mainly retained in the lung, with a detectable amount trafficking to the draining lymph node, even within 24 hours.

Lung pathology on mice receiving either (ζ+)NP or (ζ-)NP administration was performed to observe the localization of fluorescent NPs in the airways at 72 hours (Figure 3.5). Both NP types were observed throughout the entire lung and most often appear as punctate fluorescent regions, presumably internalized into phagocytic cells. These sections were stained for $CD11c^{+}$, finding that the majority of the punctate fluorescence corresponded with this surface marker.

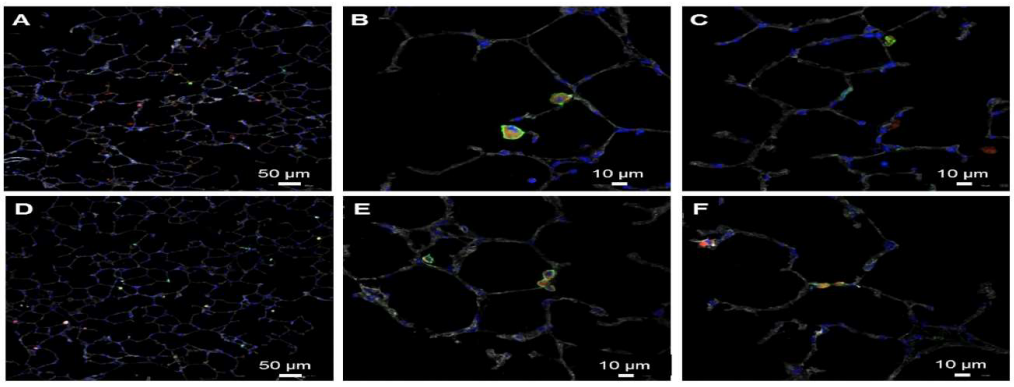

Figure 3.5. Representative immunohistochemistry of NP-treated lungs after 72 hours. Sections stained for fluorescent NPs (red), phalloidin (gray), DAPI (blue), and $CD11c^+$ (green). (A-C) (ζ^+) NPs. (D-F) (ζ^-) NPs.

3.3.2 Cationic and Anionic Nanoparticle Association in Lung Antigen Presenting Cells

To further differentiate the CD11c+ cells visually associated with NPs, we utilized flow cytometry to quantify NP uptake in three critical APC lung populations: AM, CD11b DCs and CD103 DCs. We sought to explore differences in cell associations with NPs of both charges in isolated whole lung cells at 72 hours following instillation of fluorescently-labeled NPs. The percentage of NP+ cells indicates how likely a given cell type is to associate with any amount of NPs, while the MFI lends insight to how many NPs each individual cell internalizes. The total fluorescence was calculated by multiplying the number of positive NP cells by the MFI in order to give an overall view of the total volume (related to mass) of NPs internalized; the magnitude of this value allows for comparison between NP doses and cell types to quantify cellular distribution (Figure 3.6). Representative gating used to analyze these populations is shown in Figure 3.2.

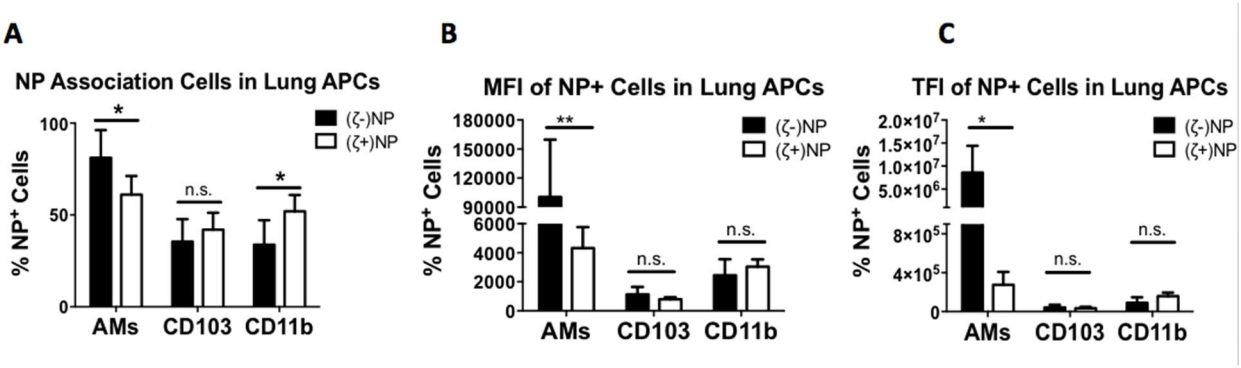

Figure 3.6 NP association in Lung APCs at 72 hours. NPs association in AMs, CD103 DCs and CD11b DCs from whole lungs of treated C57B/6 mice, n≥4 with bar representing SD. Within each population, (A) shows the percent NP positive cells and (B) shows the MFI of positive cells and (C) total fluorescence for each cell type. Statistics performed by 1-way ANOVA with Tukey multiple comparisons test with * $p \leq 0.05$, ** $p \leq 0.01$, *** $p \leq 0.001$.

Alveolar macrophages readily internalized both anionic and cationic NPs (Figure 3.6). At the NP dose given, between 60-100% of AMs were NP^+. This corresponds well with the known function of AM as the primary phagocytic cell in the lung. Interestingly, a greater percentage of AM internalized (ζ-)NPs. This is further evident in the MFI and total fluorescence intensity (FI) of these cells as (ζ-)NP were a factor of 10 higher than the corresponding (ζ+)NPs (Figure 3.6B and C). This indicates that a single AM internalized a significantly greater number of anionic NPs, suggesting that either AM have a preference towards internalization of anionic NPs, or the total availability of dosed NPs was greater than (ζ+)NPs, presumably due to other clearance methods or non-specific binding.

While the AMs showed preference to anionic NPs, both DC subtypes show increased association with cationic NPs. Slight increases in NP^+ populations were observed following (ζ+)NP administration for CD103 and CD11b DCs (Figure 3.6). A greater percentage of CD11b DCs were found to associate with (ζ+)NPs. Overall, a greater percentage of CD11b DCs were NP^+ as compared to CD103 DCs, indicating CD11b DCs found in the lung are more likely to associate with NPs at this time point. Interestingly, greater association was observed in both CD103 and CD11b DCs for cationic NPs as compared to the anionic formulation. Unlike the AM, the MFI of both NP^+ CD103 and CD11b DCs were not statistically different across the treatment groups, indicating an equivalent amount of NP internalization per cell (Figure 3.6B). Compared to AM, the MFI intensity in both DC subtypes was considerably lower as well, indicating that DCs in general associated with fewer numbers of NPs. Total fluorescence intensity between DC subtypes collected in the lung (Figure 3.6C) indicates that CD11b DCs in general associate with a greater amount of NPs than CD103 DCs, with (ζ+)NPs showing the greatest association.

3.3.3 Effect of Nanoparticle Treatment on Cellular Responses in the Lung

Differences between NP associations with different lung APCs were observed with flow cytometry, which can, in part, explain differences previously observed following vaccination with these two formulations.[10] We further hypothesized that the (ζ+)NP may have an adjuvant-like effect in the lung upon administration, which would contribute to production of local antibody responses upon vaccination.

To test this, mouse lungs were treated with both NP types and tested for cytokine production in the BALF, with PBS and CpG (a toll-like receptor, TLR, 9 agonist) as negative and positive controls. The CpG dose delivered was equivalent to previous co-delivery NP-adjuvant vaccination strategies and served as a qualitative control of known adjuvant activity.[10,13] No significant increase in IL-6 (Figure 3.7A), TNF-α, or IL-1β (not shown) levels in the BALF over saline treatment were found at 24 and 72 hours. This was in stark contrast to the effect of CpG administration to the lung, which resulted in ~1000 fold increase in inflammatory cytokine production at both time points. Minimal increase, if any, in systemic production of these same inflammatory markers was observed for all treatment types (Figure 3.7B).

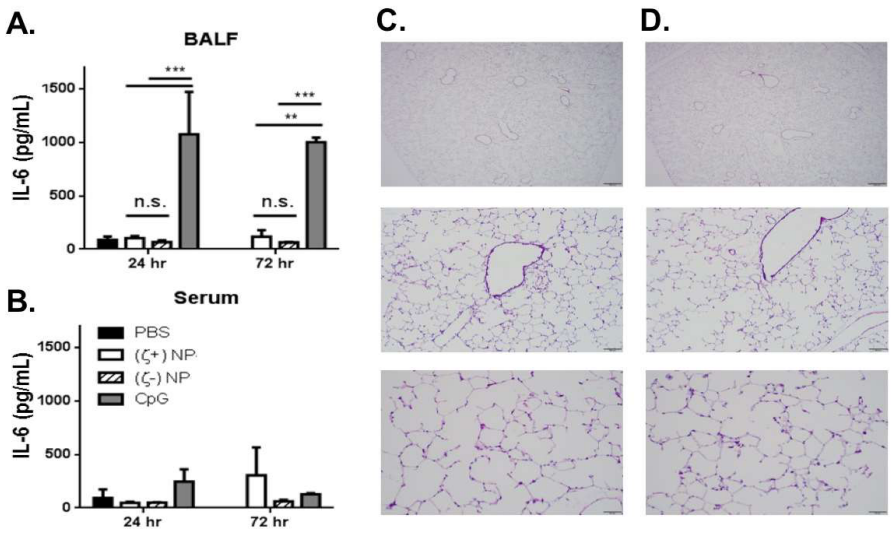

Figure 3.7. IL-6 cytokine analysis. (A) BALF and (B) serum following NP and CpG instillation at 24 and 72 hours in C57BL/6 mice, n=3 with bar representing SD. Statistics performed by 2-way ANOVA with Tukey multiple comparisons test with ** $p \leq 0.01$, *** $p \leq 0.001$. (C & D) H&E stained whole lung sections of NP treated lungs at three magnifications: (C) shows (ζ^+)NP treated and (D) shows (ζ^-)NP treated at 24 hours following NP instillation with (from top to bottom) 500 μm, 100 μm, 50 μm scale bars, respectively.

This indicates that both formulations of NPs have no increase in local or systemic inflammation over three days, a time point anticipated to be sufficient in capturing the onset of acute inflammation. The lack of acute inflammatory responses was corroborated by immunohistochemistry staining of NP-treated lungs. H&E staining of representative lung histology at 24 hours (shown in Figure 3.7C and D) and 72 hours (not shown), shows no evidence of leukocyte recruitment to the lung vasculature. Finally, we tested if (ζ+)NP administration would be detrimental to lung function, as previous studies have already shown that (ζ-)NPs are well tolerated.[55] As shown in Figure 3.8, lungs pretreated with (ζ+)NPs maintained the ability to mount an appropriate inflammatory response upon LPS stimulation in both the BALF and Serum.

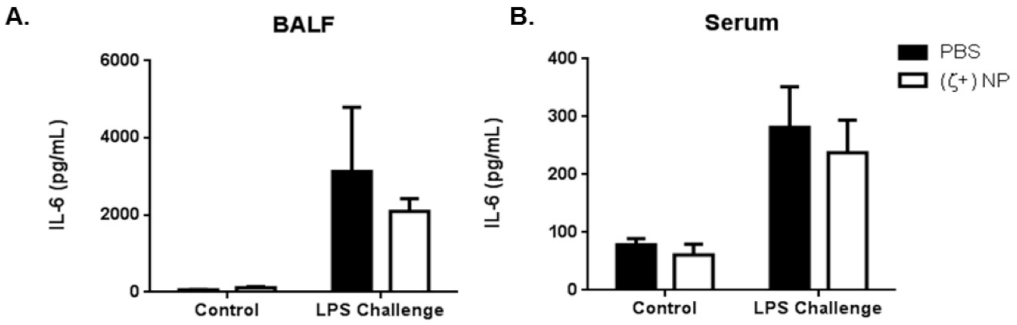

Figure 3.8 . IL-6 cytokine analysis. (A) BALF and (B) serum in C57B/6 mice which were treated with (ζ^+)NP then challenged 1 hour later with LPS, both via instillation. BALF and serum were collected 24 hours after LPS challenge, n=3. Statistics performed by 2-way ANOVA with Tukey multiple comparisons test with no statistical significance observed.

3.3.4 mRNA Expression in Lung Homogenate via Quantitative Real-Time PCR (qRT-PCR) for Immune Response Assessment

While no significant differences in cytokine levels secreted in the BALF were detected, we hypothesized that administration of either (ζ+)NP or (ζ-)NP may result in subtle changes in cytokine and chemokine production within the lung. At 24 and 72 hours following instillation, whole lungs were homogenized into a single cell suspension to perform qRT-PCR and to observe relevant cytokines and chemokines at the mRNA level, normalized to *Gapdh* (Figure 3.3). Mice treated with LPS at 24 hours were included as a reference of a known soluble mediator of inflammation; this group was excluded from our statistical analysis as it is a qualitative, and not quantitative control, and LPS inflammatory responses at the mRNA level are known to have resolved in C57BL/6 mice within 24 hours.[56] As shown in Figure 3.9, lungs treated with (ζ+)NPs were found to result in significant increased expression over untreated (UT) controls for *Ccl2* and *Cxcl10* at both 24 and 72 hours, as well as increased expression at 24 hours for *Il-10*, *Il-4*, *Il-6*, *Ifn-γ*, and *Il-12β.* In these cytokines, mRNA expression had returned to basal expression by 72 hours, indicating an acute and not sustained response to (ζ+)NPs. In contrast, lungs treated with (ζ-)NPs showed no increased expression of any of these markers when compared to UT controls. No increase in expression was observed from either NP type for *Tnf-α*, *Tgfβ-1,* or *Il-12α*.

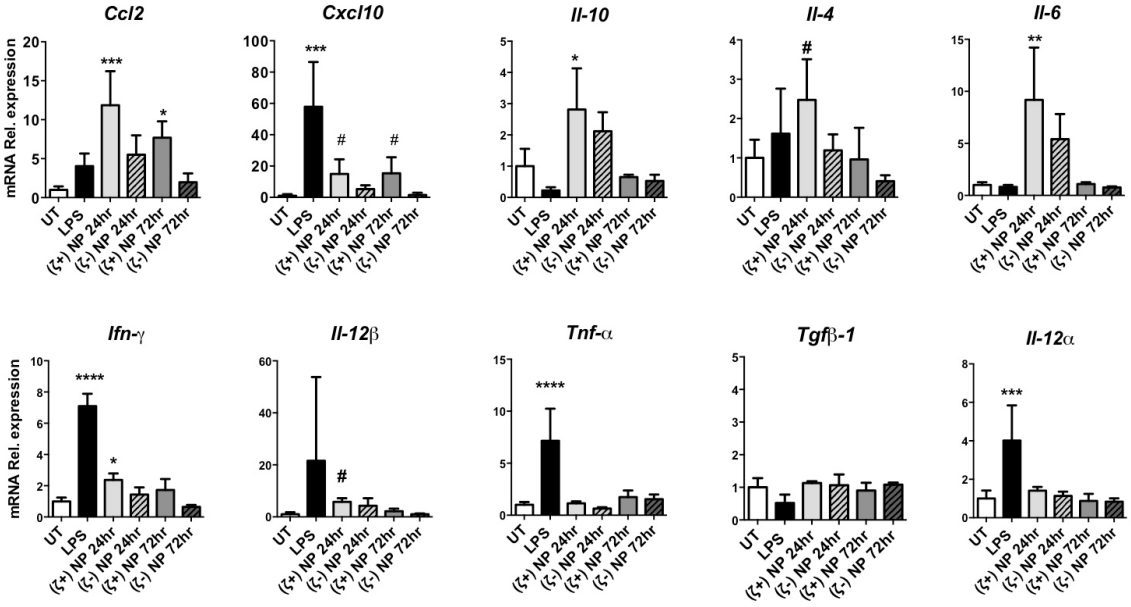

Figure 3.9. mRNA expression in Lung homogenate. qRT-PCR of *Ccl2,Cxcl10, Il-10, Il-4, Il-6, Ifn-γ, Il-12b, Tnf-α, Tgfβ-1, and IL-12a* by single cell suspensions of lung cells treated with either (ζ^+)NP or (ζ^-)NP and homogenized at 24 hours and 72 hours. Data are normalized to *GADPH* mRNA (quantity shown in Figure 3.3) and graphed as fold change over UT. UT and LPS treatments shown for 24 hours. n=4 with bar representing SD. Statistics performed by 1-way ANOVA with Dunnet's multiple comparisons test to UT control. * indicate significance including LPS in statistical analysis, # represent significance when LPS was excluded from analysis.

Both *Ccl2* and *Cxcl10* are important chemo-attractants involved in DC recruitment to the lungs.[50,51,57]As these were upregulated in lungs treated with (ζ+)NPs at both 24 and 72 hours, we sought to identify changes in lung populations following NP administration after 72 hours, allowing for a maximal effect to be detected. Using flow cytometry to differentiate AM and DC subtypes as before, we observed relative differences in the total percentage of $CD45^+$ leukocytes (Figure 3.10A), as well as the proportion of DCs between CD11b and CD103 subtypes (Figure 3.10B). Interestingly, there are no statistical differences in the relative percentage of AM of total $CD45^+$ cells, but the relative percentage of total DCs increases with NP treatment groups, with the greatest increase in the (ζ+)NP-treated group. Differences between the composition of the

DCs in the lung at this time point are more pronounced. Mice administered (ζ+)NP yielded an increased percentage of CD11b DCs in the lung, with a corresponding decrease in CD103 percentage. Anionic treatment groups showed considerably less difference, retaining a greater percentage of CD103 DCs than the cationic groups.

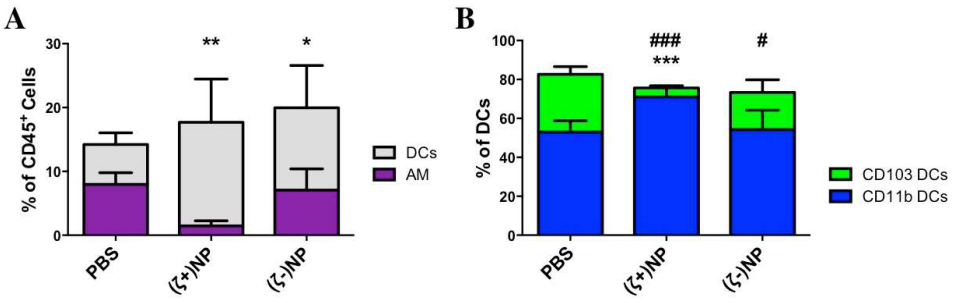

Figure 3.10. APC populations in the lung following NP treatment. (A) APC population breakdown of DCs and APCs in the whole lungs of treated C57B/6 mice after 72 hours, n≥4 with bar representing SD. Statistics performed by 1-way ANOVA with Dunnet's multiple comparisons test to PBS treatment. * indicate significant difference within DCs with * p≤0.05, ** p≤0.01, *** p≤0.001, AM n.s between groups. (B) Subtypes of $CD11c^+$ DCs in the whole lungs of treated C57B/6 mice after 72 hours, n≥4 with bar representing SD. Statistics performed by 1-way ANOVA with Dunnet's multiple comparisons test to PBS treatment. * indicate significant difference within CD11b DCs compared to PBS with * p≤0.05, ** p≤0.01, *** p≤0.001 and # indicate significant difference within CD103 DCs compared to PBS with # p≤0.05, ## p≤0.01, ### p≤0.001.

3.3.5 PEGylated and unPEGylated Nanoparticle Cellular Response and Association in the Lung

We further hypothesized that the observed decrease in residence time of (ζ-)NPs could be increased with further surface modification of a stealthing PEG layer. To test this, we first administered 80x320 nm PEGylated and unPEGylated(or (ζ-)NPs) to mice and collected BALF, serum, and lungs at 1, 7 and 28 days. LPS and PBS were used as positive and negative controls, respectively. First, BALF and serum were tested for cytokine production to confirm that the NPs

did not induce an immune response. IL-6 and MIP-2 levels were only detectable at day 1(Figure 3.11A and 3.11B). MIP-2 is a mouse macrophage inflammatory protein that plays a key role in neutrophil recruitment. The minimal inflammatory response was confirmed by immunohistochemistry staining of NP treated lungs. No change in lung architecture or infiltration of granulocytes to the lung was detected at all three timepoints (Figure 3.11 C and 3.11D).

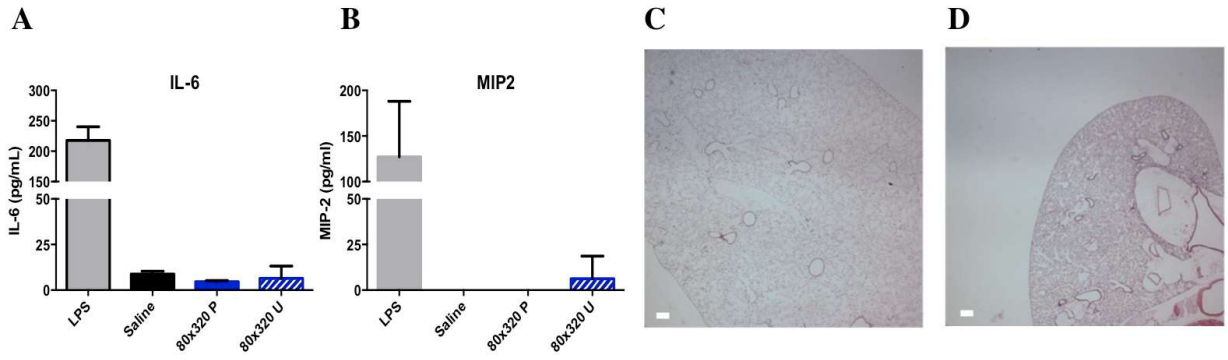

Figure 3.11. Cytokine Response for PEG and UnPEGylated particles. (A) IL-6 and (B) MIP-2 cytokine levels as determined by ELISA. Representative H&E stained lung tissue at 24 hours for (C) unPEGylated 80x320 nm particles and (D) PEGylated 80x320 nm particles with scale bar 200 μm.

After establishing no significant immune responses in the BALF, we sought to determine cellular uptake in the lung and particle retention time. Using flow cytometry and the gating scheme described earlier, macrophage and DC populations were identified and evaluated for particles containing Dylight 650 dye. The percentage of particle positive cells within a population was determined for BALF macrophages, lung macrophages, and lung DCs (Figure 3.12). BALF macrophages showed no difference in particle uptake at day 1, but by day 28 PEGylated particles were found in 60% of the macrophages compared to unPEGylated particles that were present in only 20%. Lung macrophages showed a similar trend in uptake at day 28,

with a preference for PEGylated particles. This indicates that PEGylation of particles can significantly reduce delay uptake by macrophages in the lung and extend residence time. Between day 1 and day 7, the percentage of particle positive BALF macrophages increased, suggesting that there may be free particles residing in the alveolar space which are not immediately internalized by cells in the lung. On the contrary, DCs showed an increased association with unPEGylated particles at day 1, and minimal association by day 28. These results indicate that there are significant differences in particle uptake and clearance among different resident lung cell populations.

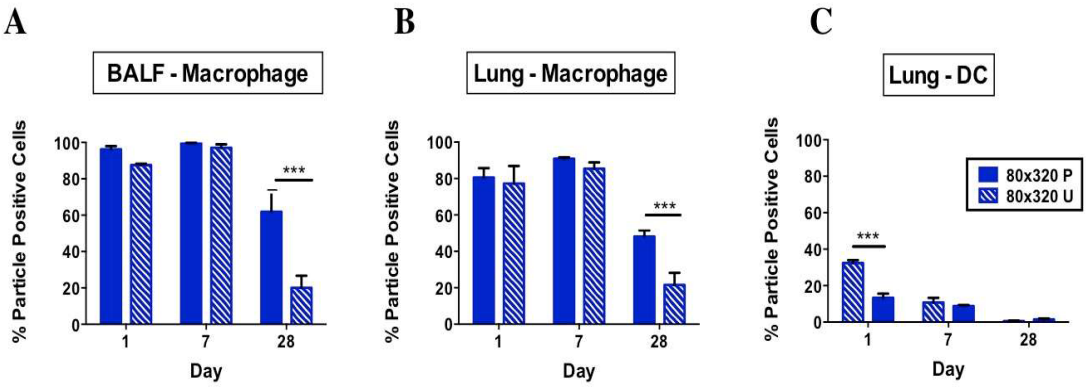

Figure 3.12. Flow cytometry analysis of PEGylated and unPEGylated particle uptake. Lung APCs associated with 80x320 nm that are PEGylated(P) and unPEGylated (U). (A) Percentage of AMs from BALF associated with particles (B)Percentage of Macrophages from lung homogenate associated with particles (C) Percentage of DCs from lung homogenate associated with particles.

3.4 Discussion

Utilization of the PRINT platform allows for investigations to independently address the influence of particle parameters (composition, degree of polymerization, surface chemistry, modulus, and geometry) on biological interactions. These studies varied a single parameter, surface chemistry, to systemically investigate the influence of NP surface charge and PEGylation

on NP cellular distribution, cytokine/chemokine production, changes in cell populations, and NP residence times in lung APCs. Our results show that cationic NPs are preferentially associated with two important lung DC populations and increase production of important lung chemo-attractants. Also, PEGylated anionic NPs maintain extended residence time in the lung.

The effect of NP surface modification on cell recruitment to the lungs is beneficial for potential pulmonary vaccine applications. Our observations of cationic NPs may account for their increased efficacy as a pulmonary vaccine carrier. Cationic NPs preferentially associated with lung DCs, while anionic NPs were more readily internalized by AMs. While AMs are considered APCs, their main function in the lung is to clear and sequester foreign material and maintain lung homeostasis[16,19,22] As a result, AMs are not the primary target of NP vaccines and it is more important to engineer particulate vaccine that target DCs, the "professional" APCs. Importantly, anionic NPs sequestered in AMs would be less successful at eliciting an adaptive immune response, as uptake in AMs represents an efficient lung clearance mechanism. The two lung DC populations studied here have both been implicated in critical immune capabilities, including stimulation of IgA production, $CD4^+$ and $CD8^+$ T cell priming, and migration to lymph nodes.[16,18,19,27–31] As both CD103 and CD11b DCs showed a trend of increased association with cationic NP, it is hypothesized that this increased DC association resulted in the previously reported result from our group demonstrating improved immune response following vaccination with cationic NPs.[10] Furthermore, the increased association observed in CD11b DCs may imply an opportunity to skew the overall lung immune status, as CD11b DCs have been implicated as a main mediator of Th2 lung responses.[30,58] These results demonstrate the importance of engineering NP surface charge to enhance association with lung DCs.

Both NP formulations, cationic and anionic, showed no acute inflammatory response systemically or locally in the BALF. However, further characterization of the lungs for mRNA expression of cytokine or chemokines showed cationic NP administration upregulated genes for two chemokines, CCL2 and CXCL10, responsible for leukocyte recruitment.[51,59] We also detected an increase in total $CD11c^+$ DCs in the lung following cationic NP administration, likely corresponding to the upregulation of these chemokines. Furthermore, the percentage of CD11b DCs from total $CD11c^+$ cells increased, likely due to recruitment of this cell type to the lung, and these cells were most commonly associated to cationic NPs in the lung. Taken together, these data suggest pulmonary administration of cationic NP administration to the lung causes recruitment of CD11b DCs to the airways, which then preferentially internalize NPs. This increased DC recruitment and NP association may account for increased antibody responses previously observed in our group for cationic NPs following pulmonary vaccination, as CD11b cells are the main driver of IgA production.[31] Increased responses to cationic NPs may also have been enhanced by upregulation of key Th1 cytokines, such as IFN-γ, Il-6, or Il-12 that can contribute to APC activation by 24 hours.[57] It is unclear at this time if this difference in cytokine/chemokine production is a result of interactions with the cationic charge on the NP or differences in the total NPs associated with DCs, as cationic NPs were more readily associated with DCs than anionic NPs.

While cationic NPs may not be ideal for an intravenous route of administration, the results generated via pulmonary delivery suggest promising opportunities for efficacious and safe pulmonary vaccine strategies, and may have implications for other mucosal surfaces as well. Pulmonary vaccination continues to gain attention as a viable approach to protect against wide variety of diseases, especially with increasing developments in dry powder administrations.[60,61]

This route offers ease of administration and the elimination of issues associated with traditionally administered vaccines such as elimination of cold chain storage and requirements for trained personnel for injections. Additionally, vaccines administered *via* the respiratory tract have demonstrated equivalent or increased local protection in the lung against various pathogens and offer systemic and distal mucosal protection.[60,62] The NPs studied here represent a model particle carrier, which can be optimized for a given antigen and route of administration. Our results suggest cationic formulations offer superior responses specifically in the lung; these NPs can promote antigen-specific responses suitable for vaccination, without overt safety concerns. Use of engineered NPs created via the PRINT platform allows for the optimization of the particle carrier for pulmonary delivery and, as suggested here, can be further adapted to carry a range of antigens to further promote mimicry of the complex pathogen surface.[4,63] This platform has the potential to increase the application of engineered particulate vaccines to combat a range of pathogens capable of being addressed by pulmonary vaccination.

The observed changes in lung populations, local changes in cytokines and chemokines, and differences in APC-NP association due to surface charge, led us to investigate the effect of altering surface chemistry (PEGylation) for targeted cell delivery. We have shown that the PEG coating provides a delay in macrophage uptake without causing an inflammatory response. This may indicate that macrophage clearance and/or turnover rates can be affected by NP surface modification prolonging particle residence time therefore acting as drug depots in the lung. Additionally, increased particle association with lung macrophages between day 1 and 7 indicates that particles may be continually taken up by the macrophages in the lung, retained within the lung tissue, and provide for sustained drug release for diseases targeting macrophages in the lung (tuberculosis). Also, PEGylated particles were not as prone to clearance, which may

be due to their ability to better interact with the mucus and surfactants in the airway. This parameter may make these particles ideal for gene delivery to treat cystic fibrosis (CF) and local delivery of therapeutics to airway cells to treat chronic obstructive pulmonary disease (COPD).

Overall, our systematic analyses investigating the effect of NP surface modification (cationic NP, anionic NP, and lastly PEGylated anionic NPs) are critical for establishing the role of NP surface parameters on pulmonary immune cell function. Our findings suggest that cationic NPs may offer increased preference towards lung DC subtypes. Specifically, cationic formulations resulted in increased DC association and modulated the local lung environment to promote recruitment and maturation of lung DCs, while avoiding extensive AM clearance. In contrast, anionic formulations were found to be immunologically inert in the lung, which may offer alternative therapeutic options towards promoting tolerance. Our findings demonstrate the importance of particle surface charge in pulmonary NP therapeutic design and will hopefully contribute to the design of novel vaccines towards a wide range of pulmonary pathogens. Furthermore, we have shown that modifying these anionic NPs by PEGylation affected particle uptake and extended retention in the lung suggesting opportunities for local lung delivery of and extended release of therapeutics. Thus far we have demonstrated our ability to fabricate monodisperse particles with varying surface modifications. Applying the knowledge from these fundamental studies of particle interactions in the lung can lead to engineering more efficient drug/biologic carriers for a variety of pulmonary delivery applications.

REFERENCES

(1) Azarmi, S.; Roa, W. H.; Löbenberg, R. Targeted Delivery of Nanoparticles for the Treatment of Lung Diseases. *Adv. Drug Deliv. Rev.* **2008**, *60* (8), 863–875.

(2) Chow, A. H. L.; Tong, H. H. Y.; Chattopadhyay, P.; Shekunov, B. Y. Particle Engineering for Pulmonary Drug Delivery. *Pharm. Res.* **2007**, *24* (3), 411–437.

(3) Pulliam, B.; Sung, J. C.; Edwards, D. a. Design of Nanoparticle-Based Dry Powder Pulmonary Vaccines. *Expert Opin. Drug Deliv.* **2007**, *4* (6), 651–663.

(4) Garcia, A.; Mack, P.; Williams, S.; Fromen, C.; Shen, T.; Tully, J.; Pillai, J.; Kuehl, P.; Napier, M.; DeSimone, J. M.; Maynor, B. W. Microfabricated Engineered Particle Systems for Respiratory Drug Delivery and Other Pharmaceutical Applications. *J. Drug Deliv.* **2012**, *2012*, 1–10.

(5) Yang, M. Y.; Chan, J. G. Y.; Chan, H. K. Pulmonary Drug Delivery by Powder Aerosols. *J. Control. Release* **2014**, *193*, 228–240.

(6) Patton, J. S.; Byron, P. R. Inhaling Medicines: Delivering Drugs to the Body through the Lungs. *Nat. Rev. Drug Discov.* **2007**, *6* (January), 67–74.

(7) Patton, J. S.; Brain, J. D.; Davies, L. a; Fiegel, J.; Gumbleton, M.; Kim, K.-J.; Sakagami, M.; Vanbever, R.; Ehrhardt, C. The Particle Has Landed--Characterizing the Fate of Inhaled Pharmaceuticals. *J. Aerosol Med. Pulm. Drug Deliv.* **2010**, *23 Suppl 2*, S71–S87.

(8) Euliss, L. E.; DuPont, J. A.; Gratton, S.; DeSimone, J. Imparting Size, Shape, and Composition Control of Materials for Nanomedicine. *Chem. Soc. Rev.* **2006**, *35* (11), 1095–1104.

(9) Blank, F.; Stumbles, P.; von Garnier, C. Opportunities and Challenges of the Pulmonary Route for Vaccination. *Expert Opin. Drug Deliv.* **2011**, *8* (5), 547–563.

(10) Fromen, C. A.; Robbins, G. R.; Shen, T. W.; Kai, M. P.; Ting, J. P. Y. Controlled Analysis of Nanoparticle Charge on Mucosal and Systemic Antibody Responses Following Pulmonary Immunization. *Proc. Natl. Acad. Sci. U. S. A.* **2015**, *112* (2), 488–493.

(11) Fromen, C. A.; Shen, T. W.; Larus, A. E.; Mack, P.; Maynor, B. W.; Luft, J. C.; DeSimone, J. M. Synthesis and Characterization of Monodisperse Uniformly Shaped Respirable Aerosols. *Am. Inst. Chem. Eng.* **2013**, *0* (00), 405–410.

(12) Moon, J. J.; Irvine, D. J.; Huang, B. Engineering Nano- and Micro- Particles to Tune Immunity. *Adv Mater.* **2012**, *24* (28), 3724–3746.

(13) Nembrini, C.; Stano, A.; Dane, K. Y.; Ballester, M.; van der Vlies, a. J.; Marsland, B. J.; Swartz, M. a.; Hubbell, J. a. Nanoparticle Conjugation of Antigen Enhances Cytotoxic T-Cell Responses in Pulmonary Vaccination. *Proc. Natl. Acad. Sci.* **2011**, *108* (44), E989–E997.

(14) Smith, D. M.; Simon, J. K.; Baker, J. R. Applications of Nanotechnology for Immunology. *Nat. Rev. Immunol.* **2013**, *13* (8), 592–605.

(15) Kunda, N. K.; Somavarapu, S.; Gordon, S. B.; Hutcheon, G. A.; Saleem, I. Y. Nanocarriers Targeting Dendritic Cells for Pulmonary Vaccine Delivery. *Pharm. Res.* **2013**, *30* (2), 325–341.

(16) Hardy, C. L.; Lemasurier, J. S.; Mohamud, R.; Yao, J.; Xiang, S. D.; Rolland, J. M.; O'Hehir, R. E.; Plebanski, M. Differential Uptake of Nanoparticles and Microparticles by Pulmonary APC Subsets Induces Discrete Immunological Imprints. *J. Immunol.* **2013**, *191*, 5278–5290.

(17) Zhao, L.; Seth, A.; Wibowo, N.; Zhao, C. X.; Mitter, N.; Yu, C.; Middelberg, A. P. J. Nanoparticle Vaccines. *Vaccine* **2014**, *32* (3), 327–337.

(18) Sakagami, M. In Vivo, in Vitro and Ex Vivo Models to Assess Pulmonary Absorption and Disposition of Inhaled Therapeutics for Systemic Delivery. *Adv. Drug Deliv. Rev.* **2006**, *58* (9-10), 1030–1060.

(19) Guilliams, M.; Lambrecht, B. N.; Hammad, H. Division of Labor between Lung Dendritic Cells and Macrophages in the Defense against Pulmonary Infections. *Mucosal Immunol.* **2013**, *6* (3), 464–473.

(20) Hassan, M.; Lau, R. Effect of Particle Shape on Dry Particle Inhalation: Study of Flowability, Aerosolization, and Deposition Properties. *AAPS PharmSciTech* **2009**, *10*, 1252–1262.

(21) Kleinstreuer, C.; Zhang, Z.; Li, Z.; Roberts, W.; Rojas, C. A New Methodology for Targeting Drug-Aerosols in the Human Respiratory System. *Int. J. Heat Mass Transf.* **2008**, *51*, 5578–5589.

(22) Fernandes, C. A.; Vanbever, R. Preclinical models for pulmonary drug delivery http://www.uclouvain.be/cps/ucl/doc/farg/documents/FernandesVanbeverEODD2009.pdf

(23) Thiel, C. Can in Vitro Particle Size Measurements Be Used to Predict Pulmonary Deposition of Aerosol from Inhalers? *J Aerosol Med* **1998**, *11*, S43–S52.

(24) Sharma, R.; Saxena, D.; Dwivedi, A. K.; Misra, A. Inhalable Microparticles Containing Drug Combinations to Target Alveolar Macrophages for Treatment of Pulmonary Tuberculosis. *Pharm. Res.* **2001**, *18* (10), 1405–1410.

(25) Sakagami, M.; Byron, P. R. Respirable Microspheres for Inhalation: The Potential of Manipulating Pulmonary Disposition for Improved Therapeutic Efficacy. *Clin.*

Pharmacokinet. **2005**, *44* (3), 263–277.

(26) Inaba, K.; Steinman, R.; Van Voorhis, W.; Muramatsu, S. Dendritic Cells Are Critical Accessory Cells for Thymus-Dependent Antibody Responses in Mouse and in Man. *Proc. Natl. Acad. Sci. U. S. A.* **1983**, *80*, 6041–6045.

(27) Naito, T.; Suda, T.; Suzuki, K.; Nakamura, Y.; Inui, N.; Sato, J.; K, C.; Nakamura, H. Lung Dendritic Cells Have a Potent Capability to Induce Production of Immunoglobulin a. *Am. J. Respir. Cell Mol. Biol.* **2008**, *38*, 161–167.

(28) Xie, Y.; Zeng, P.; Wiedmann, T. Disease Guided Optimization of the Respiratory Delivery of Microparticulate Formulations. *Expert Opin Drug Deliv* **2008**, *5*, 269–289.

(29) Abdelwahed, W.; Degobert, G.; Stainmesse, S.; Fessi, H. Freeze-Drying of Nanoparticles: Formulation, Process and Storage Considerations. *Adv. Drug Deliv. Rev.* **2006**, *58*, 1688–1713.

(30) Furuhashi, K.; Suda, T.; Hasegawa, H.; Suzuki, Y.; Hashimoto, D.; Enomoto, N.; Fujisawa, T.; Nakamura, Y.; Inui, N.; Shibata, K.; Nakamura, H.; Chida, K. Mouse Lung cd103+ and cd11bhigh Dendritic Cells Preferentially Induce Distinct cd4+ T-Cell Responses. 2012;46:165-172. *Am. J. Respir. Cell Mol. Biol.* **2012**, *46*, 165–172.

(31) Suzuki, Y.; Suda, T.; Furuhashi, K.; Shibata, K.; Hashimoto, D.; Enomto, N.; Fujisawa, T.; Nakamura, Y.; Inui, N.; Nakamura, H.; Chida, K. Mouse CD11bhigh Lung Dendritic Cells Have More Potent Capability to Induce IgA than CD103+ Lung Dendritic Cells in Vitro. *Am. J. Respir. Cell Mol. Biol.* **2012**, *46* (6), 773–780.

(32) Steinman, R. M. Dendritic Cells: Versatile Controllers of the Immune System. *Nat. Med.* **2007**, *13* (10), 1155–1159.

(33) Hubbell, J. a; Thomas, S. N.; Swartz, M. a. Materials Engineering for Immunomodulation. *Nature* **2009**, *462* (7272), 449–460.

(34) Li, A.; Moon, J.; Abraham, W.; Suh, H.; Elkhader, J.; Seidman, M.; Yen, M.; Im, E.; Foley, M.; Barouch, D.; Irvine, D. Generation of Effector Memory T Cell-Based Mucosal and Systemic Immunity with Pulmonary Nanoparticle Vaccination. *Sci Transl Med* **2013**, *5*.

(35) Michen, B.; Graule, T. Isoelectric Points of Viruses. *J. Appl. Microbiol.* **2010**, *109*, 388–397.

(36) van der Mei, H.; Busscher, H. Bacterial Cell Surface Heterogeneity: A Pathogen's Disguise. *PLOS Pathog.* **2012**, *8*.

(37) EL-SHERBINY, I. M.; MCGILL, S.; SMYTH, H. D. C. Swellable Microparticles as Carriers for Sustained Pulmonary Drug Delivery. *J. Pharm. Sci.* **2009**, *99* (5), 2343–2356.

(38) Roberts, R. a.; Shen, T.; Allen, I. C.; Hasan, W.; DeSimone, J. M.; Ting, J. P. Y. Analysis

of the Murine Immune Response to Pulmonary Delivery of Precisely Fabricated Nano- and Microscale Particles. *PLoS One* **2013**, *8* (4).

(39) Agu, R. U.; Ugwoke, M. I.; Armand, M.; Kinget, R.; Verbeke, N. The Lung as a Route for Systemic Delivery of Therapeutic Proteins and Peptides. *Respir. Res.* **2001**, *2* (4), 198–209.

(40) Du, J.; Du, P.; Smyth, H. Hydrogels for Controlled Pulmonary Delivery. *Ther. Deliv.* **2013**, 1293–1305.

(41) Mansour, H. M.; Rhee, Y. S.; Wu, X. Nanomedicine in Pulmonary Delivery. *Int. J. Nanomedicine* **2009**, *4*, 299–319.

(42) Muralidharan, P.; Mallory, E.; Malapit, M.; Don, H.; Mansour, H. M. Inhalable PEGylated Phospholipid Nanocarriers and PEGylated Therapeutics for Respiratory Delivery as Aerosolized Colloidal Dispersions and Dry Powder Inhalers. *Pharmaceutics* **2014**, *6* (2), 333–353.

(43) Bayard, F. J. C.; Thielemans, W.; Pritchard, D. I.; Paine, S. W.; Young, S. S.; Bäckman, P.; Ewing, P.; Bosquillon, C. Polyethylene Glycol-Drug Ester Conjugates for Prolonged Retention of Small Inhaled Drugs in the Lung. *J. Control. Release* **2013**, *171* (2), 234–240.

(44) Youn, Y.; Kwon, M.; Na, D.; Chae, S.; Lee, S.; Lee, K. Improved Intrapulmonary Delivery of Site-Specific PEGylated Salmon Calcito- Nin: Optimization by PEG Size Selection. *J Control. Release* **2008**, *125*, 68–75.

(45) Koussoroplis, S. J.; Paulissen, G.; Tyteca, D.; Goldansaz, H.; Todoroff, J.; Barilly, C.; Uyttenhove, C.; Van Snick, J.; Cataldo, D.; Vanbever, R. PEGylation of Antibody Fragments Greatly Increases Their Local Residence Time Following Delivery to the Respiratory Tract. *J. Control. Release* **2014**, *187*, 91–100.

(46) Merkel, O. M.; Beyerle, A.; Librizzi, D.; Pfestroff, A.; Behr, T. M.; Sproat, B.; Barth, P. J.; Kissel, T. Nonviral siRNA Delivery to the Lung: Investigation of PEG-PEI Polyplexes and Their in Vivo Performance. *Mol. Pharm.* **2009**, *6* (4), 1246–1260.

(47) Meenach, S. A.; Anderson, K. W.; Zach Hilt, J.; McGarry, R. C.; Mansour, H. M. Characterization and Aerosol Dispersion Performance of Advanced Spray-Dried Chemotherapeutic PEGylated Phospholipid Particles for Dry Powder Inhalation Delivery in Lung Cancer. *Eur. J. Pharm. Sci.* **2013**, *49* (4), 699–711.

(48) Patel, B.; Gupta, V.; Ahsan, F. PEG-PLGA Based Large Porous Particles for Pulmonary Delivery of a Highly Soluble Drug, Low Molecular Weight Heparin. *J. Control. Release* **2012**, *162* (2), 310–320.

(49) Ibricevic, A.; Guntsen, S.; Zhang, K.; Shrestha, R.; Liu, Y.; Sun, J. PEGylation of Cationic, Shell-Crosslinked-Knedel-like Nanoparticles Modulates Inflammation and Enhances Cellular Uptake in the Lung. *Nanomedicine Nanotechnology, Biol. Med.* **2013**,

9, 912–922.

(50) Rose, C. J.; Sung, S.; Fu, S. Significant Involvement of ccl2 (mcp-1) in Inflammatory Disorders of the Lung. *Microcirculation* **2003**, *10*, 273–288.

(51) Deshmane, S.; Kremlev, S.; Amini, S.; Sawaya, B. Monocyte Chemoattractant Protein-1 (mcp-1): An Overview. *J. Interf. cytokine Res.* **2009**, *29*, 313–326.

(52) Perry, J.; Reuter, K.; Kai, M. P.; Herlihy, K.; Jones, S.; Luft, J. C.; Napier, M. E.; Bear, J. E.; Desimone, J. M. Pegylated Print Nanoparticles: The Impact of Peg Density on Protein Binding, Macrophage Association, Biodistribution, and Pharmacokinetics. *Nano Lett.* **2012**, *12*, 5304–5310.

(53) Shen, T. W.; Fromen, C. A.; Kai, M. P.; Luft, J. C.; Rahhal, T. B.; Robbins, G. R.; DeSimone, J. M. Distribution and Cellular Uptake of PEGylated Polymeric Particles in the Lung Towards Cell-Specific Targeted Delivery. *Pharm. Res.* **2015**.

(54) Robbins, G. R.; Truax, A. D.; Davis, B. K.; Zhang, L.; Brickey, W. J.; Ting, J. P.-Y. Regulation of Class I Major Histocompatibility Complex (MHC) by Nucleotide-Binding Domain, Leucine-Rich Repeat-Containing (NLR) Proteins. *J. Biol. Chem.* **2012**, *287* (29), 24294–24303.

(55) Robbins, G. R.; Roberts, R. a.; Guo, H.; Reuter, K.; Shen, T.; Sempowski, G. D.; McKinnon, K. P.; Su, L.; DeSimone, J. M.; Ting, J. P.-Y. Analysis of Human Innate Immune Responses to PRINT Fabricated Nanoparticles with Cross Validation Using a Humanized Mouse Model. *Nanomedicine Nanotechnology, Biol. Med.* **2015**, *11* (3), 589–599.

(56) Johnston, C.; Finkelstein, J.; Gelein, R.; Oberdorster, G. Pulmonary Cytokine and Chemokine Mrna Levels after Inhalation of Lipopolysaccharide in c57bl/6 Mice. *Toxicol. Sci.* **1998**, *46*, 300–307.

(57) Pesce, I.; Monaci, E.; Muzzi, A.; Tritto, E.; Tavarini, S.; Nuti, S.; De Gregorio, E.; Wack, A. Intranasal Administration of Cpg Induces a Rapid and Transient Cytokine Response Followed by Dendritic and Natural Killer Cell Activation and Recruitment in the Mouse Lung. *J. Innate Immun. 2*, 144–159.

(58) Larhrib, H.; Martin, G.; Marriott, C.; Prime, D. The Influence of Carrier and Drug Morphology on Drug Delivery from Dry Powder Formulations. *Int. J. Pharm.* **2003**, *257*, 283–296.

(59) Dong, S.; Zhang, X.; He, Y.; Xu, F.; Li, D.; Xu, W.; Wang, H.; Yin, Y.; Cao, J. Synergy of Il-27 and Tnf-Alpha in Regulating cxcl10 Expression in Lung Fibroblasts. *Am. J. Respir. Cell Mol. Biol. 48*, 518–530.

(60) Tonnis, W.; Kersten, G.; Frijlink, H.; Hinrichs, W.; de Boer, A.; Amorij, J. Pulmonary Vaccine Delivery: A Realistic Approach? *J. Aerosol Med. Pulm. Drug Deliv.* **2012**, *25*, 249–260.

(61) Sou, T.; Meeusen, E.; de Veer, M.; Morton, D.; Kaminskas, L.; McIntosh, M. New Developments in Dry Powder Pulmonary Vaccine Delivery. *Trends Biotechnol.* **2011**, *29*, 191–198.

(62) Neutra, M.; Kozlowski, P. Mucosal Vaccines: The Promise and the Challenge. *Nat. Rev. Immunol.* **2006**, *6*, 148–158.

(63) Galloway, A.; Murphy, A.; DeSimone, J.; Di, J.; Herrmann, J.; Hunter, M.; Kindig, J.; Malinoski, F.; Rumley, M.; Stoltz, D.; Templeman, T.; Hubby, B. Development of a Nanoparticle-Based Influenza Vaccine Using the Print Technology. *Nanomedicine* **2013**, *9*, 523–531.

CHAPTER 4. Pulmonary Delivery of Butyrylcholinesterase as a Model Biologic to the Lung[3]

4.1 Introduction

Pulmonary delivery of biologics is an emerging alterative therapeutic approach to the traditional parenteral route of administration. The lung enables local delivery with a large surface area for absorption of proteins, as well as potential for a non-invasive systemic delivery [1,21] Delivery of biologics, including active enzymes, to the lung is of particular interest for multiple diseases. For example, cystic fibrosis patients are currently treated with inhalation of recombinant human DNase, an enzyme that aids in breaking down the sputum build up in the lungs.[3] Patients with pulmonary oxidative stress benefit from antioxidant enzyme, such as superoxide dismutase and catalase, in order to prevent lung injury.[4] Even systemic diseases have been shown to benefit from inhaled biologics; inhaled insulin has demonstrated optimal bioavailability and safety via deep lung delivery with a recent FDA approval of Afreeza®.[5,6]

Many challenges remain for successful enzyme delivery to the lungs, including maintaining biological activity and providing efficient aerosol formation. Lacking these properties, pulmonary delivery of enzymes becomes cost prohibitive and infeasible.[1,7,8] To

---

[3] This chapter has been previously published in the following:

Rahhal TB, Fromen CA, Wilson E, Kai MP, Shen TW, Luft JC, DeSimone JM. Pulmonary Delivery of Butyrylcholinesterase as a Model Protein to the Lung. Molecular Pharmaceutics. March 2016.

date, only a handful of successful inhalable proteins are on the market, with Pulmozyme® (DNase based treatment for Cystic Fibrosis), being the main example.[1] Even though this product is used in the clinic, numerous issues exist including administration via nebulizer (which is not a convenient method due to the bulky nature of the device), the lack of universal enzyme stability, and the susceptibility to protein degradation.[1] Recent progress in dry powder inhaler (DPI) development provides new opportunities for formulations with increased protein stability, overcoming many of the traditional challenges associated with nebulizers. Utilizing particles from a DPI device that could deliver enzymes such as DNase or antioxidant enzymes in a targeted method would advance current treatment options. It has been widely shown that aerosol size and shape effect residence time, rate of phagocytosis, and success of particulate treatments in the lung.[8–12] However, the balance between protein stability, particle formulation, and aerosol characteristics remains a challenge in realizing the potential of DPI therapeutics, particularly for successful administration of an active enzyme or biologic to the lung with high efficiency.[13]

To further explore the feasibility and properties of an enzyme delivered to the lung as a dry powder, we investigated butyrylcholinesterase (BuChE) as a model enzyme. BuChE is an endogenous enzyme synthesized by the liver, which serves as a catalyzer for the hydrolysis of esters in choline. BuChE can be potentially used in a diverse array of applications, such as a future prophylactic measure against organophosphate (OP) exposure or for treatment of patients with pseudocholinesterase deficiency. OP poisoning remains a serious global health concern, with both accidental and deliberate exposure leading to thousands of deaths annually.[14] As a prophylactic measure, BuChE scavenges OPs through a covalent bond at the active site, which leads to the inactivation of itself and the OPs.[15] Human BuChE has been delivered systemically

by intravenous (i.v.), intraperitoneal (i.p.), or intramuscular (i.m.) routes, with the latter two having a mean residence time of approximately 50 hours in mice; however this showed limited neutralization of inhaled OPs in guinea pigs.[16,17] Rosenberg *et al*. introduced a new approach to address OP poisoning by creating a 'pulmonary bioshield' using pulmonary delivery of BuChE to lungs with a polyethylene glycol (PEG)-modified recombinant macaque BuChE. Orotracheal administration prior to nerve gas exposure in mice showed a dose-dependent protection against toxicity, indicating the benefits of BuChE administration directly to the airways.[18] In addition to protection and scavenging for OP exposure, inhaled BuChE could be used as a supplement to patients with pseudocholinesterase deficiency, an understudied condition where 1 in 3000 people have trouble breaking down certain anesthetics due to an abnormality in endogenous BuChE.[19,20] These patients also suffer toxicity from common medicines, such as lidocaine and prilocaine.[21,22]

To achieve efficient lung deposition of BuChE, we employed Particle Replication in Non-wetting Templates (PRINT®) technology to fabricate BuChE particles for pulmonary delivery as a potential self-administered DPI. PRINT is a top-down particle fabrication technology that allows the engineering of precisely defined particles by exquisitely and independently controlling particle characteristics such as size, shape, chemical composition, and surface chemistry. Previous work by the lab has shown controlled deposition in the lung as a function of PRINT particle shape and size, as well as adaptability for use with several biologics.[8,23,24] However, these biologics were not tested extensively in actual lung administration. The flexibility of the PRINT platform lends itself to further optimization of BuChE protein parameters to enhance particle deposition with accurate fabrication of uniform particles. We sought to provide a better understanding of the lung environment, retention and activity of our

model enzyme, BuChE. Furthermore, our studies investigated BuChE distribution in *in vivo* models post-orotracheal administration, as well as the associated immune responses. Utilizing PRINT to meet the formulation challenge in pulmonary delivery, we also developed a novel 1 μm cylindrical BuChE particle to demonstrate a balanced formulation that maintains protein activity and has ideal aerosol characteristics.

4.2 Methods

4.2.1 Animals

Male mice were housed in pathogen-free facilities at the University of North Carolina at Chapel Hill and treated at 6 weeks of age. Standard guidelines for care and use of laboratory animals as approved by the Institution of Animal Care and Use Committee at UNC were followed. *Foxn1*$^{nu/nu}$ (Nude) mice were bred in-house; C57BL/6 and BALB/c mice were obtained from Jackson Laboratories.

4.2.2 Protein Source

Tetrameric Equine Butyrylcholinesterase (referred to as BuChE in this paper) (ID#C7512) at $\geq$ 10 U/mg was purchased from Sigma Aldrich and used directly with no further purification. Specifically, lot SLBB2114V (50 U/mg solid as reported by Sigma) was used for instillation studies and lot SLB7404V (19.7 U/mg solid as reported by Sigma) was used in particles for dry powder insufflation studies. Lastly, a high purity eqBuChE stock (ID#C4290), lot SLB1774V (331 U/mg solid as reported by Sigma), was used to demonstrate transformability of particle fabrication. Equine BuChE is 88% homologous with murine BuChE, 93% homologous to human BuChE and is an accepted translational model for human BuChE.[25] Furthermore, several researchers have shown that homologous systems do not result in anti-

BuChE antibodies[26,27]and have used non-homologous systems to establish proof of concept.[17,26,28–30]

4.2.3 Orotracheal Administration and Residence of BuChE

Mice were dosed with BuChE orotracheally at a maximum volume of 50 µl at 80 mg/kg with n=3 per study. BuChE activity was confirmed prior to dosing. Mice were anesthetized using isofluorane, placed on a 45 degree board by their upper incisors, the tongue was held away from the trachea and the dose was administered to the back of the mouth using a pipette. The nose was gently clamped so that the mouse could aspirate the liquid into the lung. At each time point, mice were anesthetized with ketamine, then blood was collected and centrifuged for plasma analysis. Broncheoalveolar lavage fluid (BALF) was collected from the lungs using 1x PBS (1 mL, Sigma Aldrich) at 24, 48, 72, 96, 120, and 168 hours with a single flush for protein analysis and two sequential flushes for cell collections. Cells were separated from BALF samples via centrifugation. Protocols adapted from previous work.[18,24,31]

For biodistribution analysis, a 3 wt% Dylight 680 tagged BuChE mixture (Fisher Scientific, USA) was administered orotracheally. Manufacturer's instructions were followed for Dylight 680 tagging with an optimized 3-fold ratio of dye to protein (Figure 4.1) where a minimal activity loss was detected in the tagged BuChE. BuChE activity of the 3 wt% mixture was measured before administration to insure proper dosing based on activity. BALF and Plasma were collected as stated above. Following a 10 ml PBS perfusion, organs were harvested, followed by detection via *in vivo* imaging system (IVIS) Lumina optical imaging (emission filter Cy5.5 and excitation filter 675 nm). Radiant efficiency per gram was measured for all organs, plasma (100 µl), and BALF (100 µl). Saline treated mice were harvested at 0, 24, 96, and 168 hours. BuChE treated mice were harvested at 24, 48, 72, 96, and 168 hours.

20 µg of lipopolysaccharide (LPS) was administered as a positive control for inflammatory immune responses, 1x PBS was administered at 50 µl as a negative control and an untreated group was also included in all studies.

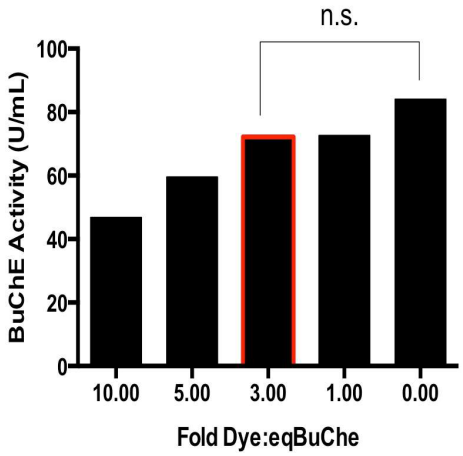

Figure 4.1 Activity of eqBuChE Tagged with Dylight680. eqBuChE was tagged at different ratios to optimize activity and detection. A 3 fold ratio of dye: BuChE was found to have minimal activity loss and adequate detection. (n.s., not significant; Two-way ANOVA with Tukey's multiple comparisons test)

4.2.4 Cytokine Measurements

The levels for IL-6, TNF-α, KC and MIP2 were measured in BALF and plasma samples using xMAP technology and Luminex Assays (RD Systems) with the assistance of the UNC Cytokine & Biomarker Analysis Facility on BALF and Plasma samples. Select samples were tested using BD OptEIA kits (following manufacturer's instructions) to confirm Luminex Assay results (data not shown).

4.2.5 Flow Cytometry

Cells from BALF samples were blocked with anti-CD16/32 (FC block, eBioScience) and stained with CD11c-PE (BioLegend), CD45-PacificBlue (BioLegend), Ly6G Alexa700

(BioLegend), SiglecF-APC (BDPharmingen). The gating scheme (Figure 4.2), briefly, consists of looking at CD45+ cells (leukocytes), then CD11c+ to differentiate alveolar macrophages, followed by Ly6g+ indicating Neutrophils, or SiglecF- indicating dendritic cells. CD11c-SiglecF+ indicated alveolar macrophages. Gating scheme based on work by Guilliams *et al.*[32] Cells were fixed using 2% PFA in PBS. All data were collected using the Beckman Coulter CyAn ADP and analyzed using FlowJo Software (Tree Star).

4.2.6 Particle Fabrication

BuChE particles were fabricated as discussed in Chapter 2. For particle *in vivo* studies, Dylight680-tagged BuChE at 10 wt% was used in the formulation (Figure 4.1).

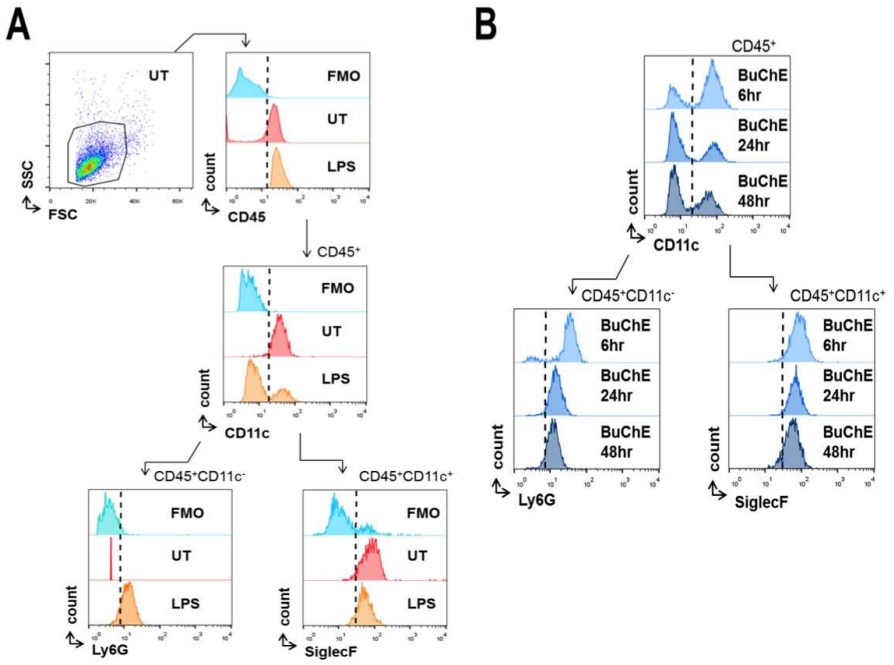

Figure 4.2. Representative Flow Cytometric Analysis of BALF Cells. (A) Gating scheme used to define three major lung cell populations: Granulocytes CD45+CD11c-Ly6G+, Macrophages $CD45^{+}CD11c^{+}$SiglecF+, Dendritic cells (DCs) $CD45^{+}CD11c^{+}$SiglecF-. Blue curves are fluorescence minus one (FMO) controls used to set gates. Red curves are untreated (UT) samples. Orange curves represent LPS controls at 24 hours. (B) Representative flow cytometry plots of BALF cells following BuChE instillation at 6, 24, and 48 hours.

4.2.7 Enzyme Activity Measurements

Activity was determined as discussed in Chapter 2.

4.2.8 Cascade Impactor Lung Deposition

BuChE particles were lyophilized in *tert*-butanol, as previously described,[8] to obtain a dry powder. The aerodynamic properties of the dry powder were characterized with an Andersen Cascade Impactor *(*ACI, ThermoScientific) in triplicate. Powder aerosols were dispersed via an insufflator device and a 3 ml syringe as the hand pump at 2 mg fill weights (Penn Century Inc., PA, USA). Standard ACI protocol was used as previously discussed.[24] Briefly, collection plates were coated with poly (ethylene glycol) MW 300. The flow rate was 28.3 L/min for 8 seconds. Deposited particles were collected using 500 µl of water, followed by flash freezing and lyophilization. Lyophilized samples were then resuspended in a concentrated volume of water for quantification of deposition per stage based on BuChE activity. It was confirmed that this corresponds directly to the relative mass theoretically deposited on each plate based on a standard of BuChE activity as it correlates to mass of protein.

4.2.9 Dry Powder Insufflation

Mice were anesthetized using ketamine, placed on a 45-degree board by their upper incisors, and a laryngoscope was used to facilitate insertion of the PennCentury insufflator device. Male C57BL/6 mice (n=3) were dosed with 1 µm cylindrical BuChE protein particles (fabricated and lyophilized as described above) at 2 mg fill weights to demonstrate potential for dry powder administration. The PennCentury was applied following standard manufacturer procedures and previously published methods.[33,34] Briefly, the dose was administered at the tidal volume of mice (200 µl) with five actuations of the air pump. The actual dose delivered was

determined by weighing the device before and after dose actuations. Following administration, the mice were placed on a heated blanket and given a reversal agent (Antisedane®) before being placed for monitoring. At each timepoint, the mice were harvested as described above. Briefly, BALF was collected with 1 mL of 1x PBS and lungs were imaged via IVIS.

4.2.10 Statistical Analysis

GraphPad Prism® v6.0 was used for statistical analyses as shown in figures and described in figure legends. Biodistribution of BuChE data was analyzed using two-way ANOVA with Tukey's multiple comparison test compared to saline at 24 hours. Cytokine response analysis and cell population distributions included two-way ANOVA with Tukey's multiple comparisons test compared to saline 24 hours with LPS excluded from analysis. BuChE activity in particles was analyzed using two-way ANOVA with Tukey's multiple comparisons test. Biodistribution of 1 μm dry powder particles was analyzed using two-way ANOVA with Tukey's multiple comparisons test compared to negative control.

4.3 Results

4.3.1 Biodistribution of Orotracheal Administrated BuChE in Nude Mouse Model

Dylight-680 tagged BuChE was utilized to monitor biodistribution of BuChE post-orotracheal administration in male Nude mice, n= 3 at 80 mg/kg (Figure 4.3). Upon harvest, lungs were lavaged and imaged via IVIS (Figure 4.3A), showing detection of BuChE up to 96 hours with significant difference over negative control up to 72 hours (Figure 4.3B). BuChE in the BALF was detected via IVIS up to 48 hours post-instillation with a significant difference over the negative control at 24 hours (Figure 4.3C) and correlated with BuChE activity that was detected up to 48 hours (Figure 4.3D). BALF BuChE concentrations were measured from the

fluid layer lining the airways of the lung. Lung concentrations were measured after broncheoalveolar lavage was collected. Comparing detection of BuChE in the lungs versus BALF at the same time point suggests uptake of BuChE by lung tissue the longer BuChE remained in the lungs.

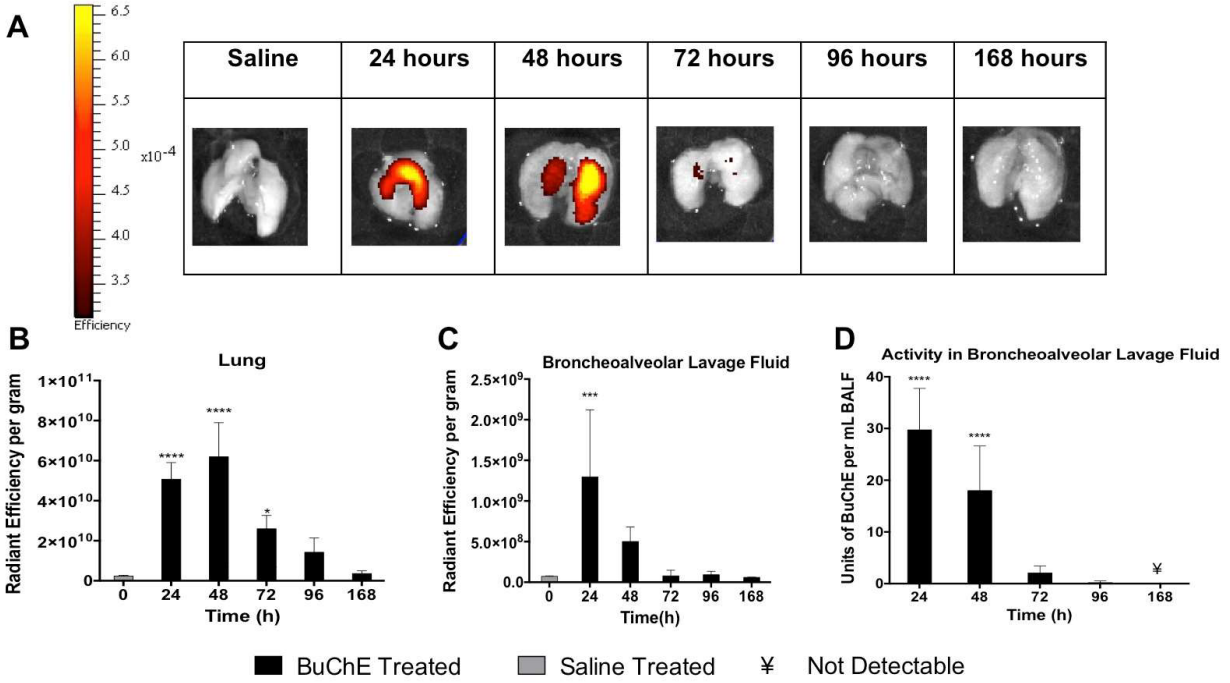

Figure 4.3. Biodistribution of BuChE. Dylight680 tagged BuChE detected post-orotracheal administration at 80 mg/kg (n=3) shown in (A) representative IVIS images of treated lungs over time (Color Bar Scale: Min= 3.13e-4,Max=6.61e-4), (B) lung and (C) BALF compartments in male Nude mice with (D) activity in the BALF measured. Results are representative of two repeated studies, n=3 each. Saline mice were included as controls. * = p< 0.05,*** = p< 0.001,****= p< 0.0001 , n.s. = not significant; two-way ANOVA with Tukey's multiple comparisons test compared to saline.

Given the increased retention of BuChE in the lungs after pulmonary instillation, other organs were analyzed for potential BuChE accumulation at each time point with no BuChE detected in the spleen, kidney, liver, or plasma compartments at any time points (Figure 4.4). No endogenous BuChE was detected in mice treated with saline orotracheally. Furthermore, no additional BuChE was detected systemically over baseline.

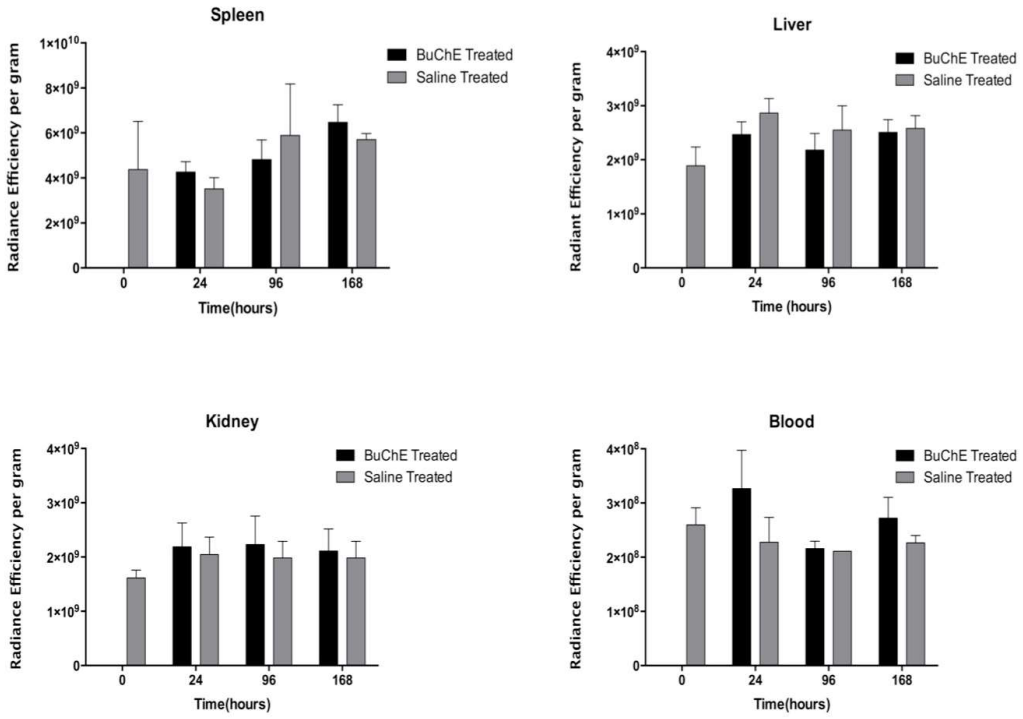

Figure 4.4. Organ Biodistribution of BuChE. Male Nude mice were orotracheally dosed at 80 mg/kg. Saline mice were included as controls. BuChE was tagged with Dylight680 for detection via IVIS.

4.3.2 Immunological Assessment of Orotracheal Administration of BuChE in Different Murine Models

Lung biology is a complex field that leaves many questions unanswered. To our knowledge, information is lacking on the biological effects in the lungs after direct biologic administration. We sought to understand the effect of BuChE administration on clearance times and immunological response in order to ultimately utilize the lung as a therapeutic target. Furthermore, previous studies have demonstrated that the particular mouse model used can affect results due to genetic/immunological variation.[35] For our initial studies, Nude mice were chosen due to their naturally low endogenous plasma BuChE levels (Table S1), which would allow for easier detection of our dosed BuChE due to higher signal to noise ratio. However, to better understand the potential immunological response, examining additional mouse models was

important to compare variance among different lung environments and better understand protein clearance from the lungs. Martin and Frevert detail how diverse the immune response is in the human lung population and the associated variances in cytokine concentrations.[36] Therefore, we used athymic Nude mice to represent a T-cell deficient lung, C57BL/6 to represent a normal human lung, and BALB/c mice to represent a typical asthmatic lung model.[37]

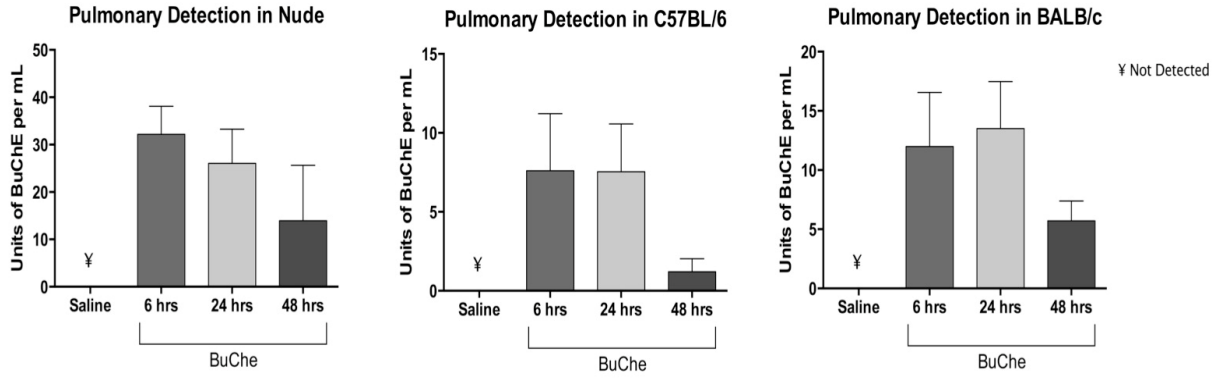

Figure 4.5. BuChE Activity Confirmation. Male Nude mice, C57BL/6 mice, and BALB/c mice were orotracheally administered 80 mg/kg BuChE (n=3). Activity as measured in BALF at 6, 24, and 48 hours to confirm presence of BuChE in the lung. Saline mice were served as negative controls.

BuChE was orotracheally administered at 80 mg/kg with saline negative control and LPS positive control treatments. BALF and plasma samples were collected at 6, 24, and 48 hours. BuChE activity was confirmed throughout (Figure 4.5). We tested cytokine levels of TNF-α, IL-6, KC, and MIP-2 in each mouse model in both the BALF (Figure 4.6) and plasma (Figure 4.7).[35,38] Alveolar epithelium derived cytokines and macrophage-derived cytokines (TNF-α, IL-6, and IL-8) were tested.[36] MIP-2 and KC are the murine homologues to human IL-8.[39] Overall, the Nude mice exhibited a greater initial increase in all cytokine levels than the BALB/c or C57BL/6 mice, respectively, however, the cytokine response subsided between 24 and 48 hours in all three strains.

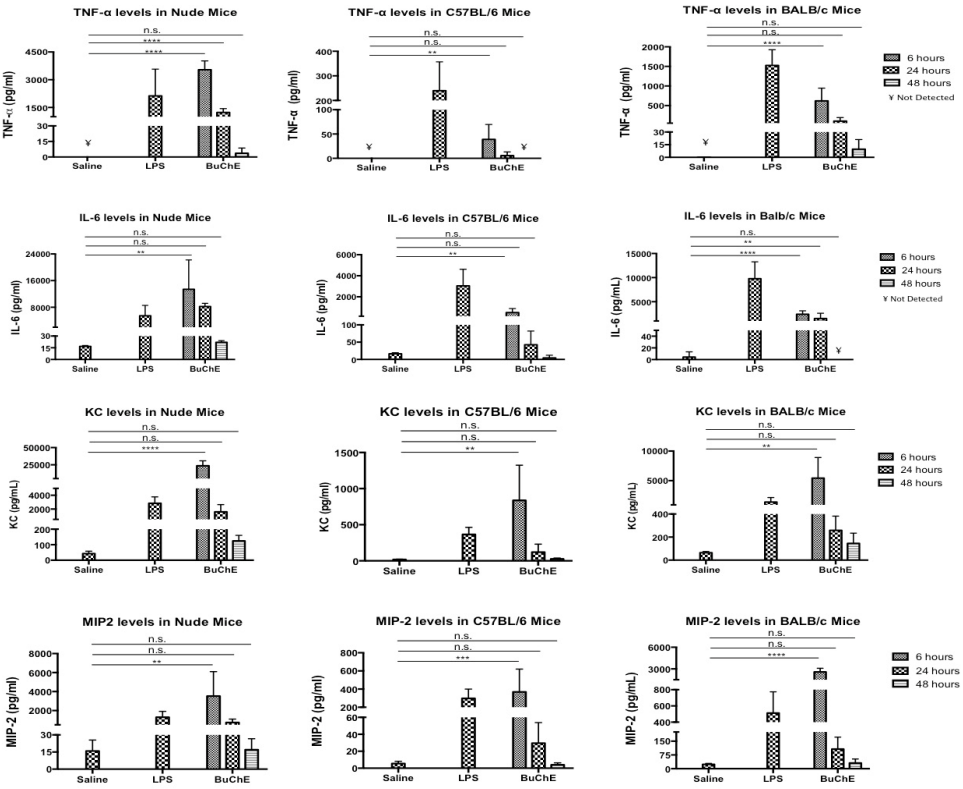

Figure 4.6. Cytokine Responses following BuChE Administration to the Lung. Male Nude, C57BL/6, and BALB/c were orotracheally administered 80 mg/kg BuChE (n=3). (A) TNF-α (B) IL-6 (C) KC and (D) MIP2 Cytokine levels were measured in BALF at 6, 24, and 48 hours. Negative control (saline) and positive control (LPS) were also included. * = $p < 0.05$, ** = $p < 0.01$, *** = $p < 0.001$,****= $p < 0.0001$, n.s. = not significant; two-way ANOVA with Tukey's multiple comparisons test compared to saline 24 hours with LPS excluded from analysis.

Furthermore, to determine the effect of BuChE pulmonary administration on cell recruitment in the lung, flow cytometry was used to examine the relative cell populations of macrophages, granulocytes, and dendritic cells in the BALF (Figure 4.8). Representative flow cytometric analysis of BALF cells is shown in Figure 4.2. A clear influx of granulocytes was seen at 6 hours in all three strains, with the Nude mice having a greater influx than the BALB/c or C57BL/6 mice. However, the granulocyte levels decreased to near saline levels by 48 hours in all three-mouse strains. It is important to note that commercial source of administered BuChE was found to contain endotoxins (data not shown).

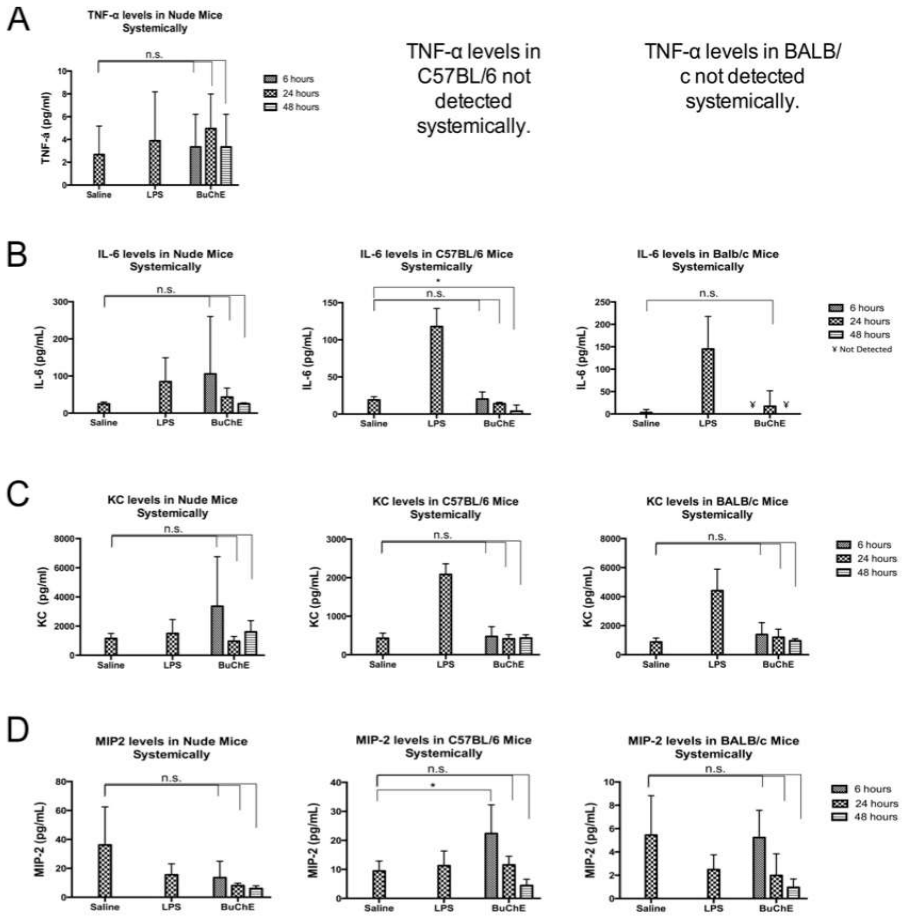

Figure 4.7. Systemic Cytokine Levels. Male Nude, C57BL/6, and BALB/c were orotracheally administered 80 mg/kg BuChE (n=3) with (A) TNF-α (B) IL-6 (C) KC and (D) MIP2 Cytokine levels measured in Blood at 6, 24, and 48 hours.* = $p < 0.05$, n.s. = not significant; two-way ANOVA with Tukey's multiple comparisons test compared to saline 24 hours with LPS excluded from analysis.

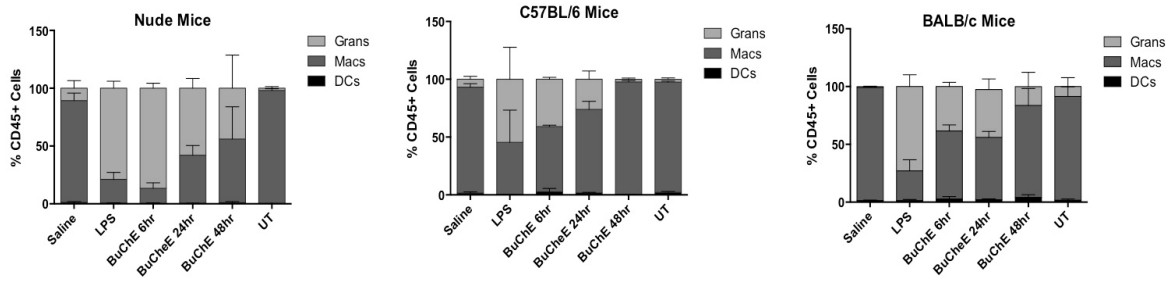

Figure 4.8. Leukocyte Population in the BALF following BuChE Administration to the Lung. Male Nude, C57BL/6, and BALB/c were orotracheally administered 80 mg/kg BuChE (n=3). Flow cytometry analysis in each mouse strain shows macrophages, granulocytes, and dendritic cell distribution. Negative controls (untreated and saline) and positive control (LPS) were also included. * = $p < 0.05$, ** = $p < 0.01$, *** = $p < 0.001$,****= $p < 0.0001$, n.s. = not significant; two-way ANOVA with Tukey's multiple comparisons test compared to saline 24 hours with LPS excluded from analysis.

4.3.3 Fabrication and Utilization of PRINT BuChE Protein Particles to Demonstrate Pulmonary Cascade Impactor Deposition

1 μm cylinder particles were fabricated as described in Chapter 2, with activity maintained throughout. As shown in chapter 2, particle composition was 98% BuChE, 1.15% lactose, and 0.51% glycerol for particles used in cascade impaction studies and *in vivo* (Figure 2.5B). BuChE particles were then lyophilized for dry powder deposition analysis. Aerosol sizing was performed from a PennCentury insufflator device with an ACI, which is typically used to correlate to human lung deposition for particles (Figure 4.9A).[40] PennCentury is routinely used for precise dry powder delivery to mice; therefore utilizing the PennCentury device allows us to compare *in vitro* data to *in vivo* studies.

A

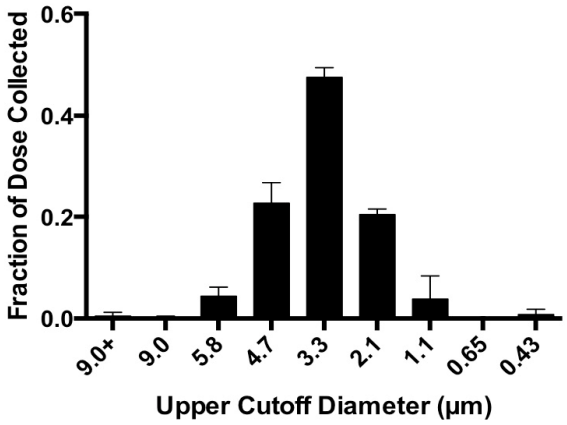

B

Aerosol Properties

N=3	Average ± std. dev.
Dose (U)	51.80 ± 7.01
MMAD(µm)	2.77 ± 0.06
GSD	1.39 ± 0.03
FPF (% emitted dose)	52.90 ± 4.16

Figure 4.9. Andersen Cascade Impaction (ACI). Distributions plotted as (A) fraction of dose deposited based on activity detected on each stage for particles aerosolized via PennCentury with Mass median aerodynamic diameter (MMAD), geometric standard deviation (GSD), and fine particle fraction (FPF) determined (B).

PRINT 1 µm cylindrical particles fell within the respirable range with aerodynamic properties indicative of deposition in peripheral airways, as compared to larger particles.[8,41] The average mass median aerodynamic diameter (MMAD) was determined to be 2.77 µm with an average geometric standard deviation (GSD) of 1.39 and a fine particle fraction (FPF) of 52.90% based on percent-emitted dose that was less than 5 µm (Figure 4.9B). Aerosols generated from these particles show potential for ideal deposition in the human lung with implications beyond the scope of current clinical standards.

4.3.4 Dry Powder Insufflation of PRINT BuChE Protein Particles in C57BL/6 Mouse Model

After assessment of dispersion properties, 1 µm BuChE cylindrical dry powder particles tagged with Dylight-680 were administered to C57BL/6 male mice to demonstrate DPI

administration utilizing a PennCentury insufflator. BuChE particle distribution was determined in the BALF and lungs with an average percent dose delivered reported in Figure 4.10A based on the amount of dose that left the chamber. BuChE particles were detected in the lungs using IVIS imaging with detection up to 72 hours and significant difference over the untreated baseline up to 48 hours (Figure 4.10B). BuChE in the BALF was detected up to 48 hours with significant difference from untreated controls (Figure 4.10C) and a corresponding detection of activity for 48 hours (Figure 4.10D).

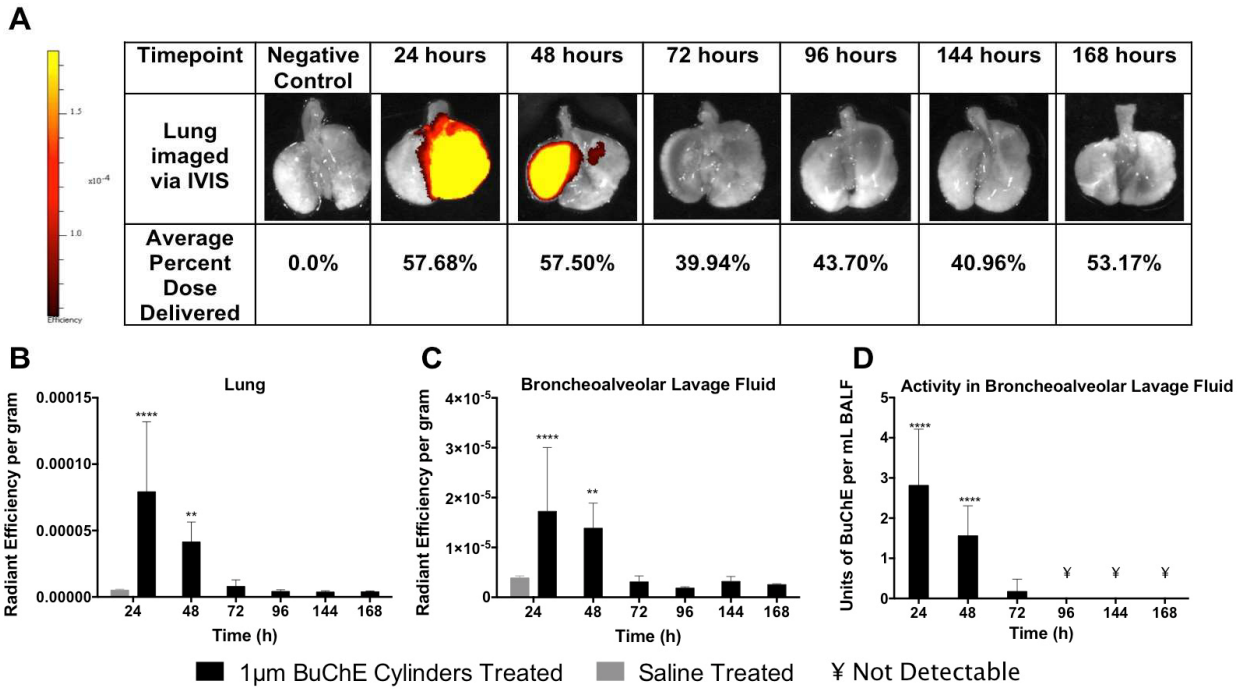

Figure 4.10. Biodistribution of 1 µm BuChE Dry Powder Particles. Dylight680 tagged BuChE detected post-insufflation administration at 2 mg/mouse (n=3) shown in (A) representative IVIS images of treated lungs over time with average percent dose delivered (Color Bar Scale: Min=6.67e-5, Max=1.76e-4), (B) lung and (C) BALF compartments in male C57BL/6 mice with (D) activity in the BALF measured. Untreated mice were included as controls. ** = $p < 0.01$,****= $p < 0.0001$; two-way ANOVA with Tukey's multiple comparisons test compared to negative control.

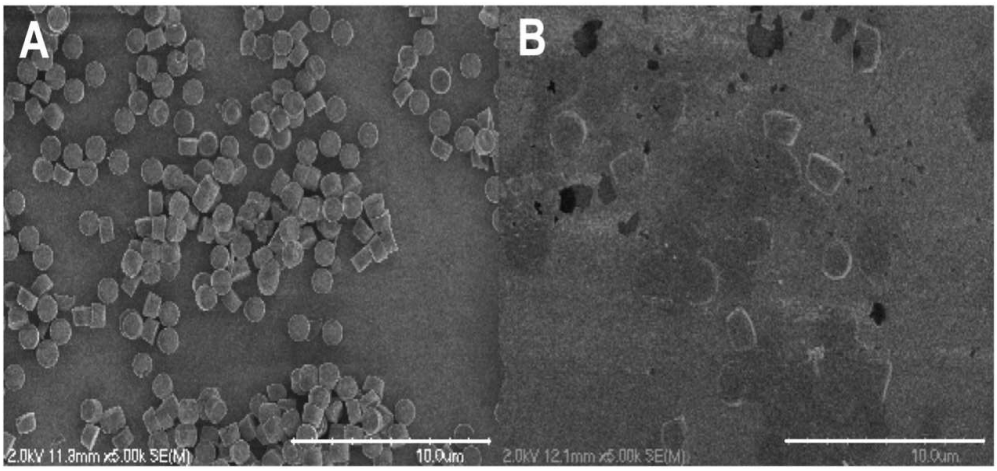

Figure 4.11. PRINT® BuChE in Aqueous Environment. 1 μm cylindrical BuChE particles in (A) isopropanol and (B) following 1 second incubation in water**.** Scale bar: 10.0 μm

4.4 Discussion

Utilizing biologics in pulmonary delivery that have both optimal aerosol characteristics and biological stability is a critical goal for the field. Diseases ranging from cystic fibrosis, pulmonary hypertension, asthma, and lung malignancies, not to mention patients with lung transplants rejection[1,7,13] could benefit from direct local treatment using dry powder particles, which can be easily administered in a targeted, non-invasive manner.[42] Our studies utilize BuChE for its potential use in treatment for organophosphate poisoning or pseudocholinesterase deficiency. Furthermore, our work serves to provide foundational studies for biologic based particles administered via dry powder inhalation. For example, adapting our methods to manufacture particulate human growth factor (HGF) could provide the opportunity to maintain HGF activity while providing good aerosol characteristics for treating growth deficiency via an inhaled route of administration.[1,13] The studies presented here examined pulmonary administration of BuChE *in vivo* to better understand local lung profiles and any resulting

immunological implications. Importantly, fabricated particulate BuChE maintained enzymatic activity, optimal deposition characteristics and subsequently displayed ideal deposition profiles.

We first tested free BuChE via orotracheal instillations to create a baseline comparison for our dry powder particle studies. Without further chemical modifications, the PRINT formulation was instantly dissolvable upon instillation, allowing us to directly relate our particle formulation to the free BuChE molecule studied in aqueous *in vivo* environments (Figure 4.11). In our initial studies, orotracheally administered BuChE was readily detectable in the BALF and lungs. BALF BuChE concentrations represented the amount of enzyme residing in the fluid layer lining the airways of the lung. Lung concentrations represented BuChE amounts remaining in the lung after broncheoalveolar lavage. To our knowledge, BuChE detection and retention in lungs has not been previously addressed, but its presence could be indicative of why previous studies have shown protection against OPs after pulmonary administration of BuChE.[18] It is hypothesized that as BuChE deposits in lungs, it adheres to or is taken up by cells and tissue, as seen in the 48-hour spike followed by a gradual clearance from tissue after 72 hours (Figure 4.3). It is likely removed through multiple clearance mechanisms of the lung, including involvement of peptidases and lung absorption.[2,41] Additionally, the main alveolar epithelium barrier restricts systemic exposure of larger proteins (>50 KDa) delivered to the lung, explaining the lack of significant BuChE levels in the bloodstream after lung deposition.[41,43] Current data show the absence of BuChE in plasma, spleen, kidneys, or liver up to 168 hours, however, future exploration of BuChE detection in blood after 168 hours with dosing of higher BuChE activity may yet offer opportunities for systemic detection.

Cell distribution and cytokine levels in lungs are important to understanding immunological response to direct BuChE treatment and future translation of enzyme delivery to

the lung. There was no endogenous BuChE detected in the BALF; therefore we were interested if administration of an enzyme non-native to the lung would have adverse responses. Another essential component to assessing immune response is to mimic the diverse lung population of human patients. We sought to do this by comparing three mouse models representing varied lung immune responses: a T-cell deficient lung (athymic Nude mice), a normal human lung (C57BL/6 mice), and an asthmatic lung (BALB/c mice).[37] Many therapeutics are not effective due to unintentional stimulation of the host immune response affecting residence time and potentially being harmful to the host, therefore it is important to assess the implications of BuChE administration.[44,45] Furthermore, the immunological consequence of delivering active particulate enzyme to the lung is largely understudied. Previously published work demonstrated minimal immune response with pulmonary delivery of non-biologically active PRINT formulations of different shapes and sizes.[11,12] Utilizing saline- and LPS-treated mice as our negative and positive controls, respectively, we observed that BuChE-treated mice initially showed an influx of granulocytes, followed by a restoration of baseline cell populations at 48 hours. This indicated an acute response to the administered protein, which was alleviated 48 hours post-instillation. It is important to note that active BuChE is still detectable in the BALF and lungs at 48 hours. Furthermore, in all mouse models, there was an initial influx in cytokine levels post-administration of BuChE in the lungs, which then decreased within 48 hours to normal levels. All mouse models showed cell distribution and cytokine level recovery in this time period, with Nude mice having a slightly more severe initial influx, BALB/c with an intermediate influx, and C57BL/6 with the least influx. This suggests that the athymic Nude mice have a delay in immune protection, while normal mice react rapidly to control the immune response. The initial influx in cytokine levels in all strains within BALF can be attributed to the actual addition of protein to

lungs, but was more likely due to endotoxin associated with the unformulated commercially available protein. This protein is routinely used in research studies[28,29] and contains <1 EU/μg of protein, which is the typical endotoxin content of most commercially available proteins but sufficient to potentially elicit an innate immune response.[46] Further studies need to be conducted with endotoxin-free BuChE to shed light on the source of inflammation. However, these promising results show that current BuChE administered directly to the lungs will not cause a severe, long-term immune response. Therefore, it can be predicted that protein particles will be a safe treatment option despite the diverse human lung population.

After establishing how free BuChE acts in the lungs and investigating immune responses, we used PRINT technology to develop a BuChE dry powder particle formulation to provide efficient delivery of BuChE to the lung. With the amenability of PRINT, we were able to formulate the particles with our choice of BuChE source, allowing us to vary particle dose based on the activity concentration of the BuChE utilized in fabrication while maintaining composition profiles of greater than 90% active BuChE content (Figure 2.5). The fabricated 1 μm BuChE particle aerosol showed promise for deep lung delivery into the alveolar region due to a high fraction being in the respirable range (less than 5 μm).[8,43,47] Based on accepted translation of ACI data to the respiratory tract, 2-3 μm MMAD would have a theoretical deposition near the secondary bronchi.[48] However, several studies have shown that this can be altered due to numerous variables, including flow rate and person to person variability, potentially resulting in deeper deposition near the terminal bronchi.[41,48] Furthermore, a low GSD of 1.39 was determined, which indicated minimal aggregation and thorough dispersion of this formulation (Figure 4.9).[24] This supported the use of 1 μm BuChE cylinders for pulmonary delivery via DPI. In comparison, our commercial source of BuChE does not have particle size properties amenable

to dispersion in the insufflator, as it was too bulky for dispersion using this method. Thus, the PRINT BuChE particle formulation is an ideal candidate for controlled and efficient BuChE airway deposition.

Successful *in vitro* testing of PRINT BuChE particles demonstrated the ability for targeted deposition; therefore, confirming a residence time comparable to free BuChE was necessary. The dry powder particles were detectable in both the lungs and BALF for 48 hours at a significant difference over baseline, with corresponding activity detection in the BALF (Figure 4.10). In comparison, the free BuChE resided in the lungs for 48 hours with some detection at 72 hours, while BuChE in the BALF lingered between 24 and 48 hours (Figure 4.3). It is important to note the difference in delivery methods of instillation, direct administration to the lung, of free BuChE, versus insufflation of the particulate BuChE. The direct instillation guaranteed the entire dose is administered. However, with dry powder insufflation, powder can be exhaled while dosing, swallowed into the stomach, etc. therefore the entire reported dose delivered does not reflect the actual dose that entered the lungs. Accordingly, it is important to assess trends and limitations in each individual study. Furthermore, PennCentury insufflation is the main way to administer dry powder particles, but it has limitations including small dose loading chamber and low dispersion of dose due to limited mouse lung capacity.[49] Utilizing this device is further limited by the expertise of the dose administrator to place the device accurately in the trachea on the first attempt. Nevertheless, this method allowed us to demonstrate the ability of our particles to have comparable residence time as free BuChE. Future studies will incorporate different pulmonary administration techniques, such as a nose-cone chamber with larger animal models. Most importantly, we have demonstrated that the particles, in current formulation, can maintain activity *in vivo* as long as the free BuChE with the advantage of targeted deposition as shown via

cascade impaction. This is promising for future translational studies utilizing our BuChE dry powder particles.

Overall, we have established that PRINT BuChE particles can provide targeted deposition as well as comparable residence time as free BuChE. The aerodynamic properties presented here can be further tuned by altering the geometric properties of the particles, which is readily achieved through the PRINT process.[8,24] Based on previous work in our lab on modifying the controlled degradation of protein particles,[23] we are now exploring ways to chemically tune the degradation of BuChE particles for extended release in a single dose administration. This approach will provide higher residence times and efficacy for future treatments, as well as adequate lung deposition characteristics, with minimal immunologic consequences. Future studies will translate application to larger animal models and the use of other biologics, including human BuChE. This work demonstrates effective and safe delivery of BuChE as a DPI formulation, which offers potential for novel clinical treatments.

REFERENCES

(1) Hertel, S. P.; Winter, G.; Friess, W. Protein Stability in Pulmonary Drug Delivery via Nebulization. *Adv. Drug Deliv. Rev.* **2014**, *93*, 79–94.

(2) Azarmi, S.; Roa, W. H.; Löbenberg, R. Targeted Delivery of Nanoparticles for the Treatment of Lung Diseases. *Adv. Drug Deliv. Rev.* **2008**, *60* (8), 863–875.

(3) Pressler, T. Review of Recombinant Human Deoxyribonuclease (rhDNase) in the Management of Patients with Cystic Fibrosis. *Biologics* **2008**, *2* (4), 611–617.

(4) Muzykantov, V. R. Review; Delivery of Antioxidant Enzyme Proteins to the Lung. *Antioxisdants Redox Signal.* **2001**, *3* (1), 39–62.

(5) Patton, J. S.; Brain, J. D.; Davies, L. A.; Fiegel, J.; Gumbleton, M.; Kim, K.-J.; Sakagami, M.; Vanbever, R.; Ehrhardt, C. The Particle Has Landed--Characterizing the Fate of Inhaled Pharmaceuticals. *J. Aerosol Med. Pulm. Drug Deliv.* **2010**, *23 Suppl 2*, S71–S87.

(6) Fala, B. L.; Writer, M. Afrezza (Insulin Human) Inhalation Powder Approved for the Treatment of Patients with Type 1 or Type 2 Diabetes. *Am. Heal. Drug Benefits* **2015**, *8* (March).

(7) Mansour, H. M.; Rhee, Y. S.; Wu, X. Nanomedicine in Pulmonary Delivery. *Int. J. Nanomedicine* **2009**, *4*, 299–319.

(8) Garcia, A.; Mack, P.; Williams, S.; Fromen, C.; Shen, T.; Tully, J.; Pillai, J.; Kuehl, P.; Napier, M.; DeSimone, J. M.; Maynor, B. W. Microfabricated Engineered Particle Systems for Respiratory Drug Delivery and Other Pharmaceutical Applications. *J. Drug Deliv.* **2012**, *2012*, 1–10.

(9) Muro, S.; Garnacho, C.; Champion, J. A.; Leferovich, J.; Gajewski, C.; Schuchman, E. H.; Mitragotri, S.; Muzykantov, V. R. Control of Endothelial Targeting and Intracellular Delivery of Therapeutic Enzymes by Modulating the Size and Shape of ICAM-1-Targeted Carriers. *Mol. Ther.* **2008**, *16* (8), 1450–1458.

(10) Champion, J. a; Mitragotri, S. Role of Target Geometry in Phagocytosis. *Proc. Natl. Acad. Sci. U. S. A.* **2006**, *103*, 4930–4934.

(11) Robbins, G. R.; Roberts, R. a.; Guo, H.; Reuter, K.; Shen, T.; Sempowski, G. D.; McKinnon, K. P.; Su, L.; DeSimone, J. M.; Ting, J. P.-Y. Analysis of Human Innate Immune Responses to PRINT Fabricated Nanoparticles with Cross Validation Using a Humanized Mouse Model. *Nanomedicine Nanotechnology, Biol. Med.* **2015**, *11* (3), 589–599.

(12) Roberts, R. a.; Shen, T.; Allen, I. C.; Hasan, W.; DeSimone, J. M.; Ting, J. P. Y. Analysis of the Murine Immune Response to Pulmonary Delivery of Precisely Fabricated Nano- and Microscale Particles. *PLoS One* **2013**, *8* (4).

(13) Shoyele, S. A.; Slowey, A. Prospects of Formulating Proteins/peptides as Aerosols for Pulmonary Drug Delivery. *Int. J. Pharm.* **2006**, *314* (1), 1–8.

(14) Hulse, E. J.; Davies, J. O. J.; Simpson, a. J.; Sciuto, A. M.; Eddleston, M. Respiratory Complications of Organophosphorus Nerve Agent and Insecticide Poisoning. Implications for Respiratory and Critical Care. *Am. J. Respir. Crit. Care Med.* **2014**, *190* (12), 1342–1354.

(15) Darvesh, S.; Hopkins, D. a; Geula, C. Neurobiology of Butyrylcholinesterase. *Nat. Rev. Neurosci.* **2003**, *4* (February), 131–138.

(16) Doctor, B. P.; Saxena, A. Bioscavengers for the Protection of Humans against Organophosphate Toxicity. *Chem. Biol. Interact.* **2005**, *157-158*, 167–171.

(17) Genovese, R. F.; Lu, X. C. M.; Gentry, M. K.; Larrison, R.; Doctor, B. P. Evaluation of Purified Horse Serum Butyrylcholinesterase in Rats. **1993**.

(18) Rosenberg, Yvonne J. ; Laube, Beth; Mao, Lingjun; Jiang, Xiaoming; Abanto, Segundo; Lee, Keunmyoung D. ; Adams, R. Pulmonary Delivery of an Aerosolized Recombinant Human Butyrylcholinesterase Pretreatment Protects against Aerosolized Paraoxon in Macaques. *Chem Biol Interact* **2013**, *203* (1), 167–171.

(19) Soliday, F. K.; Conley, Y. P.; Henker, R. Pseudocholinesterase Deficiency : A Comprehensive Review of Genetic, Acquired, and Drug Influences. *AANA* **2010**, *78* (4), 313–320.

(20) Pseudocholinesterase Deficiency.

(21) Gordley, K. P.; Basu, C. B. Optimal Use of Local Anesthetics and Tumescence. **2006**, *1* (212), 219–224.

(22) Haas, D. A. An Update on Local Anesthetics in Dentistry. *J. Can. Dent. Assoc.* **2002**, *68* (9), 546–551.

(23) Xu, J.; Wang, J.; Luft, J. C.; Tian, S.; Owens, G.; Pandya, A. a.; Berglund, P.; Pohlhaus, P.; Maynor, B. W.; Smith, J.; Hubby, B.; Napier, M. E.; Desimone, J. M. Rendering Protein-Based Particles Transiently Insoluble for Therapeutic Applications. *J. Am. Chem. Soc.* **2012**, *134*, 8774–8777.

(24) Fromen, C. A.; Shen, T. W.; Larus, A. E.; Mack, P.; Maynor, B. W.; Luft, J. C.; DeSimone, J. M. Synthesis and Characterization of Monodisperse Uniformly Shaped Respirable Aerosols. *Am. Inst. Chem. Eng.* **2013**, *0* (00), 405–410.

(25) Moorad, D.; Luo, C.; Saxena, A.; Doctor, P.; Garcia, G. E. Purification and Determination of the Amino Acid Sequence of Equine Serum Butyrylcholinesterase. **1999**, 219–227.

(26) Sun, W.; Luo, C.; Naik, R. S.; Doctor, B. P.; Saxena, A. Pharmacokinetics and Immunologic Consequences of Repeated Administrations of Purified Heterologous and

Homologous Butyrylcholinesterase in Mice. *Life Sci.* **2009**, *85* (17-18), 657–661.

(27) Rosenberg, Y.; Jiang, X.; Mao, L.; Abanto, S. H.; Lee, K. Development of a Prophylactic Butyrylcholinesterase Bioscavenger to Protect Against Insecticide Toxicity Using a Homologous Macaque Model. **2010**.

(28) Matzke, S. M.; Oubre, J. L.; Caranto, G. R.; Gentry, M. K.; Galbicka, G. Behavioral and Immunological Effects of Exogenous Butyrylcholinesterase in Rhesus Monkeys. *Pharmacol. Biochem. Behav.* **1999**, *62* (3), 523–530.

(29) Koetzner, L.; Woods, J. H. Characterization of Equine Butyrylcholinesterase Disposition in the Mouse. *Drug Metab. Dispos.* **2002**, *30* (6), 724–730.

(30) Broomfield, C. A.; Maxwell, D. M.; Solana, R. P.; Castro, C. A.; Finger, A. V; Lenz, D. E. Protection by Butyrylcholinesterase against Organophosphorus Poisoning in Nonhuman Primates. *J. Pharmacol. Exp. Ther.* **1991**, *259* (2), 633–638.

(31) Fernandes, C. A.; Vanbever, R. Preclinical models for pulmonary drug delivery http://www.uclouvain.be/cps/ucl/doc/farg/documents/FernandesVanbeverEODD2009.pdf (accessed Mar 16, 2015).

(32) Guilliams, M.; Lambrecht, B. N.; Hammad, H. Division of Labor between Lung Dendritic Cells and Macrophages in the Defense against Pulmonary Infections. *Mucosal Immunol.* **2013**, *6* (3), 464–473.

(33) PennCentury. Dry Powder Insufflator Instructions for Use.

(34) Duret, C.; Wauthoz, N.; Merlos, R.; Goole, J.; Maris, C.; Roland, I.; Sebti, T.; Vanderbist, F.; Amighi, K. In Vitro and in Vivo Evaluation of a Dry Powder Endotracheal Insufflator Device for Use in Dose-Dependent Preclinical Studies in Mice. *Eur. J. Pharm. Biopharm.* **2012**, *81* (3), 627–634.

(35) Jones, S. W.; Roberts, R. a.; Robbins, G. R.; Perry, J. L.; Kai, M. P.; Chen, K.; Bo, T.; Napier, M. E.; Ting, J. P. Y.; DeSimone, J. M.; Bear, J. E. Nanoparticle Clearance Is Governed by Th1/Th2 Immunity and Strain Background. *J. Clin. Invest.* **2013**, *123* (7), 3061–3073.

(36) Martin, T. R.; Frevert, C. W. Innate Immunity in the Lungs. *Proc. Am. Thorac. Soc.* **2005**, *2* (5), 403–411.

(37) Gueders, M. M.; Paulissen, G.; Crahay, C.; Quesada-Calvo, F.; Hacha, J.; Van Hove, C.; Tournoy, K.; Louis, R.; Foidart, J. M.; Noël, A.; Cataldo, D. D. Mouse Models of Asthma: A Comparison between C57BL/6 and BALB/c Strains Regarding Bronchial Responsiveness, Inflammation, and Cytokine Production. *Inflamm. Res.* **2009**, *58* (12), 845–854.

(38) Corwin, E. J. Understanding Cytokines. Part I: Physiology and Mechanism of Action. *Biol. Res. Nurs.* **2000**, *2* (1), 30–40.

(39) Singer, M.; Sansonetti, P. J. IL-8 Is a Key Chemokine Regulating Neutrophil Recruitment in a New Mouse Model of Shigella-Induced Colitis. *J. Immunol.* **2004**, *173* (6), 4197–4206.

(40) Mitchell, J.; Newman, S.; Chan, H.-K. In Vitro and in Vivo Aspects of Cascade Impactor Tests and Inhaler Performance: A Review. *AAPS PharmSciTech* **2007**, *8* (4), E110.

(41) Sakagami, M. In Vivo, in Vitro and Ex Vivo Models to Assess Pulmonary Absorption and Disposition of Inhaled Therapeutics for Systemic Delivery. *Adv. Drug Deliv. Rev.* **2006**, *58* (9-10), 1030–1060.

(42) El-Gendy, N.; Bailey, M. M.; Berkland, C. Particle Engineering Technologies for Pulmonary Drug Delivery. In *Controlled Pulmonary Drug Delivery*; Smyth, H., Hickey, A. J., Eds.; Springer: New York, NY, 2011; pp 283–312.

(43) Patton, J. S.; Fishburn, C. S.; Weers, J. G. The Lungs as a Portal of Entry for Systemic Drug Delivery. *Proc. Am. Thorac. Soc.* **2004**, *1* (4), 338–344.

(44) Manke, A.; Wang, L.; Rojanasakul, Y. Mechanisms of Nanoparticle-Induced Oxidative Stress and Toxicity. *Biomed Res. Int.* **2013**, *2013*, 942916.

(45) Sharp, F. A.; Ruane, D.; Claass, B.; Creagh, E.; Harris, J.; Malyala, P.; Singh, M.; O'Hagan, D. T.; Pétrilli, V.; Tschopp, J.; O'Neill, L. A. J.; Lavelle, E. C. Uptake of Particulate Vaccine Adjuvants by Dendritic Cells Activates the NALP3 Inflammasome. *Proc. Natl. Acad. Sci. U. S. A.* **2009**, *106* (3), 870–875.

(46) Watanabe, J.; Miyazaki, Y.; Zimmerman, G. a.; Albertine, K. H.; McIntyre, T. M. Endotoxin Contamination of Ovalbumin Suppresses Murine Immunologic Responses and Development of Airway Hyper-Reactivity. *J. Biol. Chem.* **2003**, *278* (43), 42361–42368.

(47) Lewis, D.; Copley, M. Inhaled Product Characterization Calculating Particle-Size Distribution Metrics. *Pharm. Technol.* **2011**, 33–37.

(48) Dunbar, C.; Mitchell, J. Analysis of Cascade Impactor Mass Distributions. *J. Aerosol Med.* **2005**, *18* (4), 439–451.

(49) Hoppentocht, M.; Hoste, C.; Hagendoorn, P.; Frijlink, H. W.; Boer, A. H. de. In Vitro Evaluation of the DP-4M PennCenturyTM Insufflator. *Submitt. to Eur. J. Pharm. Biopharm. (under Revis.* **2014**, *88*, 153–159.

CHAPTER 5. Summary and Outlook[4]

5.1 Summary and Future Work

In this work, we utilized the Particle Replication in Non-wetting Templates (PRINT) technology for precisely controlled particles to investigate the relationship between varying particle parameters and therapeutic application. We engineered particles of different particle composition and surface chemistry to specifically investigate their biodistribution and cellular interaction in the lungs. Lastly, we engineered unique biologic-based particles that remain active and demonstrate ideal deposition characteristics, unlike the common particle fabrication platforms.

We first assessed 80x320 nm cylindrical poly(lactic-co-glycolic-acid) (PLGA) nanoparticle (NP) stability in order to predict *in vivo* degradation rates (Chapter 2). Further work in the lab showed the 80x320 nm particles had reduced uptake in the spleen and liver compared to 200x200 nm particles.[1] Based on the reduced clearance of the 80x320 nm particles, we fabricated even smaller docetaxel loaded PLGA particles at 55x70 nm that had an increased loading and extended release kinetics. The DeSimone lab has since compared the biodistribution of the 80x320 nm particles to the smaller 55x70 nm particles to determine the influence of

[4] Reproduced in part from:

Robbins GR, Fromen CA, Rahhal TB, Luft JC, Wang AZ, Pecot CV, DeSimone JM. Non-Intravenous Routes of Delivery: Aerosol Therapy for Cancer Management. Cancer Nanotechnology Plan. Nov. 2015.

particle size on tumor accumulation with a different composition, hydrogels.[2] The biodistribution of these NPs was compared *in vivo* and found that the smaller (55x70 nm) NPs accumulated more in the liver and less in the spleen, with enhanced tumor accumulation compared to the larger NPs (80x320 nm).[2] This finding in conjunction with release kinetics for the PLGA 55 x 70 nm NPs provides promising evidence for the efficacy of smaller therapeutic NPs. Future studies looking at the pharmacokinetics and biodistribution of the smaller, 55x70nm, PLGA: docetaxel NPs *in vivo* would be beneficial to confirm if they are better suited for direct tumor targeting, particularly pulmonary diseases like lung cancer.

Chapter 2 highlighted two other compositions of interest, hydrogels and biologic-based, for PRINT particle fabrication. We explored these two compositions in more depth in Chapters 3 and 4 respectively. We have discussed PLGA and hydrogel compositions as well as biologics. However, there is an array of potential compositions that can be employed with PRINT. For example, chitosan is a natural polymer that allows for increased retention on mucus layers, has shown high encapsulation efficiency, and has high thermal stability, making it an ideal candidate for PRINT particle fabrication.[3] Future work exploring different compositions will expand our application of PRINT technology to improving therapeutics.

Utilizing the PRINT platform allowed us to focus independently on surface chemistry of hydrogel particles and how it affects biodistribution and cellular mechanisms in the lung (Chapter 3). We sought to compare association and uptake of particles with different surface chemistry to two main lung cells, alveolar macrophages (AMs) and dendritic cells (DCs). Our findings show cationic particles are preferentially associated with DCs, which lends useful for vaccine development that relies on DC antigen uptake, as DCs can travel to the lymph nodes and initiate an immune response. However, we investigated further and noted an increase, after

cationic particle administration, in chemokine/cytokine mRNA expression specific to recruitment of DCs to the lung. We confirmed this finding by observing changes in the lung population after administration, noting an increased DC population with cationic particle administration compared to untreated and anionic particle treatments. These findings help establish the potential application of utilizing cationic particles for pulmonary vaccines.

On the other hand, anionic particles were preferentially taken up by AMs. Targeting AMs could be beneficial for delivering therapeutics to target bacteria that remain in the AMs, like tuberculosis. Therefore, we sought to extend the anionic particle residence time by further altering surface chemistry with the incorporation of a PEG coating. PEGylated particles had an extended residence time of 28 days and delayed macrophage association. Providing this understanding of particle surface modification on cellular recruitment and association is important for advancing the development of pulmonary therapeutics. Tuberculosis treatments currently include a cocktail of antibiotics. A promising treatment would be direct delivery to the AMs, and a better approach would be to incorporate multiple drugs into one formulation or dose.[4] Future work would include incorporation of cargo into the modified hydrogel matrix for targeted delivery of AMs. Furthermore, the effect of size and shape on biodistribution can be investigated. It has been shown that macrophages have preferential association angles resulting in a high uptake of spherical particles and minimal uptake of worm-like particles.[5,6] We can employ PRINT to fabricate different particles of controlled shape and size to further understand which has a preferential association with AMs. After establishing an understanding of AM-particle association, and characterizing aerosol characteristics for the different shapes, we can engineer particles for new therapeutic opportunities to treat pulmonary diseases.

After establishing the impact of particle composition on therapeutic delivery, and investigating various surface modifications, we investigated the incorporation of a biologic into the PRINT platform for ultimate therapeutic application (Chapter 4). We successfully utilized a model protein, butyrylcholinesterase (BuChE), for fabricating cylinders within the respirable particle range. Our particles consisted of greater than 90% protein that remained active throughout processing, demonstrated central lung deposition, and had minimal inflammatory response. This formulation can be used for tackling organophosphate poisoning, or for preventing deaths in patients with pseudocholinesterase deficiency. Furthermore, we can translate our work with BuChE to other biologics of interest for treating pulmonary diseases, like cystic fibrosis (CF). CF is currently treated with DNase to break up the sputum build up in the lungs.[7] We can engineer DNase particles to potentially reduce the dosing frequency while improving efficacy.

There is an expanse of future work that can be done with BuChE biologic particles. Future work should include *in vivo* testing with larger rodents and canines using alternative pulmonary administration tools such as nose cone chambers. This can expand on residence time information and deposition, as these lung models would better relate to humans. To extend release time of the BuChE particles, a novel cross linker should be developed that would be cleavable in the lung environment. Another characterization feature that would be beneficial is to develop a high performance liquid chromatography method that can detect BuChE concentration directly. This would provide a more accurate composition analysis of the particles and can be adapted for any future biologic particle. Furthermore, we are currently working on recombinant human BuChE and have produced active monomeric and tetrameric formulations. Next steps include fabricating PRINT particles using the huBuChE for ultimate administration to humans.

Overall, we have shown that we can engineer particles with different compositions, surface modifications, and applications for use with pulmonary diseases. Furthermore, particle engineering can be very impactful on improving clinical outcomes by reducing the dose frequency patients need, overall reduction in healthcare costs, and improvement of patient quality of life.[8]

5.2 Outlook

At its current state, pulmonary diseases, including lung cancer, asthma, CF, and chronic obstructive pulmonary disease (COPD), make up more than $150 billion a year in health care costs.[9] There is a clear need to address the treatment of these diseases and reduce the associated costs by providing alternative, more effective treatment options. Our work has provided new avenues for exploration of targeted pulmonary treatments that can impact current standard of care in the clinic.

Patients with COPD or asthma or even both take multiple drugs to alleviate the inflammation in the bronchiole region. Current treatments have several problems including, systemic exposure and toxicity, lack of dual-drug, single administration therapies, limited dry powder options, and minimal dose consistency.[8] The key is to target delivery to the different regions of the lung, including mid-lung and alveolar space, with precisely defined particles. Current technologies do not provide precise control over shape and size that ultimately contribute to the aerodynamic diameter needed for this targeted deposition. PRINT provides a fabrication platform for well-controlled particles that are suitable for direct delivery to any region in the lung with none to minimal systemic exposure. Additionally, we have shown the amenability of PRINT particles to dry powder formulations providing an improved method for delivering therapeutics without the associated losses exhibited in current pressurized metered

dose inhalers (pMDI).[8] Overall, utilizing our understanding of particle compositions, surface chemistry, and targeted delivery we can employ PRINT to address many issues in treating pulmonary diseases.

With PRINT, we can also explore the creation of a combination particle. We can engineer two PRINT particles, each loaded with one drug, and dose them simultaneously using our ability to create dry powders that maintain the needed aerosol characteristics. The uniformity available by PRINT allows for controlling the issue of having equal drug concentrations dosed.[8] Each particle can be made in an identical manner with different drugs, and then characterized to ensure loading is equal. The second proposed method is to utilize two smaller particles, each loaded with one drug, then load them into a larger particle resulting in a mothership particle that can be used for its aerodynamic characteristics but then it rapidly releases the drug loaded particles, which have controlled release. We can utilize the high loading and controlled release kinetics of the PLGA particles discussed, as well as the hydrogel or biologic based larger particles as motherships. Another approach would be to fabricate a particle with both drugs loaded in equal concentration; this would take advantage of their complimentary mechanisms of action when administered.[8]

Furthermore, NP therapeutics in the lung represent an area of great potential, especially for treating cancer. The extensive research and success in particle formulations for intravenous NP therapies can be readily translated to lung administration with minimal reformulation. To date, most aerosol therapies have involved delivery of 1-5 μm sized particles, due to their aerodynamic properties and their assumed deposition in the lung.[10] Even chemotherapy liposome formulations evaluated in clinical trials as nebulized aerosols were on the order of ~1 μm.[11–13] More recent NP formulations (<200 nm) could offer tremendous benefits to the three aspects of

cancer management: drug delivery (including enhanced tumor uptake), mucosal diffusion, and lymph trafficking.[14]

However, delivery concerns will need to be addressed in order for NPs to deliver and deposit at high efficiencies in the airways. Typical drugs are potent and damaging to normal tissue, therefore direct delivery may induce lung injury.[15] The suggested solution is to design a treatment with independently tunable aerodynamic properties for controlled deposition in the region of interest within the lung.[14] Additionally, advancement of particle-based lung therapies will require continued optimization of inhaled delivery devices.[16,17] The ability to engineer particles of different shapes, sizes, compositions, and surface chemistries provides useful for pursuing pre-clinical pulmonary studies for a wide range of therapeutics as suggested here.

Pulmonary administration provides a unique advantage of a more stable, accessible, and non-invasive therapeutic delivery options for a multitude of diseases. However, there is a lack in providing a local, targeted treatment that can reduce frequency of doses and systemic side effects, while improving efficacy.[18] We have opened new doors for pulmonary treatments with our articulately engineered particles, while seeking to address the gaps in translating the application of nanotechnology to pulmonary treatments in the clinic. We hope to see an expansion in the realm of particulate pulmonary delivery of therapeutics as it can address current unmet needs in disease management.

REFERENCES

(1) Chu, K. S.; Hasasn, W.; Rawal, S.; Walsh, M. D.; Enlow, E. M.; Luft, J. C.; Bridges, A. S.; Kuijer, J. L.; Napier, M. E.; Zamboni, W. C.; DeSimone, J. M. Plasma, Tumor and Tissue Pharmacokinetics of Docetaxel Delivered via Nanoparticles of Different Sizes and Shapes in Mice Bearing SKOV-3 Human Ovarian Carcinoma Xenograft. *Nanomedicine* **2013**, *9* (5).

(2) Reuter, K. G.; Perry, J. L.; Kim, D.; Luft, J. C.; Liu, R.; DeSimone, J. M. Targeted PRINT Hydrogels: The Role of Nanoparticle Size and Ligand Density on Cell Association, Biodistribution, and Tumor Accumulation. *Nano Lett.* **2015**, *15* (10), 6371–6378.

(3) Pulliam, B.; Sung, J. C.; Edwards, D. a. Design of Nanoparticle-Based Dry Powder Pulmonary Vaccines. *Expert Opin. Drug Deliv.* **2007**, *4* (6), 651–663.

(4) Sharma, R.; Saxena, D.; Dwivedi, A. K.; Misra, A. Inhalable Microparticles Containing Drug Combinations to Target Alveolar Macrophages for Treatment of Pulmonary Tuberculosis. *Pharm. Res.* **2001**, *18* (10), 1405–1410.

(5) Champion, J. a; Mitragotri, S. Role of Target Geometry in Phagocytosis. *Proc. Natl. Acad. Sci. U. S. A.* **2006**, *103*, 4930–4934.

(6) El-sherbiny, I. M.; El-baz, N. M.; Yacoub, M. H. Review Article Inhaled Nano- and Microparticles for Drug Delivery. **2015**, 1–14.

(7) Pressler, T. Review of Recombinant Human Deoxyribonuclease (rhDNase) in the Management of Patients with Cystic Fibrosis. *Biologics* **2008**, *2* (4), 611–617.

(8) Weers, J. G.; Bell, J.; Chan, H.-K.; Cipolla, D.; Dunbar, C.; Hickey, A. J.; Smith, I. J. Pulmonary Formulations: What Remains to Be Done? *J. Aerosol Med. Pulm. Drug Deliv.* **2010**, *23 Suppl 2*, S5–S23.

(9) The Cost of Lung Disease.

(10) Crowder, T.; Rosati, J.; Schroeter, J.; Hickey, A.; Martonen, T. Fundamental Effects of Particle Morphology on Lung Delivery. *Pharm. Res.* **2002**, *19*, 239–245.

(11) Knight, V.; Kleinerman, E.; Waldman, R.; Giovanella, B.; Gilber, B.; Koshkina, N. Nitrocamptothecin Liposome Aerosol Treatment of Human Cancer Subcutaneous Xenografts and Pulmonary Cancer Metastases in Mice. *Ann N Y Acad Sci* **2000**, *922*, 151–161.

(12) Knight, V.; Koshkina, N.; Waldrep, J.; Giovanella, B.; Gilbert, B. Anticancer Effect of 9-Nitrocamptothecin Liposome Aerosol on Human Cancer Xenografts in Nude Mice. *Cancer Chemother Pharmacol* **1999**, *44*, 177–186.

(13) Gagnadoux, F.; Hureaux, J.; Vecellio, L.; Urban, T.; Le Pape, A.; Valo, I.; Montharu, J.;

Leblond, V.; Boisdron-Celle, M.; Lerondel, S.; Majoral, C.; Diot, P.; Racineux, JL; Lemarie, E. Aerosolized Chemotherapy. *J. Aerosol Med. Pulm. Drug Deliv.* **2008**, *21*, 61–70.

(14) Mansour, H. M.; Rhee, Y. S.; Wu, X. Nanomedicine in Pulmonary Delivery. *Int. J. Nanomedicine* **2009**, *4*, 299–319.

(15) Kuzmov, A.; Minko, T. Nanotechnology Approaches for Inhalation Treatment of Lung Diseases. *J. Control. Release* **2015**, *219*, 500–518.

(16) Kleinstreuer, C.; Seelecke, S. Inhaler System for Targeted Maximum Drug-Aerosol Delivery, 2011.

(17) Darwiche, K.; Zarogoulidis, P.; Karamanos, N. K.; Domvri, K.; Chatzaki, E.; Constantinidis, T. C.; Kakolyris, S.; Zarogoulidis, K. Efficacy versus Safety Concerns for Aerosol Chemotherapy in Non-Small-Cell Lung Cancer: A Future Dilemma for Micro-Oncology. *Future Oncol.* **2013**, *9* (4), 505–525.

(18) Kunda, N. K.; Somavarapu, S.; Gordon, S. B.; Hutcheon, G. A.; Saleem, I. Y. Nanocarriers Targeting Dendritic Cells for Pulmonary Vaccine Delivery. *Pharm. Res.* **2013**, *30* (2), 325–341.